October 2019

DRIVERS and CONSEQUENCES of CARBON USE EFFICIENCY - and ITS MEASUREMENT in SOIL

Grace Pold

DRIVERS AND CONSEQUENCES OF CARBON USE EFFICIENCY - AND ITS MEASUREMENT IN SOIL

A Dissertation Presented

by

Alice Grace Meadows Põld

Submitted to the Graduate School of the
University of Massachusetts Amherst in partial fulfillment
of the requirements for the degree of

DOCTOR OF PHILOSOPHY

September 2019

Graduate Program in Organismic and Evolutionary Biology

DRIVERS AND CONSEQUENCES OF CARBON USE EFFICIENCY - AND ITS MEASUREMENT IN SOIL

A Dissertation Presented

by

Alice Grace Meadows Põld

Approved as to style and content by:

Kristen M. DeAngelis, Chair

Erin Conlon, Member

Jim Holden, Member

Seeta Sistla, Member

Paige Warren, Program Director
Graduate Program in Organismic and Evolutionary Biology

ACKNOWLEDGMENTS

First and foremost, I would like to thank my trusty bikes, Donkey and Gretchen, for providing steady transport to and from the lab.

I would like to thank my labmates — and in particular Luiz Horta and Gina Chaput — for providing great company, encouragement, and intellectual input.

Thank you to the many people - scientists and not - who developed the intellectual basis for my work.

Thank you to my parents for the emotional and snack-related support that greatly smoothed the science-making process.

Thank you to the numerous undergrads who inadvertently served as guinea pigs for my mentoring experiments.

Thank you to the US taxpayers, for funding my research through the US Department of Energy, and the American Association of University Women, who funded my dissertation writing year. Funding also came from a UMass Graduate School Dissertation Research grant, and a UMass OEB Research grant.

Thank you to my committee members for putting up with and eagerly helping me with my questions.

Finally, I would like to extend my thanks to Kristen DeAngelis for allowing me to run wild most of the time, but not being afraid to reign me in when needed.

ABSTRACT

DRIVERS AND CONSEQUENCES OF CARBON USE EFFICIENCY - AND ITS MEASUREMENT IN SOIL

SEPTEMBER 2019

ALICE GRACE MEADOWS POLD

B.Sc., MCGILL UNIVERSITY

MS, UNIVERSITY OF MASSACHUSETTS AMHERST

Ph.D., UNIVERSITY OF MASSACHUSETTS AMHERST

Directed by: Professor Kristen M. DeAngelis

Soils serve as massive carbon sinks, but their ability to continue this ecological service is contingent on how the resident soil microbial community will respond to the ongoing climate crisis. One key dimension of the microbial response to warming is its carbon use efficiency (CUE), or the fraction of carbon taken up by an organism which is allocated to growth rather than respiration. However, the scientific community is still in the early stages of understanding the drivers, consequences - and even accurate measurements of - CUE. In this dissertation, I first quantified the variability of CUE and its responsiveness to temperature and substrate for soil bacteria grown in the lab. I subsequently implemented this knowledge into a plant litter decomposition

model to determine how including organism-level variation in CUE alters projected soil carbon stocks in a warmer world. Finally, I completed a series of numerical simulations to evaluate how robust a commonly-used method of measuring CUE in the field is to changes in the microbial community present.

I found that CUE was highly variable and depended on both substrate and temperature in a bacteria-specific manner. No robust genetic or genomic markers of CUE or its temperature dependence emerged, indicative of the wide diversity of bacteria characterized in this study. Nonetheless, efficiency tended to decrease with warming moreso in taxa which were already characterized by high efficiency, causing a degree of homogenization in CUE at higher temperatures. Introducing variation in CUE temperature sensitivity to the litter decomposition model DEMENT caused additional litter carbon loss under warming, which indicates the possible importance of accounting for CUE as a niche dimension for species sorting to act upon in decomposition models. Finally, I found the ^{18}O-H_2O method of measuring CUE in mixed soil communities is particularly susceptible to misleading results when the assumption of extracellular water being the sole source of oxygen to DNA is violated. Overall, my results indicate that understanding microbial physiology is essential to both the accurate measurement and projection of CUE under the global climate crisis, but that explaining the genomic underpinning of this physiological variation remains a challenge.

CONTENTS

LIST OF TABLES

Table **Page**

LIST OF FIGURES

Figure **Page**

INTRODUCTION

Research impetus

Human activities have changed the composition of the atmosphere to an unprecedented degree over the past 150 years, driving the Earth's climate into unknown territory (120). Earth System Models (**Box 1**) predict anything from a 2°C to a 7°C increase in temperature for eastern North America (120), and anything between a 253 Pg increase to a 72 Pg decrease in soil organic carbon storage by 2100 (278). Low confidence in climate projections can be attributed to a combination of uncertainties in the structure, parameterization, and assumed stable state starting values of carbon cycle modules within these models (40; 92; 277). In particular, while the deterministic portion of physical processes can be modeled with sufficient computational power, biology is a tangled mess of many known and unknown interacting components following a series of poorly-understood rules, for which the relative importance of each is only beginning to be uncovered. Because of this complexity, Earth System Models have historically simplified biologically-mediated processes such as photosynthesis and soil respiration to first-order reactions (213; 293).

However, these biological processes are not just driven by fixed pools of enzymes responding in a predictable manner to increased temperature, but rather communities of ecologically divergent organisms that interact both with their abiotic environment and each-other (6; 33; 115; 247; 249). Plant biologists have successfully

incorporated the leaf-level physiological mechanisms by which climate change affects photosynthesis and leaf respiration into Earth System Models (248), but the integration of analogous soil parameters has lagged behind (293). This can be attributed to the fact that although soil carbon stocks are approximately 4x larger than terrestrial vegetation pools, their diminution is driven by the activity of generally inconspicuous and poorly understood microbial communities whose processes cannot simply be "scaled up" (293). As such, parsing clear mechanistic drivers of microbial temperature response has proven challenging. Nonetheless, recent work has shown that changing the structure of soil carbon models to explicitly include these biotic drivers of soil carbon flux offers promise for further improving projections of soil carbon stocks (12; 24; 167; 252; 294).

Soil microbial communities respond to climate change by shifting their taxonomic and/or functional composition (61; 224; 227; 222), and/or by changing their physiology (41; 91; 106; 108; 285). Changes in functional and taxonomic composition represent one way in which physiological responses play out, and can be readily detected by sequencing the total soil community (61; 227), making the abundant publicly-available meta-omic datasets a potential goldmine for clues to a better understanding of microbially-mediated processes. However, large redundancies in the functions completed by soil organisms, and commonalities in many of the pathways used by cells to process carbon (247), mean linking this data to ecosystem processes such as soil respiration response to warming remains challenging. Furthermore, the great diversity of genes and organisms present in soil also means that, even if we could generate perfect correlations between nucleic acid and carbon cycling data, incorpo-

rating the entire genetic repertoire of the microbial community into carbon models is not a realistic goal. Instead, genetic signatures of changes soil carbon processing must be identified. Identification of the parameters of microbial physiology with the greatest influence on soil carbon stocks, and determination of readily-measured correlates of these traits, therefore offers promise for improving global biogeochemical models (279).

One parameter that projected soil carbon stocks have been demonstrated to be sensitive to is carbon use efficiency (CUE - **Box 1**) (12; 294), which describes the fraction of carbon which is assimilated by a microbe. Although models including microbial physiology have the potential to predict soil carbon stocks better than those which "black-box" microbes (294), the current implementation of CUE as a rigid, biologically-insensitive parameter can lead to poor soil carbon estimates (24; 105). As such, there has been a recent rush to measure CUE and attempts to parse out its drivers in soil (70; 71; 91; 95; 106; 257; 262; 263; 304). Nonetheless, a number of technical and intellectual barriers have limited how useful these measurements can be to understanding the fate of soil carbon in a warmer world (12; 96; 95).

In this dissertation, I evaluate the environmental, genomic, and phylogenetic drivers of carbon use efficiency (CUE), and assess how incorporating these drivers of CUE affect both its measurement and the sensitivity of soil carbon stock projections to climate change. To this end, I addressed four questions:

1. Do bacteria differ in their environmental sensitivity of CUE?

2. Is there a set of genes or genomic traits which consistently correlates with temperature sensitivity of CUE?

3. How does incorporating variability in microbial physiology into models of the carbon cycle affect projections of soil carbon stocks under climate change?

4. How does ignoring the underlying biology of organisms distort measurements of CUE made on soil samples?

Box 1: Acronyms and vocabulary
CUE - Carbon Use Efficiency (CUE) - the fraction of carbon taken up by an organism that ends up in biomass rather than being respired
ESM - Earth System Models - climate models that incorporate interactions between physical, chemical, and biological processes
Growth yield - the fraction of a substrate taken up that is incorporated into biomass; differs from CUE for carbonaceous compounds in that it also accounts for losses due to incomplete oxidation (for example acetate in addition to CO_2)
Km - half-saturation constant - parameter in the Michaelis-Menten equation; the concentration of substrate at which enzyme activity is half its maximum value (V_{max}).
Phylogenetically-conserved traits - organism characteristics that are more likely to exist or be in a state more similar in organisms that share an ancestral lineage than for organisms selected at random from the phylogenetic tree.
Redox potential - a measure of the tendency of one compound to take electrons from another
Spin-up - the stage of a model in which it is run until a steady state value is achieved, at which point disturbances such as warming treatment are added and the response is examined. "Results" from the spin-up stage are discarded, but the parameter values are carried forward for the evaluation stage
V_{max} - rate of a reaction under substrate-saturated conditions

Drivers of CUE

Chemoorganoheterotrophs face tradeoffs in resource allocation to biomass and energy production with every molecule of organic carbon they consume (218). Acquiring carbon from the environment may require the production of extracellular enzymes and membrane transporters, the former of which requires energy (ATP) to build and the latter for which ATP may be needed to run. Growth also requires the investment of energy and reducing power. For instance, the generation and poly-

merization of biosynthetic precursors into cell components also requires energy in the form of ATP (269), such that degradation of carbon storage compounds like polyhydroxyalkanoates releases energy for the cell. Furthermore, microbes must expend reducing power stored in NADH in order to convert many food sources into biomass (237). The reducing power and energy required to sustain the uptake and metabolism of substrates comes from the oxidation of other substrate, such that carbon taken up by a cell can only be incorporated into biomass once all its other basic bioenergetic maintenance needs have been met (i.e. cell growth and therefore positive CUE can only occur with that carbon available beyond what must be used to keep the cell alive) (218). As such, the CUE of an organism is expected to be subject to a range of intrinsic and extrinsic determinants of microbial maintenance costs and cell construction needs. Despite numerous studies into what these determinants are, inconsistent methodologies have historically prevented determination of which intrinsic and extrinsic factors best predict CUE (96; 181; 255).

Extrinsic drivers

Extrinsic determinants of CUE - or those which act in a manner generally independent of organism identity - include factors such as carbon quality, nitrogen availability, oxygen, temperature, competition, and pH. The effect of these parameters on CUE can be studied at the community level and can be attributed to influences on maintenance costs, imbalance between the supply and demand for resources, and differences in the theoretical energy yield of different substrates (181).

Substrate quality

A key determinant of CUE is how amenable a given substrate is to being incorporated into biomass. Polymeric substrates such as lignin and cellulose must be depolymerized before they can be taken up by the cell, which means that a cell must reallocate resources from growth to enzyme production (8). After this depolymerization step, the resultant monomers and dimers must be taken up by the cell. While some molecules such as glycerol and ethanol are able to freely diffuse across the membrane, others must enter the cell through transport proteins, either passively or through proton exchange (4). Therefore, some carbon sources require a greater resource investment than others to acquire. After entering the cell, compounds enter metabolism at different stages and are, therefore, differentially allocated to biomass (anabolism/assimilation) or energy production (catabolism). As such, community-level CUE in soil showed a positive correlation with the cellulase:phenol oxidase enzyme potential as a proxy for carbon quality (272). Highly oxidized compounds such as oxalic acid require expending considerable reducing power (NADH) if they are to be incorporated into biomass (240), and also only yield small amounts of energy compared to glucose. As such, the CUE of soil microbial communities on oxalic acid or phenolic compounds is substantially lower than that on glucose (91; 270). Other features, including whether they inhibit other metabolic pathways (135), where compounds enter central metabolism, which components of the cell they are converted into (104), and how rapidly those components are recycled are also likely to be important for CUE (100). Finally, it is feasible that the effect of carbon quality on

CUE will depend on the historic nourishment regime of the bacteria; bacteria previously exposed to carbon-limited conditions are able to metabolize a much broader range of substrates than those subject to carbon replete ones (119). Cometabolism can, in the case of using a non-assimilable energy source and a low-energy carbon source, increase the degree to which carbon is conserved (100). Nonetheless, CUE is generally expected to increase with the degree of reduction of a compound.

Temperature

Increased temperature is often observed to reduce CUE (91; 181). The mechanism for this has not been confirmed yet, but one hypothesis is that microbial maintenance costs increase with temperature due to increased protein turnover (181), need for saturation of lipids in the cell membrane (108), or a heat stress response (181). Another possible cause is the dependence of the number of energy conserving sites in the electron transport chain on temperature (110). Alternatively, CUE may increase in soil if elevated temperatures favour the desorption of chemically-labile, high C:N compounds from mineral surfaces (55). Other researchers have reported that temperature does not affect intrinsic CUE (71), and that the apparent decrease in CUE with warming may indeed be due to methodological artifacts or increased microbial turnover (106). In particular, Djikstra *et al.* (2011) found that while the primarily-anabolic pentose phosphate pathway was halved by elevated temperature, CUE showed a small *increase* at higher temperatures. More recent community-level work shows that microbes are able to adapt to local temperature. In this process,

growth increases moreso than respiration, such that CUE should also increase with temperature (28). This may be underlain by decreases in substrate affinity even with small increases in temperature, effectively starving microbes (201). Therefore, the effect of CUE to elevated temperatures appears contingent on microbial physiology, substrate choice, and method used to measure the response.

Nitrogen availability (substrate C:N ratio)

An apparently undisputed driver of CUE for both isolates and soil communities is the C:N ratio of the substrate. Biomolecules have fixed ranges of carbon and nitrogen, and cells require a certain fraction of these biomolecules to exist. Only rarely are elements in the substrate a microbe consumes present in exactly the same ratio it needs to maintain and build new biomass, so nitrogen or carbon will be preferentially mineralized to regain the desired elemental ratio (193). As such, substrates with high C:N ratios or nitrogen limiting conditions are expected to be associated with low CUE (129; 181).

Oxygen availability

As the strongest biological oxidizer and the best terminal electron acceptor, the presence of oxygen can play a central role in CUE. Due to its high redox potential, oxygen is able to capture electrons that have traveled further along the electron transport chain and, therefore, generated a greater electrochemical gradient than other terminal electron acceptors (84). Under conditions of low oxygen, organisms must

either ferment molecules (use internal electron acceptors), or use terminal electron acceptors such as nitrate with lower redox potential. Therefore, the amount of energy they can get from a given substrate is reduced when organisms cannot use oxygen. In addition to its effect on direct oxygen-dependent steps of metabolism, anaerobic conditions have been shown to decrease the fraction of carbon going through the anabolic pentose phosphate pathway, and to increase the fraction going through glycolysis (70; 71). It is important to note that, although low oxygen conditions are expected to reduce biomass yield, reduced CUE will not necessarily be detected because CO_2 is the only waste product typically measured. Furthermore, while energy yield from a substrate may be greater under aerobic conditions, the cost of biosynthesis and for cell maintenance (ex. due to oxidative damages) are lower under anaerobic conditions (114). Therefore, a general effect of oxygen availability on CUE is challenging to predict *a priori*.

Competition and connectivity

An additional environmental determinant of CUE is that of competition. Bacteria differ in their competitive strategies (see "oligotophs and copiotrophs", below), or how they behave in the presence of abundant substrate. Like a pig at a slop bucket, a bacterium may either opt to eat as much as possible, in which case it will do so messily and produce a lot of waste, or do so more slowly and possibly put on less weight, but with less waste. This decision to eat cleanly (be efficient) can be influenced by the environment an organism finds itself in, such that *Lactococcus lactis* growing with a limited amount of glucose in an environment free from competition

evolved slower but more efficient growth compared to its ancestor which grew in a free-for-all environment (19). Another way to look at this is that where resources are privatizable, there will be incentives to use that resource most efficiently. Low soil moisture essentially provides this privatization of resources for bacteria, since they cannot traverse the air-filled pores present in all but the most saturated soils (286). Therefore, moderate reductions in soil moisture are expected to increase CUE by promoting the privatization of resources (233). Indeed, CUE was observed to be greatest at very low moisture in a xeric ecosystem (111). However, traits associated with movement through the soil matrix may only be costly for CUE under high moisture, when motility is both most beneficial and expressed (62).

An additional feature of competition relevant to CUE is that of cheating strategy. As noted above, the production of enzymes requires considerable resource investment, so releasing them into the environment where they and their substrates may be pirated by other cells is a risky business. As such, some bacteria may "cheat" and not produce extracellular enzymes, instead depending on the monomers produced by other organisms' enzymes. Such cheating is temporarily favoured when privatization of resources is not possible, but eventually leads to enzyme producers ceasing to produce enzyme when they are less likely to reap the benefits of their investment (ex. in a well-mixed environment) (7; 10). In soil, lower soil moisture limits enzyme diffusion and is therefore expected to favour extracellular enzyme production. However, as a counterargument, interactions between organisms may lead to increased CUE if cross-feeding occurs. As one example, amino acids can be grouped based on precursor demands, where some amino acids are more efficiently produced from glu-

coneogenic substrates and others are more efficiently produced from glycolytic ones (290). Therefore it is conceivable that one organism fermenting glucose and producing amino acids could transfer gluconeogenic substrates such as lactate to another organism, which in turn uses it to produce and then share the remaining amino acids with the original donor.

pH

As both an important driver of bacterial community structure (88), and a potential stressor, pH is expected to influence CUE. In a meta-analysis of global soils, Sinsabaugh *et al.* (2016) found a weak but significant CUE minimum at a pH of 5.4, which they attributed to differences in the bacterial to fungal ratio. pH is also expected to affect the availability of nutrients and toxic metals such as aluminum, which may also indirectly affect CUE through the reallocation of resources to stress response rather than growth. Direct effects of pH on CUE may be conferred by virtue of the need to express novel antiporters or change metabolism to include more organic acids at high pH (25; 207). However, not only do bacteria isolated from the same soil show a range of pH optima, but pH optima are phylogenetically conserved (124). This indicates that the degree of stress response (and, therefore, reduction in CUE) that bacteria show to pH is likely to differ between organisms and be phylogenetically conserved.

"Intrinsic" determinants and markers of CUE

So-called "intrinsic" determinants of CUE are those features which are encoded in the genetic or epigenetic imprint of a cell. Although the manifestation of many of these intrinsic determinants is expected to be affected by the extrinsic factors noted above (290), the identification of genetic determinants of CUE would offer promise for interpreting carbon cycling data in light of environmental meta-omic data. Many of these factors have been examined in the context of growth yield in model organisms such as *Escherichia coli*, which is similar but not identical to CUE (**Box 1**).

Trophic strategy: "oligotrophs" vs. "copiotrophs"

There is a long-held assumption that some microbes are inherently more efficient than others. Central to this is the observation that, while some organisms maintain slow but steady growth independent of resource availability ("oligotrophs"), others undergo boom-bust growth cycles (297; 138). These "copiotrophs" rapidly reproduce in times of plenty, but die back when resources are more limited. Many other organisms lie somewhere between these two extremes of trophic strategy (185). Fierer (2007) suggested that soil oligotrophs may also be efficient growers, thereby linking trophic strategy with CUE. Soil oligotrophs are thought to be characterized by a combination of genomic and physiological traits, including the capacity for high-affinity uptake and co-metabolism of multiple substrates at low concentrations, low ribosomal RNA operon copy number, and high growth yield. More recently, Roller and Schmidt (237) proposed that oligotrophs are likely to show inherently high growth

efficiencies because of their dominance under conditions generally associated with efficient growth. Indeed, in another paper, Roller *et al.* (238) demonstrated that CUE on succinate is negatively correlated with both maximum growth rate and ribosomal RNA operon copy number for eight terrestrial and aquatic bacteria.

Assuming the proposed connection between CUE and trophic strategy holds, genes indicative of trophic strategy could be used to infer efficiency. For instance, Lauro *et al.* (154) found that aquatic oligotroph genomes were enriched in genes for lipid metabolism, while genes for motility, transcriptional machinery, and chitinase activity were enriched in the genomes of copiotrophs. In a similar vein, a much greater fraction of protein coding genes are transcriptionally controlled in marine copiotrophs compared to oligotrophs (57). Studies with the opportunistic aquatic oligotroph *E. coli* have also shown that there is less catabolite repression under carbon limitation, so the bacterium can utilize a broader range of carbon sources (119). This is similar to what is expected for obligate oligotrophs, and shows that one way in which microbes may adapt to low resource conditions is through the production of diverse, high-affinity and non-specific transporters (138). However, since terrestrial bacteria are fundamentally different from aquatic bacteria (298), the genes and genomic features determining CUE may also be distinct between terrestrial and aquatic organisms. That said, if organisms characterized by "oligotrophic" traits are not more efficient than "copiotrophic" ones, then any proposed relationships between genome content and efficiency are no longer expected to hold.

I propose six gene classes and genome features, which may serve as indicators of trophic strategy and, therefore, be correlated with CUE_{max}. First, copiotrophs may

activate motility genes to actively seek out food in moist soil (117; 165; 244), whereas oligotrophs are not expected to do so. Second, given the prevalence of reductive cell division in copiotrophs under low carbon conditions, and rapid cell membrane growth under high carbon conditions (165), copiotrophs are expected to have higher transcriptional activity and abundance of genes for the generation and processing of cell wall components. Third, oligotrophs are also expected to have larger plasmids than copiotrophs; these plasmids may interact with chromosomally encoded genes, as hypothesised for the oligotroph *Ancylobacter vacuolatus*, which showed fast growth rates that were sensitive to carbon concentration following plasmid removal (306). Fourth, given the generally low abundance of individual substrates in the environment most of the time, oligotrophs are expected to have a more diverse suite of genes for the transport and metabolism of compounds. Fifth, because of the general lack of response to changing nutrient conditions (139), oligotrophs are expected to have more constitutively-expressed proteins than copiotrophs, which actively sense and respond to the environment in order to best allocate resources. That is, simple, unregulated metabolisms of oligotrophs have low maintenance costs compared to the strategy of actively sensing and responding to the environment that copiotrophs use (112). Finally, organisms capable of growth under low carbon conditions are expected to use ions such as sodium in place of the more membrane-permeable H+; this should be seen as an increase in the ratio of sodium:H+ symporters with maximum CUE (114). Roller *et al.* (2016) also highlight chemotaxis, thiamine biosynthesis, and phosphoenolpyruvate:carbohydrate phosphotransferase systems as being more abundant in fast-growing, inefficient copiotrophic organisms.

While many of these adaptations to oligotrophy may enable cells to avoid physiologically expensive stress responses (38), the "average" cost of maintaining diverse transporters may exceed the pulsed costs of stress response. Therefore, it is feasible that oligotrophs are, on average, less efficient than copiotrophs under the luxurious lab conditions generally considered amenable for growth, but more efficient under rapidly changing or low quality environments.

High and low yield central metabolism

Central to the "oligotroph-copiotroph" dichotomy is the assumption that organisms face a fundamental growth rate-efficiency tradeoff, in which high growth rates are associated with wasteful metabolism and low biomass yields (170). Numerous mechanisms for this tradeoff have been proposed, including that reactions do not proceed if the energy of the reactants is equal to the energy of the products (215); the high energetic costs of protein production (192); imbalance between anabolism and catabolism (282); and protection from oxidative stress (171). On the other hand, efficiency may be *higher* at high growth rates if maintenance energy is a fixed quantity, because any additional carbon taken up beyond that required for maintenance will be directed to growth. As a result of these apparently conflicting results, Lipson (2015) predicted that yield should show a hump-shaped relationship with growth rate that is underlain by three growth strategies (170). Under conditions of nutrient limitation, starvation, and other physiological stress, microbes take on a stress-tolerance strategy in which they have very low growth rates and low yields,

instead allocating resources to storage of materials to help them survive the stress. In very resource-rich conditions or under "hot but not too hot" temperatures, microbes are expected to take on a race-to-the-bottom growth strategy, and grow fast but inefficiently. However, under conditions of energy limitation, at the low end of the organism's temperature range, and in spatially structured environments, microbes are expected to show intermediate growth rates with high yield; that is, yield is maximized at intermediate growth rates.

These switches between high and low yield growth have been studied using metabolic models of central metabolism. For instance, while many organisms have both the Embden-Meyerhoff-Parnas (EMP) and the Entner-Doudoroff (ED) glycolytic pathways, many have just one or the other. The EMP pathway yields a much more controlled release of energy, such that two ATP result from glycolysis, but this steady release of energy requires a substantially greater enzyme investment in order to keep the same flux as the lower-yielding, but faster, ED pathway (90). Anaerobes, which have weak oxidative phosphorylation compared to aerobes, are enriched in the nitrogen-expensive but higher-energy-yielding EMP pathway, whereas aerobes are relatively enriched in the ED. It has been proposed that since central metabolism may account for up to half of an organism's proteome, it is feasible that organisms may not have sufficient room in their cells to support the large quantities of proteins required to maintain fast but efficient flux via the EMP pathway (282). However, whether similarly strong tradeoffs between growth rate and efficiency occur in "oligotrophic" bacteria characterized by low maximum growth rates is unclear. I posit that organisms whose genomes encode more complex (more nodes, higher net-

work connectivity) central metabolism will have lower CUE_{max} due to the costs of regulating and running these alternative pathways (245), but less environmentally-responsive CUE because of the wider range of ways in which metabolism can be optimized.

Phylogenetic determinants of carbon use efficiency

Some authors have argued for the existence of differences in CUE at high taxonomic levels. For instance, communities dominated by fungi have been suggested to be more efficient than those dominated by bacteria (257; 275), presumably because the CN ratio of their biomass is higher. However, fungus-dominated communities may instead just be able to access different carbon pools to bacteria (3; 261) and/or be present in soils characterized by edaphic parameters more amenable to higher CUE (257; 275; 261). Alternatively, CUE may respond to different abiotic factors in bacteria than in fungi (129). If groups of organisms *do* differ in maximum attainable CUE, this may be due to genetically encoded physiological constraints, such as the need for carbon allocation to abundant peptidoglycan in Gram positive organisms, transporters spanning both membranes in Gram negative bacteria, or abundant intracellular membranes in Verrucomicrobia (158). However, despite these considerable differences in cell chemistry and biosynthetic precursor requirements, metabolic modeling predicts that CUE on glucose is insensitive to Gram positive: Gram negative: fungal ratio (71). This contrasts with the expectations of Gommers (1988) that fungi should have higher CUE than bacteria on glucose, but lower on acetate

because of differences in metabolic precursor demands on biosynthesis. As such, the influence of phylogeny on CUE may be in its coherent response to environmental variables, such as temperature, drought or nitrogen availability (15; 71; 195).

Another key correlate of CUE may be ribosomal RNA operon copy number (rrN). rrN sets the upper limit to growth rate in bacteria (136), such that up to 75% of transcriptional effort may be allocated to generating ribosomes under rapid growth (52). rrN is strongly phylogenetically conserved, such that it can be predicted in unsequenced genomes based on the values of close relatives (130). "Oligotrophic" phyla such as Acidobacteria are capable of slow growth in nutrient-poor environments and typically have low rrN, while fast-growing copiotrophic groups such as Betaproteobacteria and Bacteroidetes have high rrN (86). Whether rrN itself is a determinant of CUE, or merely a stand-in for other conserved drivers of CUE is unclear, however.

Interplay between biotic and abiotic drivers of CUE

The numerous aforementioned biotic and abiotic factors may influence CUE both alone and in interaction with other factors. For instance, taxa grown on the same mixed substrate media may differ in their CUE as a virtue of preferring uptake of organic acids over sugars (67). Interspecific competition may also interact with nitrogen availability to impact CUE (186). Specifically, fungal monocultures grown under nitrogen-replete conditions showed lower CUE at higher temperatures, but those grown under nitrogen limited conditions did not. When two fungi were co-

cultured, CUE was always lower than expected based on values when species were grown alone, and the negative effect of temperature on CUE was apparent for isolates grown under both high and low N conditions. Due to differences in the stringent response machinery and degree of stress required to induce its activation (39), it is also expected that the CUE of oligotrophs and copiotrophs should respond differently to stressors. As a further example, due to differences in metabolic precursors required for biomass synthesis in, say, bacteria and fungi, growth may be more efficient for bacteria than fungi on some substrates, and more efficient for fungi than bacteria on others (100; 269). Quorum sensing provides a final example of how biotic and abiotic factors can interact to affect CUE; late in exponential phase, quorum sensing has been observed to lead to reduced expression of many genes involved in the uptake and metabolism of glucose (101).

I explore a number of these hypotheses in Chapter 1 of this dissertation.

Modeling the carbon cycle

In light of the aforementioned factors, it seems apparent that CUE is not a fixed factor and so should not be modeled as such. Indeed, how or why CUE is high or low under a given scenario (8; 105), or in one kind of community or another (258; 296), is essential for predicting the stability of soil carbon. For instance, if CUE is low because maintenance costs are high, then microbial biomass may decline and SOC increase (105). On the other hand, if CUE is low because enzyme production is high, then SOC pools will shrink (105). However, when additional feedbacks such as species sorting are incorporated, high enzyme production may induce increased

carbon storage (8). Together, these prior modeling results indicate that accounting for both the metabolic costs of living in and processing substrates in the environment, and in variability in these costs, are likely to be important for the fate of soil organic matter in a warmer world.

I explore this hypothesis in Chapter 2 of this dissertation.

Measuring CUE in opaque environments

In my third chapter, I complete a sensitivity analysis to see how robust soil CUE measurements are. Whereas CUE can be readily measured in liquid culture, where the microbial biomass can be separated from the growth medium, it is much more challenging to measure in soil. This is not only because a fraction of the biomass may be active at any given time (30; 210), but also because this small community is stuck within a matrix of minerals with large background carbon. Therefore, methods must be able to distinguish between new growth and old biomass, when microbial biomass typically accounts for 1% of the carbon in soil.

Since CUE is in units of carbon, perhaps the most intuitive way to measure it is using isotopically labeled carbon compounds. In this method, ^{13}- or ^{14}C labeled glucose (or less frequently cellulose (205), phenol (91; 270), or amino acids (91; 127)) are added to the soil. After a period, a sample of CO_2 is taken and evaluated for the amount of isotopically labeled carbon. The amount of label within microbial cells is also determined. This is completed using chloroform fumigation extraction, in which cells are lysed by chloroform vapour and the difference in labeled organic

carbon in lysed and unlysed samples is used as a metric of the amount of substrate carbon assimilated into biomass. In a variant of this method, position-specific isotopes of glucose and pyruvate are used in parallel incubations (71). CUE can then be determined by combining labeled respiration and microbial biomass carbon measurements with a series of assumptions about which carbons are broken off and enter which assimilatory or dissimilatory pathways.

However, one main drawback of the isotopically-labeled substrate method is that it is compound-specific. That is, you measure the CUE of the subset of the community able to use that substrate. Furthermore, it is impossible to separate substrate uptake from assimilation into biomass pools, as chloroform fumigation extraction effectively measures cytoplasmic content. Therefore, labeled carbon compounds are liable to overestimate true CUE (95; 105). As a result, methods depending on ^{18}O-H_2O (95; 262; 263; 304) or ^{13}C (179) incorporation into DNA are increasingly being used for CUE measurements.

In the ^{18}O-H_2O method of CUE determination, labeled water added to the soil is taken up by microbes and incorporated into DNA. The labeled oxygen in the DNA is then quantified using isotope ratio mass spectrometry (IRMS), and this oxygen is assumed to be directly proportionate to the amount of new DNA synthesized. The relationship between the total microbial biomass carbon at the initiation of the experiment, and total DNA extracted at the end, is then used to convert the new DNA produced to new microbial biomass carbon produced. CO_2 produced during the incubation is also measured, so CUE can be calculated. All microbes need water to live, so it is assumed that this method provides an unbiased estimate of growth.

Furthermore, since the label is specifically measured in a biomass component, and DNA replication does not occur without growth, it should provide a true measure of assimilation rather than uptake. However, the additional assumptions introduced by this method - in particular with the conversion between new DNA and microbial biomass carbon - leave it susceptible to errors. I uncover and evaluate the effect of some of these in a sensitivity analysis of the method in chapter 3.

CHAPTER 1

CARBON USE EFFICIENCY AND ITS TEMPERATURE SENSITIVITY CO-VARY IN SOIL BACTERIA

1.1 Abstract

The strategy that microbial decomposers take with respect to using substrate for growth versus maintenance is one essential biological determinant of the propensity of carbon to remain in soil. In order to quantify the environmental sensitivity of this key physiological tradeoff, we characterized the carbon use efficiency (CUE) of 23 soil bacterial isolates across seven phyla under three temperatures and up to four substrates. We identified genes associated with the temperature sensitivity of CUE in glucose media, and subsequently validated those candidate markers we had not *a priori* hypothesized to exist using 1) a subset of isolates grown on other media types, and 2) mixed bacterial communities grown on cellobiose in an artificial soil matrix. Temperature altered CUE in both an isolate- and substrate-specific manner. Our exploratory approach did not yield any genomic indicators of CUE which were consistent across datasets, and we found a positive correlation between ribosomal RNA operon copy number and CUE, opposite what was expected. We also found that inefficient taxa increased their CUE with temperature, while those with high CUE showed a decrease in CUE with temperature. Together, our results indicate

that CUE is a flexible parameter within bacterial taxa, and that its temperature sensitivity is better explained by observed physiology than genomic composition across diverse taxa. We conclude that CUE response to temperature and substrate is more variable than has been previously considered.

1.2 Introduction

Optimum allocation of resources to growth versus maintenance is central to the success of microorganisms. This "carbon use efficiency" (CUE) is the outcome of a complex interplay between biotic and abiotic factors which shape whether organisms are able to thrive or just survive in their environment. In turn, how CUE responds to a changing world is expected to have far-reaching implications for the ability of global soils to maintain vital ecosystem services such as carbon retention.

Of particular pertinence is projecting how elevated temperatures are affecting microbial physiology under climate change. In ecosystem and Earth System models, CUE is typically parameterized to be either unaffected by warming or show a homogeneous community-level decrease (8; 288; 295). In practice, however, community-level CUE increases (205; 304), decreases (91; 304), or remains unaffected by temperature (72; 91; 106; 304), with no clear explanation as to why these temperature responses differ (300) or why different responses of CUE to longer-term warming may emerge (91; 284). Organism-level CUE decreases when respiration increases more than growth with temperature; this pattern can be caused by increased protein turnover (181), changes in membrane fluidity (108), or the loss of energy-conserving

sites in the electron transport chain (110). On the other hand, CUE is expected to increase with temperature if maintenance costs are independent of growth rate, and growth rate increases with temperature (219). Effects of longer-term changes in temperature may additionally play out indirectly through chronic warming induced changes in the environment.

Chronic warming can impact the quantity and quality of substrates available through their differential production and consumption (91; 225). For example, warming increased microbial activity in the rhizosphere (301) by increasing the quantity of carbon released by roots into the soil (301), but also made those exudates richer in phenolic compounds (229). In other instances, however, warming may reduce the amount of biomass that plants allocate belowground (305), or plant inputs may just not keep pace with increased microbial demand at higher temperatures (188). In this case, labile compounds can be preferentially lost from soil, such that the remaining available substrates show signatures of a later state of decay (225). All said, these indirect effects of temperature on CUE via changes in substrate quality may be as — if not more — important than its direct effects (91; 204). This is in part because intrinsic differences in the oxidation states of substrates set an upper limit on how efficiently they are anabolized (100); energy must be invested to bring the oxidation state of carbon in organic acids to that of the cell, but not for more highly reduced lipids. Substrates also differ in their extracellular processing and uptake costs, which impacts the maximum potential yield of a substrate pool (7; 8; 91). Furthermore, alternative metabolic pathways for processing the same substrate mean that microbes may differ in how much of the energy they can capture (90). Finally, bacteria may

switch between metabolic pathways depending on temperature (175) or substrate availability (60; 121), opening the possibility of gene-by-substrate interactions in how CUE responds to temperature.

In addition to differences in efficiency due to substrate quality, bacteria may differ in their maximum possible efficiency. As such, community-level differences in CUE temperature response may be driven by shifts in who is active in addition to the direct physiological effects of warming on a fixed community. It has long been assumed that a tradeoff exists between how fast an organism can grow and growth efficiency for a given amount of substrate — the so-called growth rate-yield tradeoff (170). Bacteria with more ribosomal RNA operons are able to sustain a higher maximum growth rate (267), but also appear to grow less efficiently than those with fewer copies (238). This is proposed to be a consequence of the high energetic costs of building and running translational machinery (66), suggesting that oligotrophic bacteria are more efficient than copiotrophs. Bacteria capable of producing large amounts of extracellular enzymes or membrane-bound transporters may also be less efficient than those with more limited production capacity because substantial energy investment is required to polymerize amino acids under aerobic conditions (165; 260). The ability to produce copious and diverse extracellular enzymes may also be indicative of reduced temperature sensitivity of these taxa, however, as bacteria with diverse metabolic potentials may be better able to tune which pathways or enzymes they use in order to maintain efficiency even as the environment around them changes (189; 285). As such, genomic traits such as ribosomal RNA operon copy number or extracellular enzyme gene density may serve as "genomic markers" of bacterial

CUE and its temperature sensitivity. However, empirical support is equivocal for both the growth rate-yield (151; 170; 198; 267; 238) and enzyme cost (180; 260) hypotheses, and a number of questions regarding the genomic basis of efficiency remain. Specifically, are there genomic markers of CUE which are consistent across phylogenetically diverse soil bacteria? And can the genomic repertoire of soil bacteria be used to infer temperature responsiveness of CUE?

We sought to first quantify how soil bacterial CUE varies in its response to shifts in temperature and substrate, and second to determine whether these shifts can be predicted based on genome composition. Because it is a complex metabolic trait, we posited that CUE and its temperature sensitivity would be highly variable across taxa, but be more similar in closely-related bacteria (184). Furthermore, we posited that CUE would be negatively correlated with ribosomal RNA operon copy number (rrN) (238) and extracellular enzyme costs (8), and would decrease more in response to temperature in organisms with simpler metabolisms. To test these hypotheses, we measured the CUE of 23 soil bacteria representing seven phyla and a 50-fold difference in maximum growth rate on four media types. We then explored correlations between CUE and gene abundances using a comparative genomics approach both to test *a priori* hypotheses, and to discover potential markers of CUE using an explore and validate method.

1.3 Results

1.3.1 Variability in CUE

The bacterial isolates used in this study were primarily derived from temperate forest soil (**Table 1.1**), and were chosen to be representative of the diversity found in the soils they were derived from (61). Carbon use efficiency was determined using optical density measurements of exponentially-growing cultures to quantify growth, and infrared gas analysis measurements of carbon dioxide production rates. Assay conditions included growth at 15, 20, and 25°C, and on glucose, pyruvate, succinate, and potato dextrose broth (PDB) media.

Carbon use efficiency varied from 26 to 81% across conditions (Fig. 1.1). This variation in CUE was underlain by substantial variation in both respiration and growth rates among taxa, which did not always correlate with one-another (Fig. B.1). Using a Hartigan's dip test (177), we did not find evidence that CUE took on a multimodal distribution under any of the assay conditions, except for PDB at 15°C (Fig. B.2). CUE showed a weak positive correlation with growth rate during CUE measurements on glucose (repeated measures correlation r = 0.26, P <0.001, 270 df), PDB (r = 0.22, P = 0.02, 120 df), pyruvate (r = 0.24, P <0.01, 114 df), and succinate (r = 0.25, P <0.05, 92 df) media. CUE was more strongly negatively correlated with mass-specific respiration rate, with correlation coefficients between -0.41 (PDB; $P < 0.001$, df = 119) and -0.58 (glucose; $P < 0.001$; df = 206) across the substrates tested. Thus variation in CUE between taxa was more strongly correlated with variation in respiration between taxa than variation in growth rate was.

Table 1.1: Isolates used in CUE measurements. Taxonomy is based on 16S sequence assignment using IDTAXA (197). The explore/validate column denotes whether the organism was selected to identify candidate genomic markers in an exploratory approach, or only appeared as part of the dataset used to determine if those markers were predictive. "NA" indicates isolate did not grow on glucose media so was not used for identifying genomic markers. "+" indicates isolate from Harvard Forest; "=" indicates genome was sequenced using PacBio for this project. Genome completeness and contamination were predicted using CheckM (212)

Isolate	IDTAXA (GTDB) Taxonomy	IMG taxon ID	completeness (contamination)	Explore or Validate	Reference
AN5 +	Bacteria; Proteobacteria; Alphaproteobacteria; Rhizobiales; Rhizobiaceae; Agrobacterium	2617270923	99.98 (1.177)	explore	this study
AN6A +	Bacteria; Proteobacteria; Alphaproteobacteria; Rhizobiales; Rhizobiaceae; Agrobacterium	2619618868	99.96(0.141)	explore	this study
GAS188 +	Bacteria; Proteobacteria; Alphaproteobacteria; Rhizobiales; Beijerinckiaceae; EF018539	2693429787	97.806 (2.194)	explore	(226)
GAS232 +	Bacteria; Acidobacteriota; Acidobacteriae;Acidobacteriales; Acidobacteriaceae; Terriglobus	2690315654	100 (3.586)	explore	this study
EB95 +	Bacteria; Acidobacteria; Acidobacteriia; Acidobacteriales; Acidobacteriaceae; unclassified Acidobacteriaceae	2747843220	99.238 (1.724)	explore	this study
MT12 +	Bacteria; Proteobacteria; Alphaproteobacteria; Rhizobiales; Xanthobacteraceae; Bradyrhizobium	2690316366	99.871 (2.506)	explore	this study
MT45 +	Bacteria; Actinobacteriota; Actinobacteria; Corynebacteriales; Jatrophihabitantaceae; MT45	2690315646	95.755 (1.402)	explore	this study
GAS332 +	Bacteria; Proteobacteria; Gammaproteobacteria; Betaproteobacteriales; Burkholderiaceae; Paraburkholderia	2695420918	99.95 (1.02)	explore	this study
GAS474 +	Bacteria; Verrucomicrobiota; Verrucomicrobiae; Methylacidiphilales; GAS474; GAS474	2690315640	99.324 (4.392)	explore	(223)
GAS479 +	Bacteria; Firmicutes; Bacilli A; Paenibacillales; Paenibacillaceae; Paenibacillus O	2693429825	99.511 (0.349)	explore	this study
GAS525 +	Bacteria; Proteobacteria; Alphaproteobacteria; Rhizobiales; Xanthobacteraceae; Bradyrhizobium	2740892596	99.984 (1.599)	NA	this study
GP183 +	Bacteria; Firmicutes; Bacilli A; Paenibacillales; Paenibacillaceae; Paenibacillus E	2690316367	97.849 (1.613)	explore	this study
GAS106B +	Bacteria; Proteobacteria; Gammaproteobacteria; Betaproteobacteriales; Burkholderiaceae; Paraburkholderia	2690315676	99.95 (0.827)	validate	this study
24-YEA-27 +	Bacteria; Proteobacteria; Alphaproteobacteria; Rhodobacterales; Rhodobacteraceae; 24-YEA-8	2767802438	94.838 (1.313)	validate	this study
BS19 =+	Bacteria; Proteobacteria; Gammaproteobacteria; Enterobacterales; Enterobacteriaceae; Ewingella	2806310493	99.983 (0.536)	validate	this study
BS40 =+	Bacteria; Actinobacteria; Actinobacteriota;Actinobacteria Actinomycetales; Micrococcaceae; MA-N2	2806310496	99.039 (1.462)	validate	this study
BS60 =+	Bacteria; Proteobacteria; Alphaproteobacteria; Rhizobiales; Rhizobiaceae; P6BS-III	2806310495	100 (0.435)	validate	this study
BS71 =+	Bacteria; Actinobacteriota; Actinobacteria; Actinomycetales; Microbacteriaceae; unclassified Microbacteriaceae	2806310494	98.99 (0.631)	validate	this study
A. alpinus	Bacteria; Actinobacteria; Actinobacteria; Micrococcales; Micrococcaceae; Arthrobacter	2634166197	99.541 (1.95)	validate	(303)
C. pinensis	Bacteria; Bacteroidetes; Sphingobacteriia; Sphingobacteriales; Chitinophagaceae; Chitinophaga	644736340	99.507 (0.739)	validate	(63)
GAS86 +	Bacteria; Proteobacteria; Gammaproteobacteria; Betaproteobacteriales; Burkholderiaceae; Paraburkholderia	2695421038	99.95 (2.108)	validate	this study
GP187 +	Bacteria; Planctomycetes; Planctomycetia; Planctomycetales; Isosphaeraceae; Singulisphaera	2695420965	99,612 (5.814)	validate	this study
N. jensenii	Bacteria; Actinobacteria; Actinobacteria; Propionibacteriales; Nocardioidaceae; Nocardioides	2731957589	98.698 (1.215)	validate	(54)

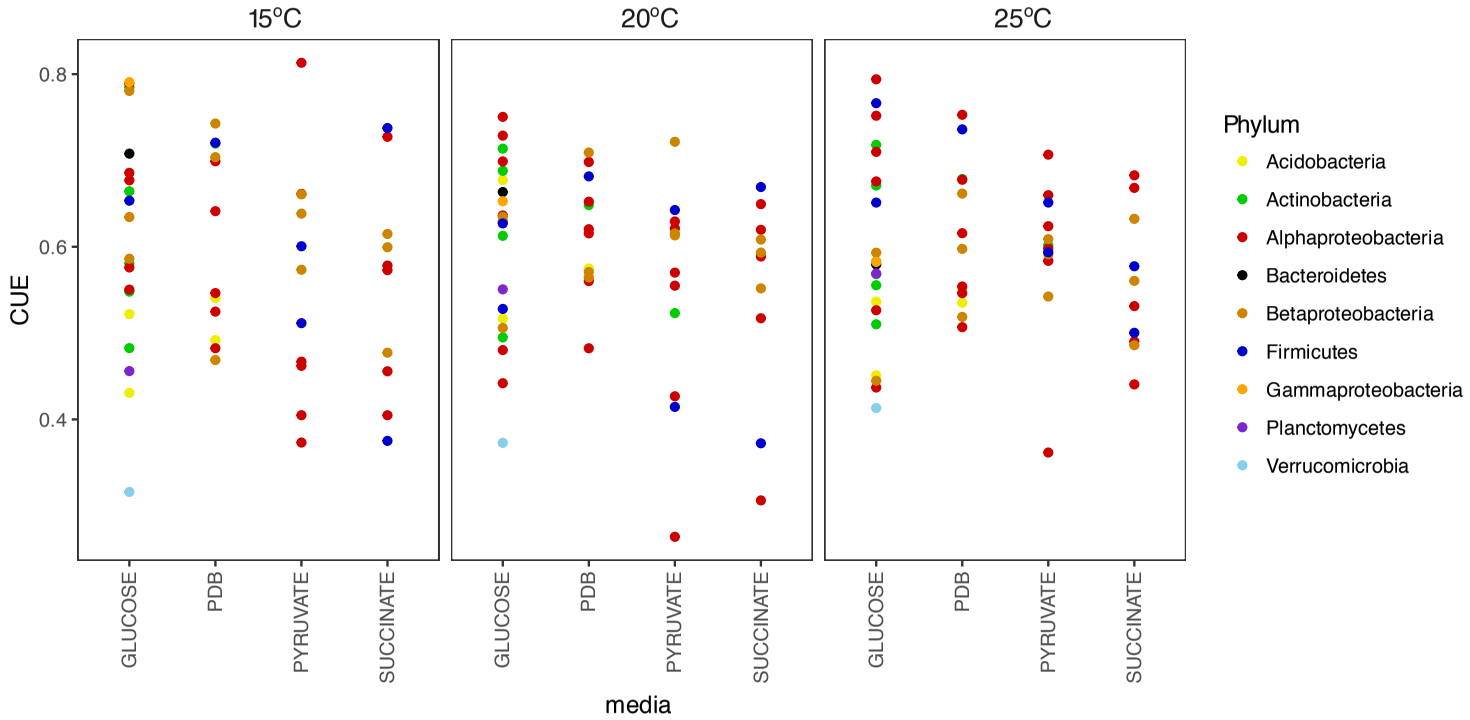

Figure 1.1: CUE of bacterial isolates, coloured by phylum and plotted against temperature and media type. Each point represents the average CUE for a given isolate and growth condition.

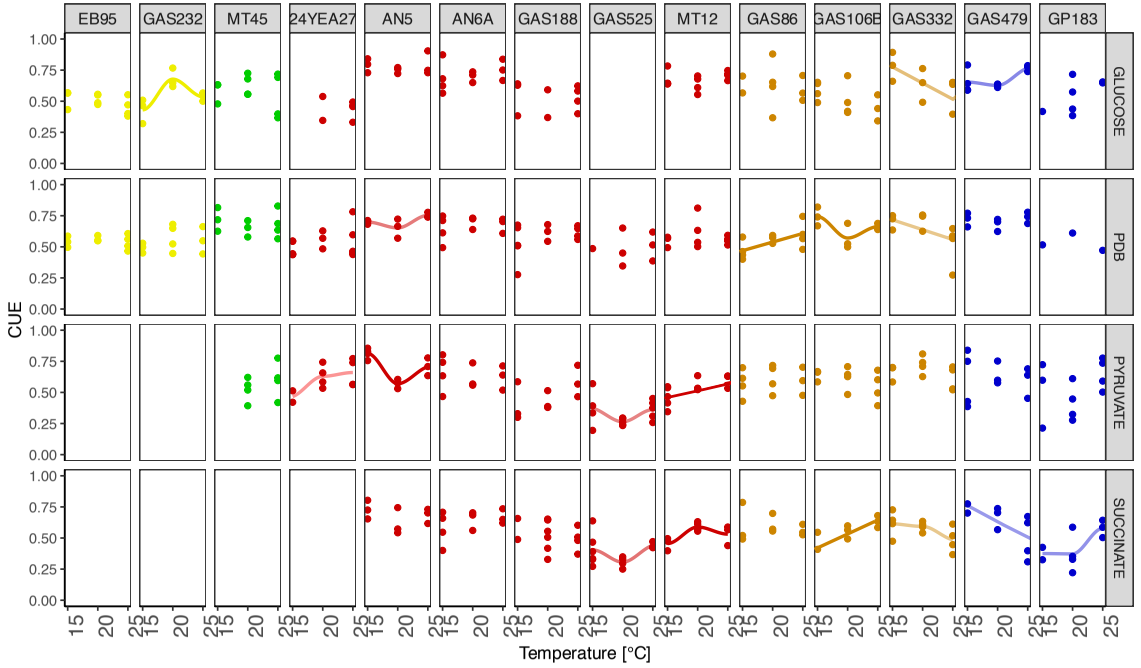

Figure 1.2: Effect of temperature and substrate type on CUE across a range of bacterial isolates. Linear and parabolic curves were fit and compared for each scenario, and curves were assigned if slope parameters were significant. An ANOVA was used to compare between models to determine if the more complex parabolic model fit significantly better than the simpler linear one. Opaque line - $P < 0.05$; translucent line: $P < 0.1$. Lines represent the trend without denoting the exact equation of the best-fit line.

1.3.2 Effect of substrate quality on CUE and its temperature sensitivity

CUE did not increase significantly with the energy content of the substrate (heat of combustion standardized to carbon content; Fig. B.3), likely because isolates differed in their ability to grow on the different substrates (Fig. B.1). The effect of temperature and media on CUE were isolate-specific (temperature*isolate interaction $F(22,476) = 2.324$, $P < 0.001$; media*isolate interaction $F(32,476) = 2.100$, $P < 0.001$ for three-way ANOVA; Fig. 1.2). This effect was underlain by variation in both growth and respiration rate of the isolates (Fig. B.1) with temperature.

Across all isolates and media, the Q_{10} of CUE varied from 0.49 to 2.63 (Fig. 1.3), equivalent to a halving to more than doubling in its value with a 10°C increase in temperature. In 71% of the cases however, CUE was unaffected by temperature over the range studied, indicating that respiration and growth often responded similarly to temperature. Substrates did not differ in their mean temperature sensitivity (Fig. B.4) or in the frequency with which the 95% bootstrap confidence intervals on Q_{10} did not overlap one for a given isolate by temperature combination (Fig. 1.3).

1.3.3 Phylogenetic conservatism of CUE and its temperature sensitivity

A phylogenetic tree was built for the isolates based on a set of conserved single-copy genes (152) using raxML (264). This tree was used as the backbone for identifying whether the CUE values observed were distributed at random in the bacterial taxa studied (Pagel's lambda = 0), whether the values are consistent with evolution following Brownian motion (Blomberg's K = 1, Pagel's lambda = 1), or whether they are comparably under- (Blomberg's K > 1) or over-dispersed (K < 1) on the phylogenetic tree. CUE did not have a consistent phylogenetic signal — it varied with

temperature and substrate. Pagel's lambda differed from zero only at 25°C, and not at 15 or 20°C on glucose (Table 1.2). On pyruvate, however, CUE correlated with phylogeny and approached the expectation under Brownian motion based on Pagel's lambda for all temperatures. Blomberg's K was typically small and less frequently different from zero than would be expected by chance, indicating that variation in CUE cannot be decisively said to vary more within than between clades. Reflecting this generally weak phylogenetic signal, knowing CUE of all remaining taxa did not help predict CUE in adjacent tips on the phylogeny except for taxa grown on glucose or pyruvate at 15°C, or for the Q_{10} between 20-25°C for taxa grown on glucose (Fig. 1.4, Fig. B.5, Fig. B.6). The estimation error for CUE on glucose was not correlated with distance to nearest sampled taxon, although it was positively correlated for pyruvate at 15°C ($\rho = 0.85$ $P < 0.01$). Estimation error for Q_{10} CUE on glucose was weakly positively correlated with phylogenetic distance ($\rho = 0.37$, $P < 0.1$), but more strongly negatively correlated for pyruvate between 15-20°C (ρ = -0.67, $P <$ 0.05).

1.3.4 Drivers of CUE

We annotated the genomes of the bacteria using IMG (47), and then tested our *a priori* hypotheses that CUE would be negatively correlated with rrN, growth rate, and transporter and extracellular enzyme investment, but positively correlated with metabolic complexity. Maximum observed growth rate (0.01-0.56 $hour^{-1}$), rrN (1-8 copies), and CUE on glucose were frequently positively correlated with one-another (Table 1.3, Fig. 1.5, Fig. B.7). CUE was not correlated with extracellular enzyme activity measured using artificial substrates, or with extracellular gene or trans-

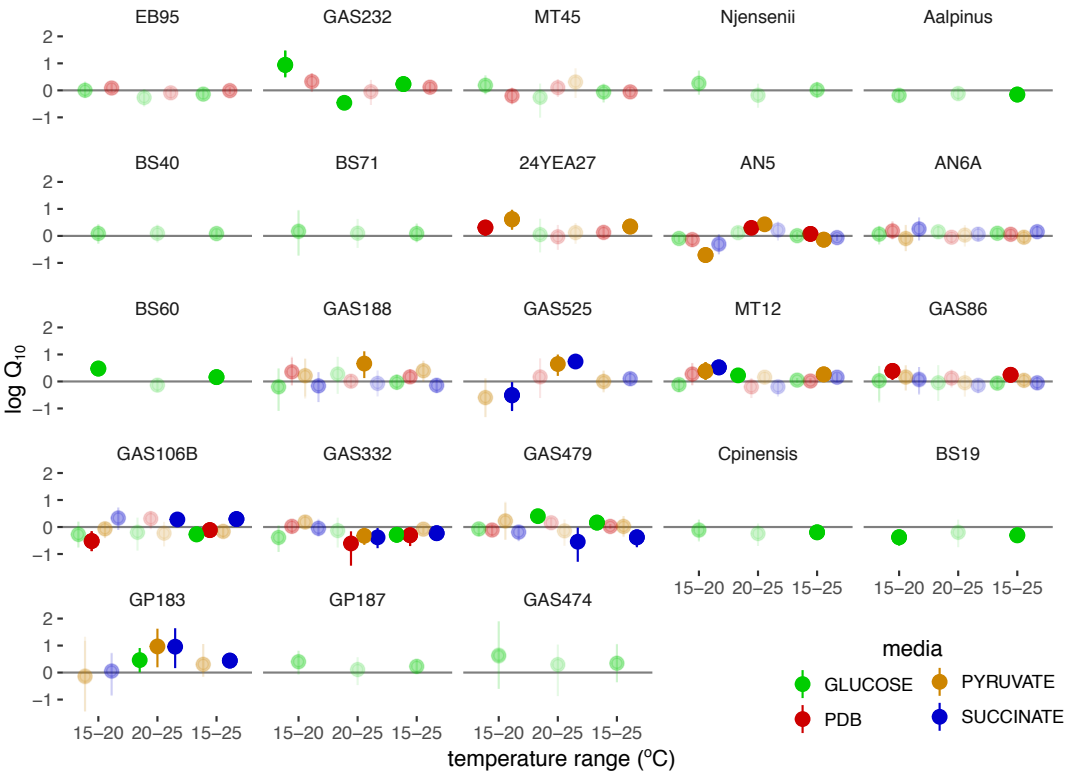

Figure 1.3: Q_{10} of CUE across three temperature ranges assayed in this study. Values are presented as the logarithm in order to center them on zero, and are coloured according to substrate. The intensity of the colour is halved when the 95% bootstrapped confidence intervals on the estimate of the raw data overlap one (i.e. CUE is insensitive to temperature), depicted here as a horizontal line.

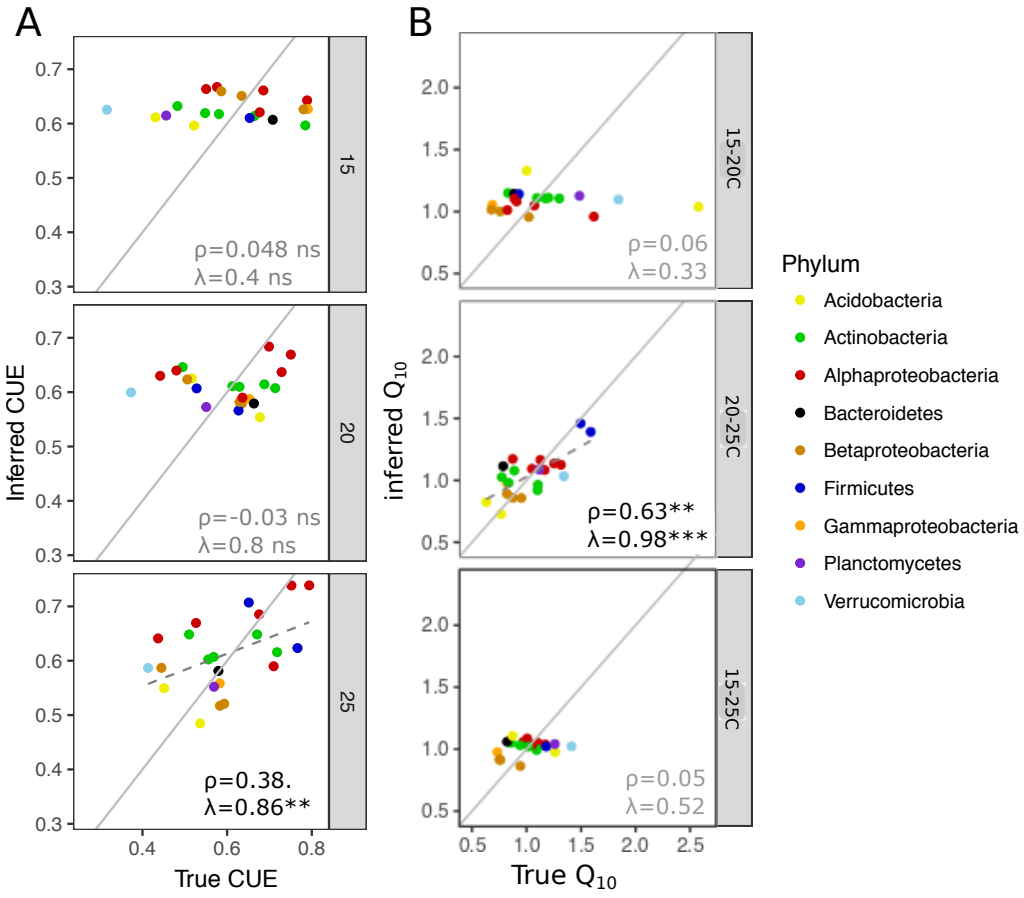

Figure 1.4: Plot of observed mean CUE (A) or CUE temperature sensitivity (B) for each isolate vs. the predicted mean CUE based on phylogenetic reconstruction using ancestral reconstruction techniques. Each point represents an isolate, the x-axis the observed mean CUE (Q10), and the y-axis the mean CUE (Q10) predicted for the isolate based on ancestral reconstruction using a phylogenetic tree whose terminal branch lengths have been scaled so the trait is best fit to a Brownian motion model. The 1:1 line, indicating perfect agreement between predicted and observed CUE, is drawn in solid grey, and the correlation for significant relationships between observed and predicted mean CUE for each isolate is drawn as a dashed line alongside the Spearman correlation coefficient (ρ) and Pagel's lambda (** $P < 0.01$,* $P < 0.05$)

Table 1.2: Phylogenetic signal of CUE and its temperature sensitivity over a range of temperatures and media types. "Temperature" denotes CUE at that temperature, while "range" denotes how CUE changes over the temperature range denoted. K denotes Blomberg's K, while λ denotes Pagel's lambda. Values for which the p-value for a test comparing values to zero is greater than 0.05 are in grey, while asterisks on black values denote $P < 0.05$ (*), $P < 0.01$ (**) or $P < 0.001$ (***). The 95% confidence intervals of K are 0.36-2.46, 0.32-2.45, 0.26-2.49, and 0.19-2.49, for a Brownian process simulated on the glucose, PDB, pyruvate, and succinate trees. The corresponding values for lambda are: 0.89-1, 0.89-1, 0.9-1, and 0.8-1.

Media	temperature (°C)	K (p)	λ (p)	range (°C)	K (p)	λ (p)
	15	0.11	0.4	15-20	0.25	0.33
glucose	20	0.11	0.8	20-25	0.70*	0.98 ***
	25	0.21	0.86 **	15-25	0.20	0.52
	15	0.1	0.48 .	15-20	0.05	0.19
PDB	20	0.83	0.88 **	20-25	0.01	0.00
	25	0.11	0.65*	15-25	0.02	0.00
	15	0.66 **	0.99 **	15-20	0.15	0.99 **
pyruvate	20	0.31 .	0.98 **	20-25	0.22	0.81
	25	0.38 .	0.99 ***	15-25	0.19	0.99 **
	15	0.17	0.62 .	15-20	0.04	0.99 **
succinate	20	0.28 .	1.00 **	20-25	0.11	0.97*
	25	0.1	0.89*	15-25	0.03	0.00

porter gene density estimated using a variety of genome annotation tools ($P > 0.2$). Likewise, we did not find a correlation between *in-silico* estimated CUE for extracellular enzyme production — which we determined using amino acid biosynthesis and polymerization costs — and the CUE observed on glucose, except at 15°C (Table 1.3). Codon bias is a measure of the degree to which a genome is optimized for rapid and efficient translation (283); based on the growth rate-yield hypothesis codon bias is expected to correlate negatively with CUE. However, the observed relation-

Table 1.3: Regression coefficients for a phylogenetic generalized least squares model fit to CUE on glucose at a given temperature versus rrN or the maximum growth rate observed across all assay conditions. Slopes are shown when the p-value is less than 0.1 (.), 0.05 (*), or 0.01 (**); - indicates the slope was not significant. Metabolic pathway count corresponds to the number of MAPLE pathways with 80% completeness. CUE for EEA production corresponds to the theoretical fraction of carbon from glucose expected to be retained in the extracellular enzymes produced by the organism, rather than being burned to produce the ATP needed to make the corresponding amino acids *de novo* and then polymerize them into the proteins.

temperature	CUE vs. GRmax	CUE vs. rrN	rrN vs. GRmax	CUE vs. log2 rrN	Metabolic pathway count	CUE for EEA production
15°C	0.41***	0.028*	7.23**	0.071**	0.0022***	2.782*
20°C	-	-	6.18*	0.039**	-	-
25°C	0.26*	0.021*	6.18*	0.052**	0.001.	-

ship between codon bias and CUE paralleled the non-negative correlation observed between CUE and maximum growth rate (Fig. B.8). We found evidence for a positive correlation between CUE on glucose at 15°C (Table 1.3) and the number of metabolic pathways annotated using MAPLE (17) (0.002 CUE metabolic pathway^{-1}; $P < 0.001$), and a weaker non-significant positive correlation at 25°C (0.001 CUE metabolic pathway^{-1}, $P < 0.1$). Similarly, the overall functional gene composition that an organism had was correlated with CUE on glucose at both 15 and 25°C, as evidenced by a significant correlation between the NMDS coordinates of a taxon's genome size-standardized KO composition and its CUE ($R^2 = 0.43$, 0.29, $P < 0.05$; envfit in vegan).

We also completed an "exploratory" analysis for markers of CUE, where we looked at all KO categories and maps to see whether they were correlated with CUE for a subset of isolates grown on glucose, and then validated them based on their consistent

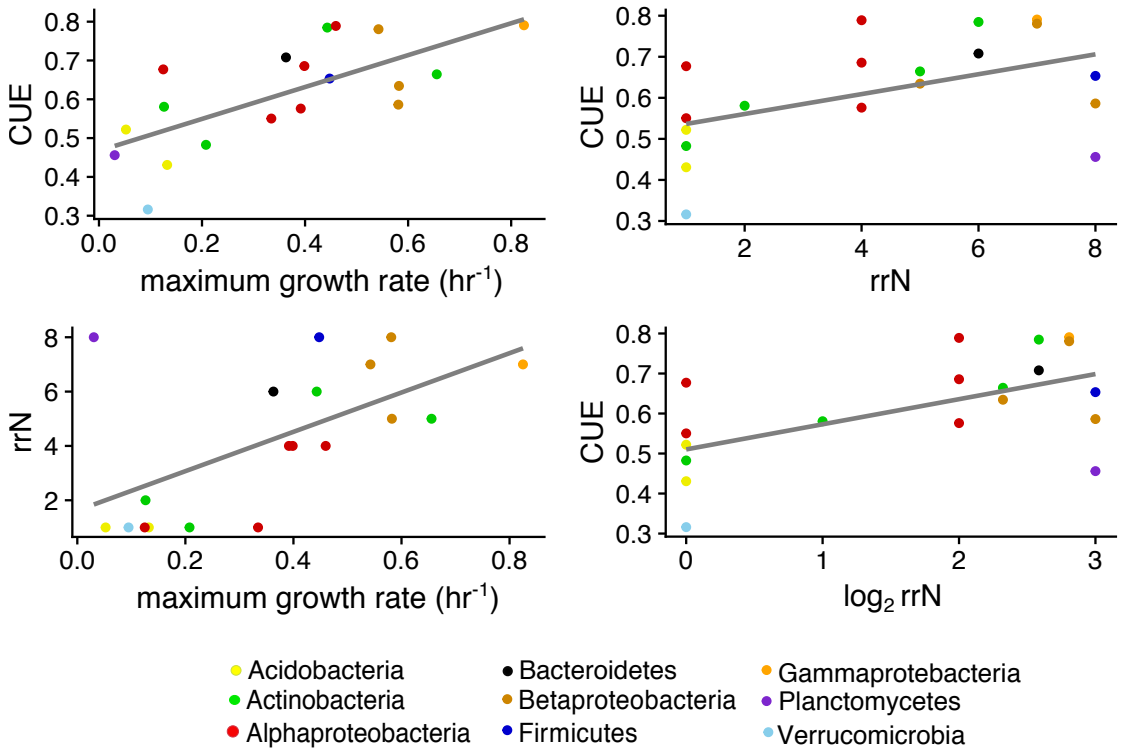

Figure 1.5: Relationships between CUE, growth rate, and rrN for bacteria grown in glucose media at 15°C. Full details can be found in Table 1.3

appearance in additional isolates and under alternative cultivation conditions. None of these candidate markers were confirmed by all three of the additional datasets intended to validate them (Figs. B.10, B.9; Table A.2).

1.3.5 Drivers of Q10

The Q_{10} of CUE tended to be lower for more efficient taxa (Fig. 1.6). This led to a homogenization of CUE at higher temperatures, with the standard error of CUE between isolates decreasing between 15-20 and 15-25°C for all substrates. The temperature sensitivity of CUE on glucose was negatively correlated with the number of metabolic pathways a bacteria had at 15-20°C (0.007 decrease in Q_{10} for every additional pathway, $P < 0.01$), and at 15-25°C (0.002 decrease, $P < 0.05$), but not 20-25°C. This corresponds to an expected decrease in CUE of 14% between 15-20°C for the isolate with the most metabolic pathways (*Ewingella* BS19; 200), to an increase of 6% for the bacteria with the fewest (*Verrucomicrobium* GAS474; 49). Extracellular enzyme-related functions increased the temperature sensitivity of CUE only for the 15-20°C temperature range on glucose (Q_{10} increases 0.01 extracellular enzyme Mbp $^{-1}$ $P < 0.01$). Q_{10} of CUE was not consistently correlated with genomic density of transporters (15-20°C: -0.016 transporters Mbp $^{-1}$; 20-25°C: +0.008 transporters Mbp $^{-1}$), and did not correlate with maximum growth rate or $\log_2$rrN (Table A.1).

As for CUE at a fixed temperature, no candidate markers of the temperature sensitivity of CUE identified in the "exploratory" glucose dataset were validated by both the microcosms and "other substrates" datasets (Figure B.11,A.3).

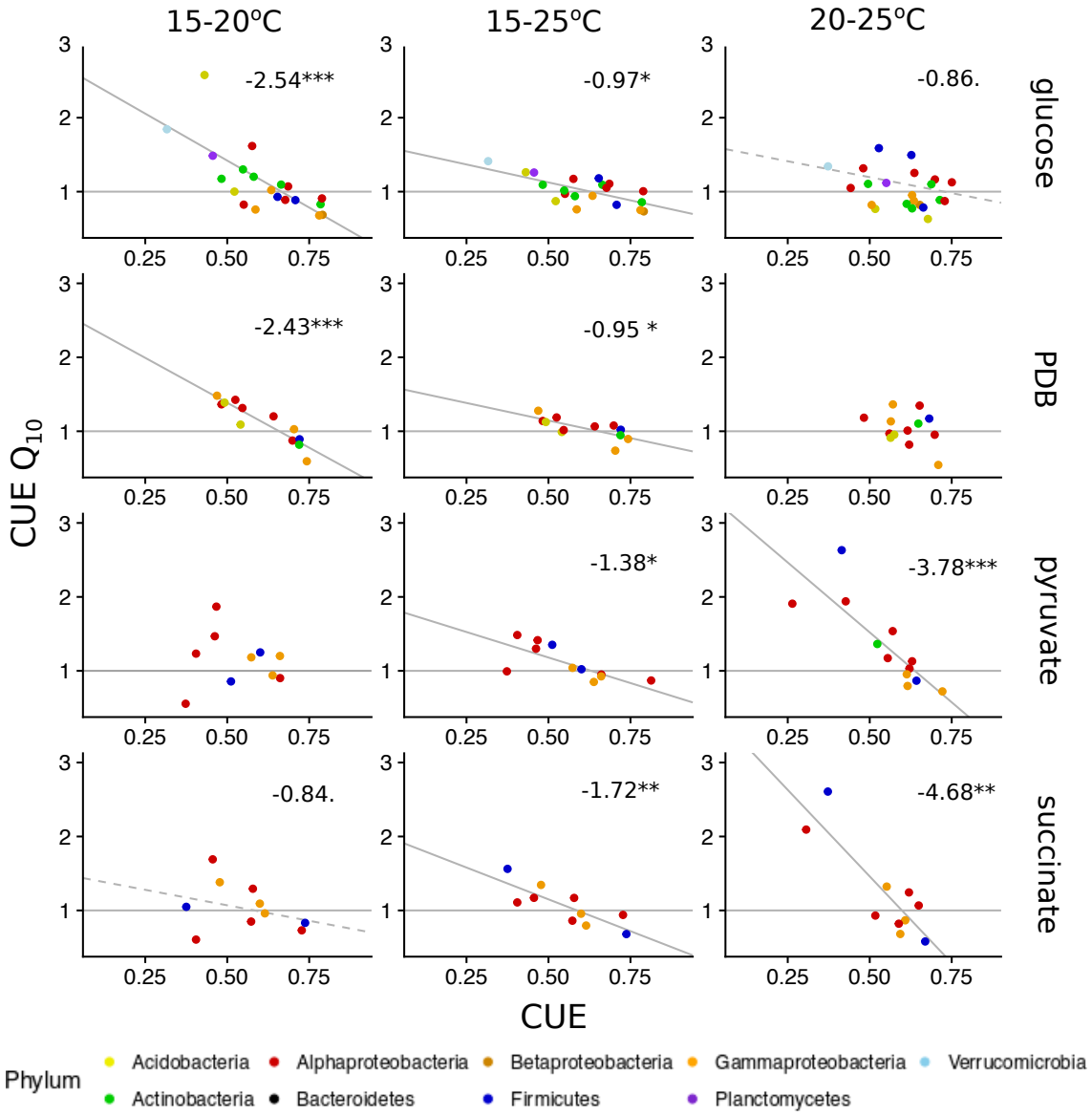

Figure 1.6: Change in CUE with temperature compared to the CUE at the starting temperature (i.e. Q_{10} between 15-20°C or 15-25°C against CUE at 15°C, or Q_{10} between 20-25°C compared to CUE at 20°C). The colour of the points is based on phylum (or class for Proteobacteria), with each point representing the mean CUE and Q_{10} for each isolate under the relevant treatment and temperature. Solid grey lines are the non-phylogenetic linear model, and dashed black lines the phylogenetic generalized least squares fit. Numbers on each plot denote the slope of the phylogenetic regression, if its p-value was below 0.1 (*** $P < 0.001$, ** $P < 0.01$, * $P < 0.05$. $P < 0.1$). Thin grey horizontal line denotes no temperature sensitivity (i.e. Q_{10} equals 1), so points above the line indicate an increase in CUE with temperature, and points below the line a decrease.

1.4 Discussion

We hypothesized that CUE would be highly variable across soil bacteria and temperatures, and this was indeed the case. The range of CUE observed for our soil bacteria was similar to that of fungi isolated from the same site (194), as well as bacteria from a wide range of ecosystems and domestication histories (238). Nonetheless, the upper limit of efficiency reported for our bacteria was 10% lower than that of the fungi, and almost 30% higher than the aforementioned bacteria grown under similar conditions. Furthermore, the range of Q_{10} values for the bacteria in the present study included a pair of stronger, more positive temperature responses (Q_{10} >1) than reported for fungi, consistent with a previous study which showed bacterial growth to be less negatively affected by higher temperatures than fungal growth (217).

The diverse temperature response of CUE we identified in this study contrasts with the homogeneous response typically assumed in models (10; 295). Although we are not the first to observe an increase in CUE with temperature for soil taxa (304), the magnitude and range of temperature responses observed across taxa is up to five times larger than has been reported for soil communities (70; 106; 168; 304). We suggest that the mute temperature responses observed for mixed communities are the result of a statistical averaging effect wherein mixtures of substrates (304) and microbal taxa (72; 91) with divergent CUE cancel each-other out. This is consistent with the observation that CUE on phenol (which can be used by a more restricted group of taxa) (99) showed a much stronger response to temperature than CUE on the more ubiquitously-used glucose (91). Consequently, taxon-level differences in CUE temperature sensitivity may only matter at the ecosystem-level for soil organic

matter cycling if they are linked to the presence of other "effect" traits involved in the uptake and processing of organic matter.

As a complex physiological trait which integrates the entire metabolic network of a cell, we hypothesized that CUE and its temperature sensitivity would be more similar in closely related organisms than expected by chance. This pattern was observed, but the degree of phylogenetic conservation was insufficient for building a predictive model of CUE in unsampled tips of the phylogeny. Poor ability to predict CUE based on phylogeny contrasts with other complex physiological traits such as oxygenic photosynthesis (184) and with apparent growth-limiting traits such as rrN (131; 238), which are assumed to be phylogenetically conserved because of low horizontal gene transfer frequency. While some of the uncertainty in predicted CUE values can be attributed to under-sampling of the phylogenetic tree, this is unlikely to be the sole factor because estimation error was never strongly positively correlated — and sometimes negatively correlated — with distance to the nearest sampled taxon on the tree. Thus, the pattern of CUE on the tree is inadequately modeled by Brownian motion, and so it must vary as a function of additional traits.

High and low efficiency organisms had different overall metabolic potentials, but few of the specific traits we proposed *a priori* to be correlated with CUE were actually correlated in the manner hypothesized. Of particular note is rrN, which has received considerable attention for its apparent role in setting the upper limit on growth rate (66; 267; 283), and in turn the ecological strategy and bacterial CUE under high nutrient conditions (238). Although we observed the expected positive correlation between rrN and maximum growth rate or codon bias, our results diverge

from previous studies (198; 238) in that CUE was positively correlated with rrN and maximum growth rate under many temperature-substrate combinations. The negative correlation between growth rate and CUE under high resource conditions was initially proposed based on the better studied and of-observed growth rate-yield trade-off (170; 238). This growth rate-yield trade-off is thought to be the consequence of balancing the speed and accuracy of translation (66; 149; 238), and has been proposed to be a central component of the copiotroph-oligotroph niche axis (86). Nonetheless, we are not the first to question (280) the ubiquity of the growth rate-yield trade-off.

Additional work has shown that bacteria can attain rapid growth under both high- and low-efficiency metabolisms. For example, selection for rapid growth in *E. coli* can result in either a high uptake, low-yield phenotype, or a moderate uptake, high-yield phenotype (151). A third dimension describing the relationship between uptake rate and yield in *E. coli* has been proposed (49), which would account for the observation that overflow metabolism is not ubiquitous, and not all organisms shift away from the pentose phosphate pathway and towards glycolysis when grown on glucose. Since we found a similar pattern of CUE increasing with growth rate and rrN even for non-fermentable substrates, this indicates that overflow metabolism is not a uniform driver of CUE and yield at high growth rates in our environmental isolates. Inconsistent relationships between maximum growth rate and yield have also been reported for aquatic Proteobacteria (198) and *Bacillus* species (280). Mechanistically it would make sense that CUE increases with growth rate if maintenance respiration (time-dependent) outstripped growth respiration (time-independent) (219), but

neither the literature (133) nor the value derived from the current dataset indicate this to be the case. Furthermore, maintenance respiration would have to be lower in fast-growing taxa than slow-growing taxa to explain the higher CUE in fast-growing taxa, which contradicts the pattern previously observed (281). Therefore, the mechanisms underlying the positive correlation between growth rate and efficiency in the present isolates remains unclear.

Our exploratory analysis searching for genomic markers of efficiency also failed to provide a substantive explanation for the observed differences in CUE between taxa. None of the markers proposed based on their correlation with CUE on glucose were consistently validated by both the "other substrates" and microcosms datasets, and those which were validated by one or the other were often found in few genomes and/or formed isolated steps in metabolism. This lack of validation by additional datasets may in part be because the substrates differ in where they enter central metabolism. Glucose may enter any of a number of pathways with different nitrogen requirements, energy yields (90), and anabolic potentials — including through the TCA cycle where pyruvate and succinate are generated — whereas pyruvate and succinate are much more limited in the diversity of pathways they can directly enter. On the other hand, the presence of interspecific interactions may explain why glucose-fed isolates and cellobiose-fed microcosms differed in the genes correlated with CUE, despite the substrates being able to enter the same metabolic pathways (59). For instance, genes which are advantageous for growth in isolation may not be advantageous in a mixed community (93; 297), or where substrates are not in a freely-available pool (215; 19). Furthermore, while we are certain that CUE was

measured during exponential phase for isolates, it is unlikely to be the case for the soil communities which were left without substrate addition for a month prior to CUE measurements. Finally, it is possible that the metagenomes inferred for the microcosm communities based on their 16S rRNA gene content do not adequately represent the true metagenomic content, as even very similar 16S genes can be associated with different functional compositions (141). Nonetheless, our results indicate that the taxa which are most efficient on one substrate are unlikely to be the most efficient on another, such that CUE is more like a dynamic response variable than a fixed ecological trait. Given that CUE varied substantially as a function of substrate — and substrate chemistry can differ substantially across soils (102) — it is possible that the temperature sensitivity of CUE, rather than its absolute value, is more useful for comparing the physiology of different microbial community compositions.

The temperature sensitivity of CUE was not consistently correlated with common soil-associated traits such as extracellular enzyme gene allocation, but could be predicted based on the value of CUE itself. Specifically, the temperature sensitivity of CUE was negatively correlated with basal CUE under many assay conditions. This could not be attributed to differences in the growth rates of organisms at the lower temperature, indicating that increasing temperatures do not preferentially favor slow growing taxa. Decreased CUE temperature sensitivity with greater basal CUE does, however, indicate that the CUE of communities should homogenize at higher temperatures as inefficient communities increase in efficiency and efficient ones less-so. This is indeed the case for the mock bacterial communities incubated in artificial soil with cellobiose, as the standard error of CUE decreased from 4.4 at 15°C to 3.8

at 20°C and 3.6 at 25°C. Nonetheless, given the possibility of different substrates becoming available at higher temperatures, and the substrate-specific divergences in CUE across taxa, the correlation between CUE and its temperature sensitivity is unlikely to hold for intact microbial communities. Accordingly Zheng *et al.* (2019) found only a very weak negative correlation between CUE and its Q_{10} across a range of different soils. Thus future work integrating the diversity of temperature responses to predict the outcome of community interactions is necessary to advance the field.

1.5 Conclusion

The objective of this study was to identify markers of CUE in soil bacteria, in order to be able to generate predictions about the taxa most sensitive to temperature. We found that fast-growing taxa are likely to grow more efficiently, and that highly efficient taxa tend to decrease in efficiency with temperature more so than those with initially low CUE. Therefore, our results are consistent with the hypothesis that maintenance respiration is a more pivotal factor in regulating soil bacterial CUE than previously recognized. Our results also challenge the idea that high ribosomal operon copy number correlates with reduced growth efficiency. Previously and *de-novo* hypothesized markers of efficiency were not consistent across assay conditions, reinforcing that CUE is an integrator of organism physiology in response to the environment more-so than a fixed parameter of their ecological strategy. Our results also suggest that communities capable of effectively retaining soil C in the present may not necessarily be the best equipped to continue to do so in the future, because the taxa able to grow most efficiently at low temperature tended to release more

substrate as CO_2 as the incubation temperature increased. Our study therefore opens the door for additional work with isolates under the more realistic soil conditions we ultimately wish to understand.

1.6 Materials and Methods

1.6.1 Isolate selection

We used 20 bacteria from our lab culture collection, and an additional three isolates from public culture collections for our study (**Table 1**). Those bacteria from our lab collection were derived from the organic and A-horizon of the Canton series underlying a temperate deciduous forest stand at the Harvard Forest Long-term Ecological Research (LTER) site, in Petersham Massachusetts. These bacteria were isolated using a range of cultivation conditions (222), and freezer stocks were prepared using the second or third streak of the original soil-derived colony. The isolates used were selected to cover the global diversity of soil bacteria (64).

1.6.2 CUE measurement

To measure bacterial CUE, isolates were grown on up to four media types at a pH of 6; this is the lowest pH all isolates were able to grow but still two pH units higher than the soil most of them were originally isolated from. The media types were: potato dextrose broth (PDB), and glucose, pyruvate, and succinate media. We ensured the cells were acclimated by transferring exponentially-growing cultures at the temperature and media used for assay conditions at least three times prior to

taking CUE measurements. Additional information on media and assay set-up can be found in the supplement.

The optical density and respiration rate of cultures were monitored throughout the exponential growth phase using a Spectronic-20 spectrophotometer at 600 nm and a Quantek instruments model 906 CO_2 analyzer, respectively. Prior to each read, tubes were vortexed vigorously to ensure solution and headspace CO_2 were in equilibrium. At least three distinct experiments starting with a new freezer stock restreak were completed for each isolate and condition assayed. A conversion factor of 130 μg carbon $OD^{-1}ml^{-1}$ was used to calculate microbial biomass carbon throughout the growth curve (BioNumber 109836), as technical challenges collecting biomass from cultures meant that MBC was underestimated in the taxa characterized by small cells.

1.6.3 Data analysis

Calculation of CUE was restricted to exponential phase, which was identified by taking the natural logarithm of biomass vs. time and finding the range of timepoints which maximized the slope. Three to ten timepoints were used per curve for this purpose, depending on the growth rate of the isolate and duration of exponential phase. When the slope of the growth rate or mass-specific respiration rate did not differ from zero (F test $P > 0.05$), the data were discarded and the experiment was repeated. CUE was calculated as:

$$CUE = \frac{\mu}{\mu * R}$$

Where μ is the intrinsic rate of increase, calculated as the slope of ln(biomass) against time, and R is the mass-specific respiration rate during the same time period (194). This is similar to the method used by Keiblinger *et al.* (2010); the use here of multiple CO_2 measurements and of the entire exponential phase is expected to improve estimate reliability. We used repeated measures correlation (20) to look at the effect of substrate quality.

1.6.3.1 Calculating temperature sensitivity

Although our experimental design was such that the same starting culture would be incubated in four different media under three different temperatures, successful concurrent cultivation under all twelve conditions was rarely achieved. Therefore, in the absence of such a blocked design, bootstrapping was used to determine uncertainty in the temperature sensitivity of CUE. In other words, the temperature sensitivity of CUE was calculated for all combinations of 15 and 25°C for a given media and isolate combination, and the standard error was calculated from this.

1.6.3.2 Genome annotation

Genome annotation was completed using the Joint Genome Institute's IMG pipeline (47). Potential extracellular enzymes were separately identified based on the presence of signal peptides using SignalP 4.1 (214) with the default D-cutoff of 0.57. This subset of ORFs was then examined for enzymes involved in litter and necromass decomposition. Carbohydrate-active and lignin-degrading enzymes were identified using dbCAN (116) v6, and additional putative extracellular enzymes for other substrates were extracted by name from the IMG annotations using "*rotease"

or "*roteinase" or "*eptidase" or "*osphatase" or "*hospholipase" annotation as keyword strings. These extracellular enzyme classes were chosen to retain consistency with functions typically assayed in soils.

Transporters were annotated using TCDB (241) and TransportDB 2.0 (81) and summed for each isolate. Identification was completed with gBlast2 (234) against the TCDB reference database downloaded on July 20th 2018, and using the TransAAP online tool against TransportDB in August of 2018. The number of metabolic pathways an organism has based on annotations with MAPLE (17) was used as a proxy for metabolic complexity (198). The envfit function in vegan (203) was used to evaluate whether CUE was correlated with differences in overall KO composition of bacterial genomes, where the initial ordination of functional gene composition was completed using NMDS of Bray-Curtis distances.

1.6.3.3 Protein production costs

We calculated the total extracellular enzyme cost as a function of amino acid biosynthesis and translation, using the amino acid biosynthesis costs presented in Kaleta *et al.* (2013) for *E. coli* with glucose as the substrate and assuming 4.2 ATP consumed per peptide bond formed (126). Assuming 26 ATP are produced per six glucose carbons, we calculated the theoretical carbon assimilation efficiency for each protein as the ratio of carbon in the protein to the carbon in the protein plus CO_2 respired making the ATP required to make the protein. The "per protein CUE" for each protein was then weighted by its expected relative expression to get a whole exoenzyme production cost. Relative expression was predicted based on codon usage bias as outlined in Appendix C.

1.6.4 Mixed bacterial communities

Cells were extracted using soil from the same Harvard Forest LTER site as the bacterial isolates using 224mM sodium pyrophosphate (266), and subsequently passed through a 0.8μm mixed cellulose ester syringe filter to remove eukaryotic cells. The filtered cell suspension was then used to inoculate an artificial soil matrix consisting of 70% acid-washed sand, 20% muffled and acid-washed silt, and 10% calcium chloride-treated bentonite clay, initially amended with mixed deciduous leaf litter DOC, 2X roller media (266), VL55 minerals and yeast extract. The communities were kept at 60% water holding capacity at 15 or 25^{o}C for four months, with weekly additions of 0.5 mg g soil^{-1} cellobiose and 0.05 mg g soil^{-1} ammonium nitrate solutions as sources of carbon and nitrogen, respectively, for the first three months.

We measured CUE using the ^{18}O-water method (262) at the same temperature the long-term incubations were completed at. The bacterial communities were sequenced at the Environmental Sample Preparation and Sequencing Facility at Argonne National lab following the Earth Microbiome Project protocol (276). Metagenomes of these communities were inferred using PICRUSt v 1.1.1 (153) with closed-reference OTUs picked in Qiime v1.9.0 (43) at 99% identity using uclust (79) against Greengenes v. 13.5 (65). We used relative abundance of the predicted KEGG ortholog gene categories as predictors of CUE. Nearest Sequenced Taxon Index (NSTI) for genomes used in functional assignment averaged 0.02 (range 0.003 to 0.072).

1.6.5 Identification of genomic markers

We focused on identifying markers of CUE on glucose, as this is the substrate for which we were able to get the most bacteria to successfully grow on. Genomic

markers of efficiency (and temperature sensitivity of efficiency) of glucose utilization were identified and validated in one of two ways. When we had an *a priori* hypothesis about the marker based on the literature, we used the full set of bacteria grown on glucose for our analysis. This was the case for rrN, codon bias (a proxy for growth rate (283)), extracellular enzyme costs, and number of metabolic pathways (198). For the others, we used a two-part process: a preliminary exploratory analysis for bacteria grown on glucose to identify candidate markers, and then a distinct validation step in which a "validating" dataset of bacteria grown on other substrates and a dataset of bacterial communities grown in artificial soil on cellobiose were interrogated for the same patterns. This exploratory analysis focused on the 5270 KEGG orthologues found in our bacterial genomes.

The identification and validation of markers in bacterial isolates was completed using phylogenetic generalized least squares in caper v1.0.1 (206). Caper uses a maximum likelihood method to infer the branch length transformations of the phylogenetic tree which minimizes phylogenetic correlation of the model residuals, thereby flexibly accounting for different degrees of phylogenetic signal in the residuals of comparable models. Genes were said to be candidate markers of efficiency at an alpha of 0.05 for the slope estimate. We used an identical approach to identify markers of efficiency in our first and second validating datasets. In the first, we required that the correlation between the candidate marker and CUE was the same for all 23 bacterial isolates on glucose as it was for the first subset of 12. The second validating dataset consisted of genes similarly correlated with CUE in at least two of the three other substrates. This criteria was selected to balance assuring robustness of markers over

multiple substrates with the fact that different substrates are likely to enter different metabolic pathways.

Our second validation method involved the cellobiose-grown mixed soil communties, for which we calculated Spearman correlation coefficients between predicted KO density and CUE. Those genes for which the approximate t-statistic had a p-value less than 0.05 for the Spearman rank correlation were kept. We considered markers of CUE from the isolates to be validated when they had the same significant direction of correlation in the isolate exploratory glucose, exploratory validating isolate glucose, and microcosm or other substrate datasets. When the validating dataset confirmed the correlation between a genomic marker and CUE that was proposed by the exploratory dataset, we examined residual plots for bias and normality for models. Model residuals were also examined to confirm removal of any phylogenetic signal using the phylosig() function in phytools v.0.6-60 (236). Proposed markers which did not meet these criteria were excluded from further analysis, which in practice meant that "rare" functions found in just a handful of genomes were routinely removed.

1.6.6 Inferring CUE based on phylogeny

The overall phylogenetic signal for CUE was calculated using the phytools package (236) for both Blomberg's K (35) and Pagel's lambda (208). We then used the rescale function in geiger (109) to scale the terminal branch lengths of the phylogeny according to this lambda so the trait matched Brownian motion. Ancestral reconstruction of CUE and its temperature sensitivity was completed on the rescaled tree using the phyEstimate() function in picante (132), where one known tip was removed

at a time and the CUE of the remaining tips was used to infer that of the removed tip.

CHAPTER 2

METABOLIC TRADEOFFS AND HETEROGENEITY IN MICROBIAL RESPONSES TO TEMPERATURE DETERMINE THE FATE OF LITTER CARBON IN A WARMER WORLD

2.1 Abstract

Climate change has the potential to destabilize the Earth's massive terrestrial carbon (C) stocks, but the degree to which models project this destabilization will occur depends on the kinds and complexities of microbial processes they simulate. Of particular note is carbon use efficiency (CUE), which determines the fraction of C processed by microbes that is anabolized into microbial biomass rather than being lost to the atmosphere as carbon dioxide. The temperature sensitivity of CUE is often modeled as a homogeneous property of the community, which contrasts with empirical data and has unknown impacts on projected changes to the soil carbon cycle under global warming. We used the DEMENT model—which simulates taxon-level litter decomposition dynamics—to explore the effects of introducing organism-level heterogeneity into the CUE response to temperature for decomposition of leaf litter under 5°C of warming. We found that allowing CUE temperature response to differ between taxa facilitated increased loss of litter C, unless fungal taxa were specifically restricted to decreasing CUE with temperature. Increased loss of litter C was

observed when the growth of a larger microbial biomass pool was fueled by higher community-level average CUE at higher temperature in the heterogeneous microbial community, with effectively lower costs for extracellular enzyme production. Together these results implicate a role for diversity of taxon-level CUE responses in driving the fate of litter C in a warmer world.

2.2 Introduction

Soil heterotrophs are central to the cycling and recycling of the 60 Gigatons of organic carbon (C) that plants deposit onto and into the ground each year. How well these litter inputs are converted into relatively stable soil organic matter depends on temperature, moisture, chemical composition, and soil mineralogy, which interact to influence microbial physiology (127; 181; 204). Predictions regarding how soil C stocks will continue to respond to climate change are, in turn, highly sensitive to how carbon use efficiency (CUE)—or the fraction of C taken up by a cell and incorporated into biomass rather than being respired—-changes with temperature (8; 12; 167; 258; 273; 294). As such, quantifying microbial decomposer CUE and its responsiveness to environmental change has been subject to intensive study (29; 68; 91; 95; 159; 179; 180; 205; 262; 263; 304).

Soil microbial communities show considerable differences in how their metabolisms respond to elevated temperatures, with their CUE increasing (205; 304), decreasing (68; 91; 205; 168; 304) or remaining unaffected by warming (72; 205; 284; 304). However, models of the soil C cycle generally assume either no change (12; 167; 295) or a fixed decrease in CUE with temperature (8; 12; 167; 294). When CUE is al-

lowed to directly increase with temperature, this temperature response is fixed across taxa (91; 300). In other instances, CUE may be modeled as fixed within taxa, such that changes in community-level CUE with warming are the result of shifts in the dominant group or groups of organisms present as a function of their dietary preferences and/or C:N ratio (258; 294). Therefore, models have thus far insufficiently accounted for how the temperature sensitivity of central metabolism may differ between microbes, such that intrinsic differences in efficiency between taxa above and beyond temperature-driven differences in substrate supply may also drive microbial community trajectories.

Variation in the temperature sensitivity of growth efficiency could be driven by differences in the rate-limiting step of central metabolic pathways (71), or in how well the proteins responsible for the extracellular processing and uptake of environmental nutrients are able to maintain activity as temperature increases (11; 13). For instance, there is some evidence that bacteria benefit more than fungi from an increase in temperature, as their growth rate was observed to decrease less rapidly with temperature above its optimum than the fungal community's did (217). Although the respiration rate for the two groups could not be isolated in that study, it is possible that they may also differ in the temperature response of CUE as a consequence of changing nutrient demands (129; 257). Therefore, the temperature range over which an an organism can maintain efficient growth is one important dimension of its niche (44), and, when combined with other "response traits" determining how they react to the environment (155), can impact their success in the environment. These response traits may in turn be linked to "effect traits" determining how an organism alters its

environment, such as extracellular enzyme production (15; 184; 279). For instance, taxa capable of growth at higher temperatures may need to produce a broader suite of enzymes and attack a wider range of substrates to support this rapid growth than slower-growing taxa.

Extracellular enzyme production is proposed to impose substantial metabolic costs on the cell, however. This is because carbon which could otherwise be allocated to growing the cell or generating the energy required to maintain it must instead be spent producing amino acids and expending ATP to link them together (125; 126). As such, extracellular enzyme production is inferred to reduce the carbon use efficiency of soil microbial communities (8; 180).

We explored whether interactions between the temperature sensitivity of intracellular (i.e. CUE) and extracellular (i.e. litter decomposing enzyme) metabolic processes of cells can explain why CUE is observed to increase with temperature in some soils, and decrease in others. We used the litter decomposition model DEMENT (6) to evaluate four hypotheses: 1) allowing temperature response of CUE to vary between taxa increases uncertainty in projected litter decomposition dynamics because more diverse phenotypic combinations exist for competitive selection (i.e. species sorting) to act upon; 2) this variation favors a community with higher CUE, in turn leading to higher microbial biomass and greater litter C loss with warming; 3) forcing the temperature response of CUE to positively co-vary with the number of enzymes an organism produces causes greater litter C loss than when the two factors vary independently, because increasing CUE with temperature offsets the increased costs against CUE associated with copious enzyme production; and 4) the

magnitude of litter carbon loss with warming is greater when the carbon-rich fungal functional group increases with warming than if only the nitrogen-rich bacterial functional group does.

2.3 Methods

2.3.1 DEMENT background and model design

DEMENT (6) is a litter decomposition model designed to simulate the loss of leaf C through time. The principal advancement of DEMENT over its predecessors is that it is both microbially- and spatially-explicit. The model is able to simulate inter- and intraspecific microbial interactions, with a primary focus on the tradeoff between the ability to take up and digest substrates, and the metabolic costs of creating and maintaining the machinery required to do so. Because these tradeoffs are both explicit and variable across taxa, DEMENT is an ideal model for evaluating how the physiology and ecology of microbes affects C stocks in a changing world. Furthermore, DEMENT allows for consideration of how diversity in responses across taxa (rather than using some cross-taxon mean) can facilitate soil C responses to climate change. Full details about the setup and execution of DEMENT are available elsewhere (6; 8; 9); here we describe the model controls on CUE which are relevant to our study.

Intrinsic CUE—the maximum CUE an organism could attain under ideal temperature and stoichiometry—is calculated for each taxon as a function of the baseline CUE at 15 °C, and the number of enzymes and transporters the taxon can produce. In turn, how much CUE is decreased due to enzyme and transporter production

Table 2.1: CUE-related model parameters mentioned in this paper.

Parameter	Value	Units	Description	Reference
C_r	0.38	dimensionless	CUE at 15°C for a taxon with no transporters or enzymes	this paper
C_e	-0.0025	enzyme^{-1}	change in CUE per extracellular enzyme gene	Allison, 2014
C_u	-0.0071	transporter^{-1}	change in CUE per transporter gene	Allison, 2014
C_t	-0.022 to 0.022	°C^{-1}	change in CUE per degree change in temperature from 15°C	this paper

depends on the cost per enzyme (C_e) and cost per transporter (C_u) (Table 2.1). The C used in enzyme synthesis is considered a loss from the cell, and is therefore not reported as microbial biomass C. The intrinsic CUE of each taxon is adjusted for temperature, decreasing by 0.016°C^{-1} by default (i.e. C_t = -0.016°C^{-1}), consistent with a global meta-analysis (230).

2.3.2 Modifications to DEMENT

Baseline CUE (C_r) was adjusted downwards from its original published value of 0.58 to 0.38 at 15°C; this not only improved model stability (Table A.4), but is also consistent with a comparative modeling study completed by Li *et al.* (2014), several ^{18}O-H_2O based CUE measurements (95; 262; 263), and for the structural components of litter modeled by MIMICS (296). We also altered the temperature sensitivity of CUE (C_t) from its default (fixed at a given cross-taxon average), to vary around the mean in different ways (Fig. 2.1). In the first set of scenarios, C_t varied independent of the taxonomic identity or number of enzymes a taxon produced. In the second scenario, C_t was limited to either increasing or decreasing as a function of the number of enzymes a given taxon had. In the third, bacteria and fungi were constrained to both have a positive C_t, both a negative C_t, or one a positive and the other a negative

C_t. In all instances, C_t was selected at random from a uniform distribution bounded by +/- 0.022$^oC^{-1}$ at the upper and/or lower limits. These values are within the range of temperature sensitivities observed for both bacterial cultures in the lab and for field communities (Fig. B.12), as well as values inferred based on modeling CUE against mean annual temperature on a global basis (256; 300). It was necessary to force the temperature sensitivity of CUE to take on a zero-centered uniform distribution so that simulation outputs in which extracellular enzyme counts were linked to the C_t could be compared to those scenarios where they were not linked, without changing the distribution of extracellular enzyme counts present in the community.

2.3.3 Running DEMENT

DEMENT v0.7.2 was downloaded from GitHub, and modified as described above. DEMENT was subsequently run on the Massachusetts Green High Performance Computing Cluster for 6,000 model days using 59 different independent starting seeds and a 100x100 grid size. "Control" runs were completed at 15^{o}C (equivalent to April to November mean soil temperature for a northern mid-latitude temperate deciduous forest (37)), while "heated" runs were completed at 20^{o}C (8). The first 1000 days of each resultant output file was excluded from the analysis because of rapid shifts in the microbial community during this time. In addition, outputs were filtered to exclude any seeds where the substrate pool was two or more times greater at the end of the model run than the median during the preceding 5000 days, indicating unrealistic, unconstrained litter accumulation. R version 3.4.0 was used for all runs and analyses (231).

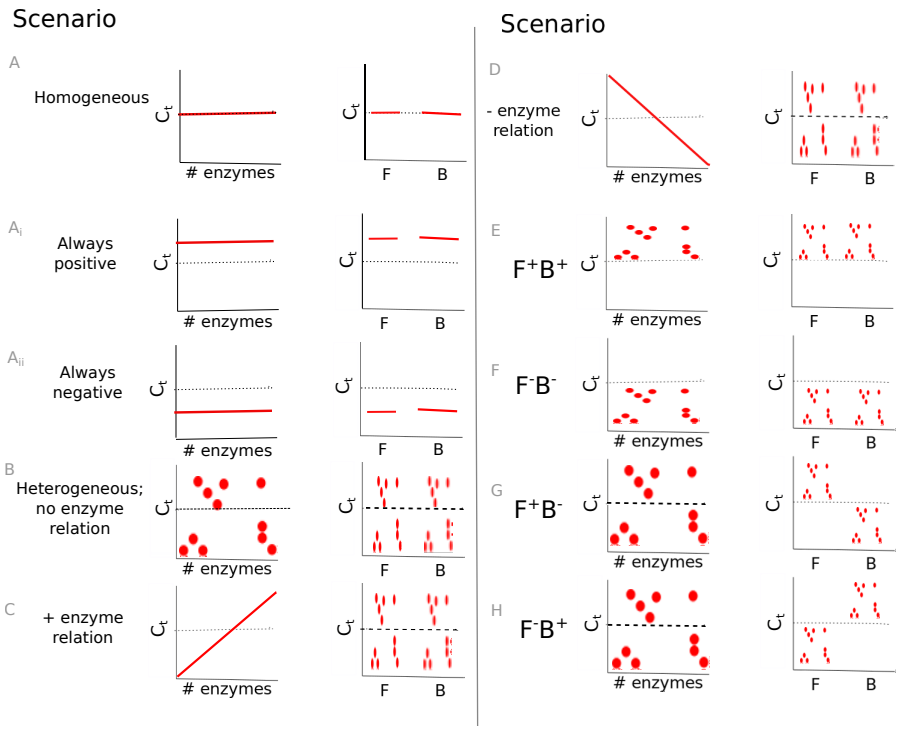

Figure 2.1: Schematic of experimental design used in this study, where CUE temperature response (C_t) varies as a function of the number of enzymes and/or taxonomic affiliation of organisms. Graphs show the effects of having homogeneous (A) or heterogeneous (B) C_t across taxa; the effect of forcing a positive (C) or negative (D) correlation between the number of enzymes and C_t; effect of fungi and bacteria both having increases (G) or decreases (H) in CUE with temperature, or with one group showing an increase while the other decreases its CUE with temperature (E,F). Horizontal dashed lines indicate a C_t of zero, and clusters of points above and below this line denote when CUE tends to increase or decrease with increasing temperature. The letters F and B in the x-axis of individual graphs denote sensitivities for fungi and bacteria, respectively.

2.3.4 Analysis of outputs

The model outputs of interest were litter organic matter (LOM), microbial biomass carbon (MBC), respiration rate, richness and diversity of the surviving community, median number of enzymes per taxon for taxa alive during the 5000-day simulation, fungal:bacterial biomass ratio for surviving taxa, and biomass-weighted CUE at 15 and 20°C. Richness was calculated as the number of taxa surviving to the end of the 5000 day run, while diversity was calculated as the median daily Shannon's H for the duration of the simulation using the vegan package (203). In order to determine whether warming and model parameterization affected model outputs, we used mixed effect models with starting seed as a random effect and warming or simulation scenario as fixed effects using lmer in lme4 v 1.1-17 (26). Data were visually assessed for normality and homoskedasticity using qqplots and residual plots following log-transformation. Significantly different pairwise differences were subsequently identified using emmeans v.1.3.0 (163), with a stringent Bonferoni-corrected p-value cutoff of $P < 0.0001$. Warming effect sizes are plotted as the natural log ratio of model outputs in heated:control scenarios.

2.4 Results and discussion

LOM and MBC content were both generally higher than observed in environmental samples, leading to MBC:LOM ratios at the high end of ranges observed in the field (2-11% vs. 1-5% (243; 299)). LOM and MBC values were within the range previously observed for simulations using DEMENT with daily litter inputs (10), but

greater than those with just a single litter pulse (6; 9; 83), indicating that these high biomass and litter C values can be attributed to these substrate inputs.

2.4.1 Intertaxon variability

To evaluate the effect of intertaxon CUE variablity on LOM stocks, we ran the model at 20°C ("heated") under two scenarios, and then compared the results to runs at 15°C ("control"). In the first "heterogeneous" scenario, C_t was assigned from a random uniform distribution bounded by -0.022 and 0.022°C^{-1} (Fig. 1A). In the second scenario, all taxa had an identical temperature sensitivity that was equivalent to the cross-taxon mean (0°C^{-1}) of the starting community in the first scenario (Fig. 1B).

Introducing intertaxon differences in CUE temperature response caused the characteristics of the initial microbial community (starting seed) to have a greater impact on litter decomposition than when all taxa had an identical temperature response (Table 2.2). This contrasts with the dampening effect proposed to explain instability in small-scale microbially-explicit models compared to their macroscale counterparts (293), whereby the additive effect of increased physiological diversity was to increase, rather than decrease, uncertainty in the present simulations. The median-standardized interquartile ranges of both MBC (0.25 vs. 0.15) and LOM (0.28 vs. 0.14) increased with the introduction of a variable C_t. Through species sorting, this heterogeneously-responding microbial community became more uneven with warming, with similar richness but lower diversity than the control community (Table 2.2). The heterogeneous communities maintained a higher median microbial biomass—driving two and a half times more LOM loss—than the homogeneous communities

(Fig. 2.2). Intriguingly, neither litter (r=0.16, p=0.23) nor microbial biomass pool sizes (r=-0.44, $P < 0.001$) positively correlated with extracellular enzyme investment; thus, a (non-significant) 28% increase in the median enzyme count is unlikely to have driven the increased decomposition under the heterogeneous scenario. Instead, increased decomposition and increased biomass are likely the consequence of elevated CUE under warming conditions.

The homogeneous community scenario tested here is akin to the "no adaptation of CUE" scenario reported in a number of other studies (12; 167; 258), because the cross-taxon mean used is zero temperature response. Our results of reduced LOM loss in the absence of acclimation are consistent with two previous studies, but contrast with others. In an ecosystem-level model parameterized for an arctic tundra system, Sistla *et al.* (2014) found that greater soil organic matter (SOM) loss occurred with warming when the microbial community was able to acclimate its CN ratio (and in turn efficiency), than when the CUE was effectively fixed. Likewise, Allison (2014) found greater potential for increased LOM accumulation under warming when there was greater absolute variation in CUE across taxa (i.e. C_r from 0.18 to 0.58 rather than 0.38 to 0.58) (8). On the other hand, a comparison of models where the microbial community is modeled homogeneously showed that soil organic matter loss increases when organisms do not adapt (167). Similarly, Wieder *et al.* found that greater SOM loss occurred if the CUE was directly insensitive to temperature than when C_t was negative (295). These microbially-explicit decomposition models vary in if and how they link CUE to microbial traits, and so our findings support

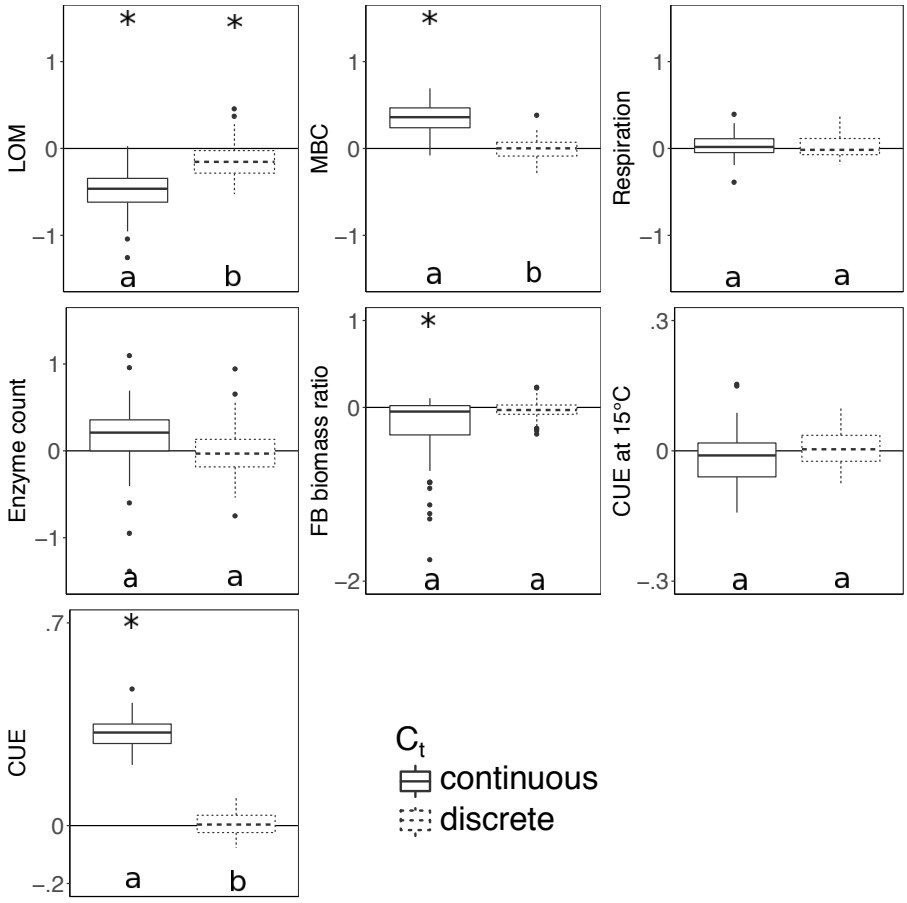

Figure 2.2: Effect of warming 5°C on C stocks and flows in simulations, reported as the natural log of the ratio of values in heated compared to control conditions. CUE temperature response either varied between taxa ("heterogeneous") or took on the fixed cross-sample mean temperature response of zero. Values above the zero line indicate warming increased the value, and values below indicate a decrease with warming. Boxplots denote 1st to 3rd quartiles with the median. Asterisks denote significant warming effect based on a paired Wilcoxon test at Bonferoni-corrected $P < 0.0001$. Letters denote warmed scenarios which are significantly different from one-another by the same criteria.

the concept that nuances in how different components of CUE respond to warming is an important control on the fate of litter C (105).

2.4.2 Confirming the role of C_t as an additional niche dimension

We allowed for CUE to increase with temperature for a subset of taxa in a way that most previous modeling efforts have not, and so it is possible that our results deviate from those of prior studies not because of variation in C_t, but rather because our simulations explore novel (positive C_t) parameter space. To facilitate comparison with previous decomposition modeling studies, we ran DEMENT simulations to test the effect of C_t being homogeneous vs. heterogeneous when CUE was either always positive (homogeneous C_t = 0.011 $^oC^{-1}$ (Fig. 2.1A_i), heterogeneous C_t = 0 to 0.022 $^oC^{-1}$ (Fig. 2.1G)) or always negative (homogeneous C_t = -0.011 $^oC^{-1}$ (Fig. 2.1A_{ii}), heterogeneous C_t = -0.022 to 0 $^oC^{-1}$ (Fig. 2.1H). In contrast to when C_t was allowed to vary over the whole spectrum of values, introducing heterogeneity in CUE did not increase inter-run uncertainty in LOM or MBC pools (Table A.5). We also found that less LOM accumulated when CUE showed a variable decrease with warming than a fixed one (Fig. B.13), which could be attributed to a reduction in MBC. By contrast, the homogeneous zero-centered and homogeneous positive C_t scenarios, and the heterogeneous zero-centered and heterogeneous positive C_t, behaved more similarly to one-another in that warming decreased LOM while increasing MBC and CUE to a greater degree in the heterogeneous than homogeneous scenarios (Table A.5). This finding reinforces the idea that if warming favors decomposer taxa capable of maintaining efficient growth, then soil C loss will be accelerated. Nonetheless, the strongly selected-for positive CUE response is rarely observed in complex soil com-

munities. This indicates that additional tradeoffs with CUE temperature response are likely at play when CUE is either unaffected or decreases with temperature, but that these tradeoffs are missing in the formulation of DEMENT used in this scenario. One such tradeoff possible to explore within the framework of DEMENT is the allocation of resources to extracellular enzyme activity.

2.4.3 Linkages between CUE temperature response and extracellular enzyme allocation

Microbes depend upon extracellular enzymes to break down substrates in the environment into digestible pieces, and enzyme activities are, like CUE, responsive to temperature (11; 94; 285). Soil extracellular enzymes often are active *in-situ* at temperatures much below their activity optima (13; 94; 225). Therefore, warming enables them to process substrates at a higher rate, increasing the supply of growth substrates to microbes. However, the affinity of enzymes for their substrates also decreases as temperature increases (11; 94); unless enzyme V_{max} increases faster with temperature than K_m, additional resources must be diverted from growth to enzyme production to maintain microbial growth substrate supply rate. Therefore, taxa may differentially-allocate resources to enzymes and so demonstrate a relationship between the temperature sensitivity of CUE and the number of enzymes they produce.

We evaluated whether litter decomposition changed its trajectory when the organisms with the greatest genomic potential to break the litter down (i.e. enzyme counts) also showed the most- or least-positive growth efficiency response to warming. In the "increase" scenario, we simulated a positive relationship between tem-

perature sensitivity of CUE and extracellular enzymes, where C_t increased linearly from -0.022°C^{-1} for organisms with no extracellular enzyme production potential to 0.022°C^{-1} for those organisms capable of producing the model maximum of 40 enzymes (Fig. 1C). In the "decrease" scenario, we simulated a negative relationship between temperature sensitivity of CUE and extracellular enzymes, where the opposite relationship was imposed with C_t decreasing with enzyme counts (Fig. 1D). These scenarios were then compared to the "heterogeneous" scenario (aka "no relation", as described above), where C_t varied across the same range, but independently of the number of enzymes an organism could produce. Therefore, the starting distribution of C_t and enzymes per taxon was identical across scenarios, and only their relationship with one-another changed.

More taxa survived to the end of the simulation when warming was applied under the "increase" scenario than either the "decrease" or "no relation" scenario (median of 13 versus 7 and 8, respectively, median absolute deviation = 2.97 in all cases). Under the "increase" scenario, taxa had 70% more enzymes each than the "no relation" scenario, and more than three times as much as the "decrease" scenario (Table 2.2). This relationship caused the CUE of surviving taxa to be 20-37% lower at 15°C for the "increase" scenario compared to the others, but this deficit was diminished at 20°C. As a result, the "increase" scenario led to higher respiration and a greater LOM loss under warming than under the "decrease" scenario, despite an overall smaller microbial biomass pool (Fig. 2.3).

How the relationship between C_t and extracellular enzymes drives favorable trait combinations can also be observed in Fig. 2.4. Surviving taxa retained a median

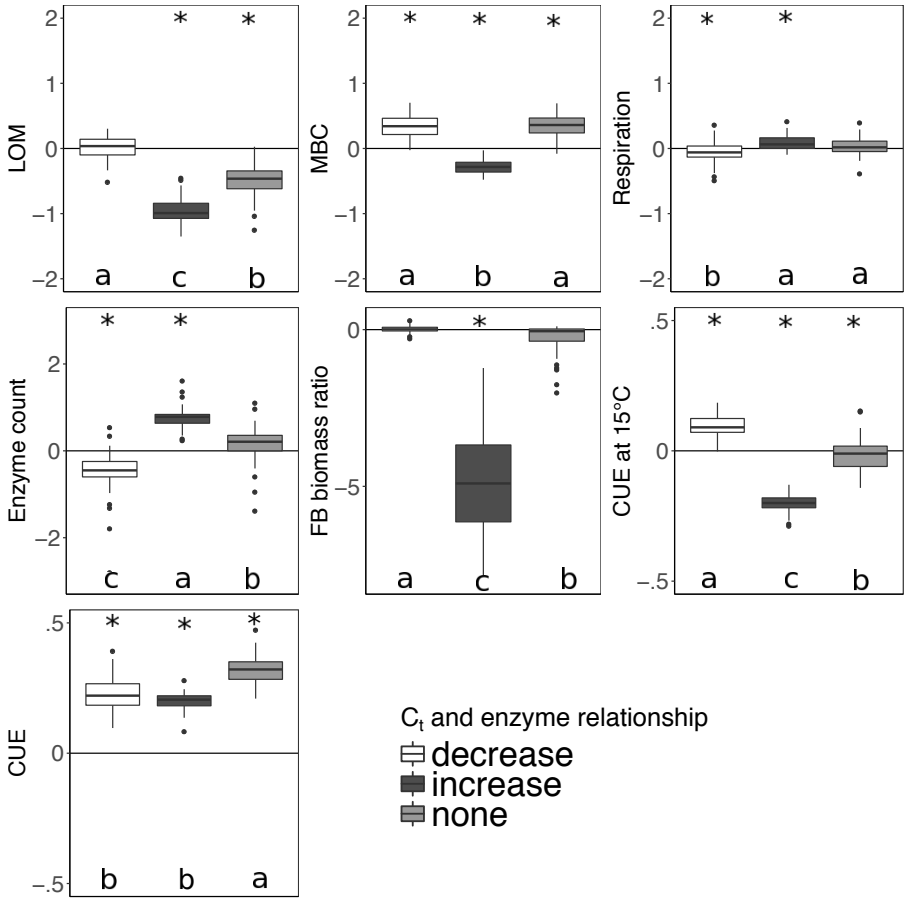

Figure 2.3: Effect of warming 5°C on C stocks and flows in simulations, reported as the natural log of the ratio of values in heated compared to control conditions. CUE temperature response was forced to increase, decrease, or remain independent of the number of enzymes a taxon could produce. Values above the zero line indicate warming increased the value, and values below indicate a decrease with warming. Boxplots denote 1st to 3rd quartiles with the median. Asterisks denote significant warming effect at $P < 0.0001$ after correcting for multiple comparisons using the Bonferoni method. Letters denote warmed scenarios which are significantly different from one-another by the same criteria.

enzyme count of at least 30 and a realized CUE temperature response of no less than $0.0158^{o}C^{-1}$ under the "increasing" scenario (ρ=0.64, $P < 0.001$), but there was no relationship between realized CUE temperature response and enzyme production under either the "decrease" or "no relation" scenarios. The selection for community capable of maintaining high CUE at high temperatures was much weaker when it was associated with reduced enzyme production. When there was no relationship between C_t and extracellular enzyme production costs, however, communities were able to attain a high realized CUE temperature response over a much wider range of median enzyme costs.

These findings indicate that response traits—which determine how an organism reacts to changes in temperature (e.g. CUE temperature response)—and effect traits—which determine how an organism alters its environment (e.g. litter decomposition potential)—interact to determine the fate of organic C. However, contrary to our hypothesis, adjusting DEMENT to allow for this tradeoff did not substantially alter how community-level CUE responds to temperature. The observation that LOM is reduced further when enzyme production is effectively cheaper contrasts with earlier work with DEMENT (8) showing smaller litter C pools under both ambient and elevated temperature when enzymes and transporters were cheaper to produce. However, our results are consistent in that microbial biomass was lower when enzyme costs are high, and that the microbial community was able to maintain a higher CUE under warming no matter the enzyme costs. The mechanisms underlying these phenomenological similarities differ, however, due to differences in how C_t was parameterized in the two sets of model simulations. Specifically, although

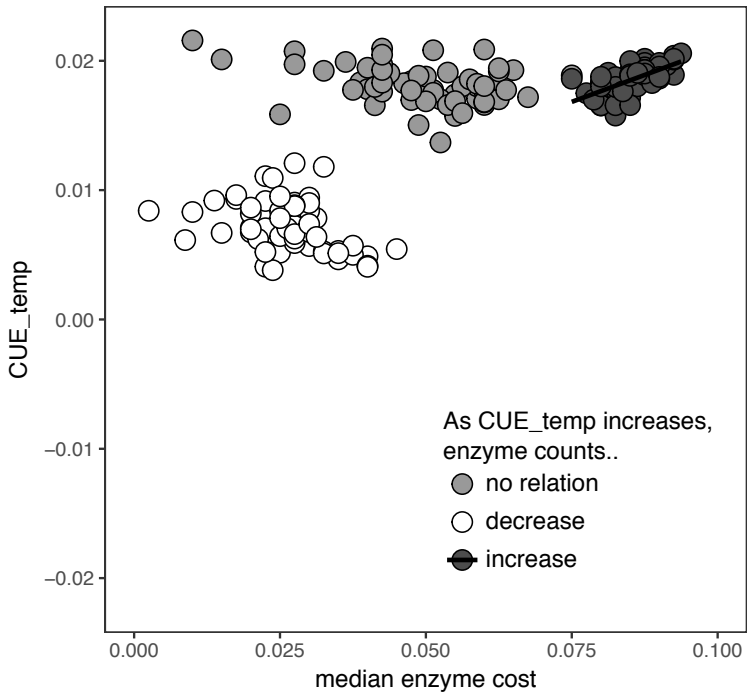

Figure 2.4: Relationship between the enzyme cost and temperature sensitivity of surviving taxa when the relationship between C_t and enzyme count is set to be positive (increase), negative (decrease), or non-existent. Each point represents the value for the median across all surviving taxa for one of 59 starting communities.

microbes were able to attain high CUE at elevated temperatures in our simulations by balancing the benefits of elevated CUE at higher temperatures with the costs of enzyme production against CUE, CUE always decreased with temperature in earlier work with DEMENT (8). Furthermore, enzyme production costs varied both with and independently of enzyme counts in previous DEMENT simulations (8).

Increased CUE is likely needed to offset the costs of extracellular enzyme production if taxa are to remain competitive at elevated temperatures within the framework of DEMENT, but empirical support for correlations between temperature sensitivity of CUE and enzyme investment are needed to best put these inferences to use. By examining correlations between the number of enzymes an organism can produce and its CUE temperature response at the end of the DEMENT model run, we see that there is likely to be either no or a positive correlation between the two variables, rather than a negative one (Fig. 2.5). Limited data from bacterial isolates grown in the lab also support this, whereby CUE temperature response is either positively correlated or uncorrelated with the number of enzymes produced (Chapter 1). Furthermore, although the mechanisms underlying the isolate response remain unclear, it is consistent with the scenario of C_t and enzyme counts being positively correlated. Specifically, we found isolates with lower CUE at 15°C (more extracellular enzymes in DEMENT) were more likely to have a positive CUE temperature response than those with a higher CUE (fewer enzymes in DEMENT). Together, these insights support a synergism between CUE temperature response and enzyme production, rather than a tradeoff. Because our DEMENT simulations indicate that selection for organisms characterized by high, positive CUE temperature responses with warm-

ing can alter both the directionality and extent of projected C loss, we propose it is important for other models to explore how possible increases—rather than just decreases—in C_t affect terrestrial C projections.

2.4.4 Ecological relevance of microbial metabolic diversity—bacteria vs. fungi

Across scenarios, fungi generally dominated the microbial biomass C pool (Table 2.2), as is typical for litter decomposition ((46), and references therein). This pattern occurred despite generally lower biomass-weighted CUE for surviving fungal taxa, and preferential loss of fungal taxa across most scenarios. The lower CUE for surviving fungi was not driven by higher enzyme costs than for bacteria, as median biomass-weighed enzyme costs were not statistically different ($P > 0.4$) and differed by less than one enzyme for the two groups. To test whether modeled differences in fungal vs. bacterial cell sizes and stoichiometry were driving this pattern, we tested how forcing differences in C_t in the two groups would impact the decomposition rate.

DEMENT was run with CUE simulated to respond: 1) negatively to temperature for all fungi and positively for all bacteria (F-B+; Fig. 1E); 2) negatively for all bacteria and positively for all fungi (F+B-; Fig. 1F); 3) positively for all bacteria and fungi (F+B+; Fig. 1G); or 4) negatively for all bacteria and fungi (F-B-; Fig. 1H). Minimum and maximum C_t were set to -0.022 °C and 0.022 °C, respectively.

Litter C accumulated at higher rates with warming when fungal C_t was negative, regardless of the bacterial C_t (Fig. 2.6, blue, orange). This is consistent with the observation that the CUE of surviving fungi was lower at the simulation temperature in seven out of the eleven scenarios. Because fungi have higher CNP ratios than

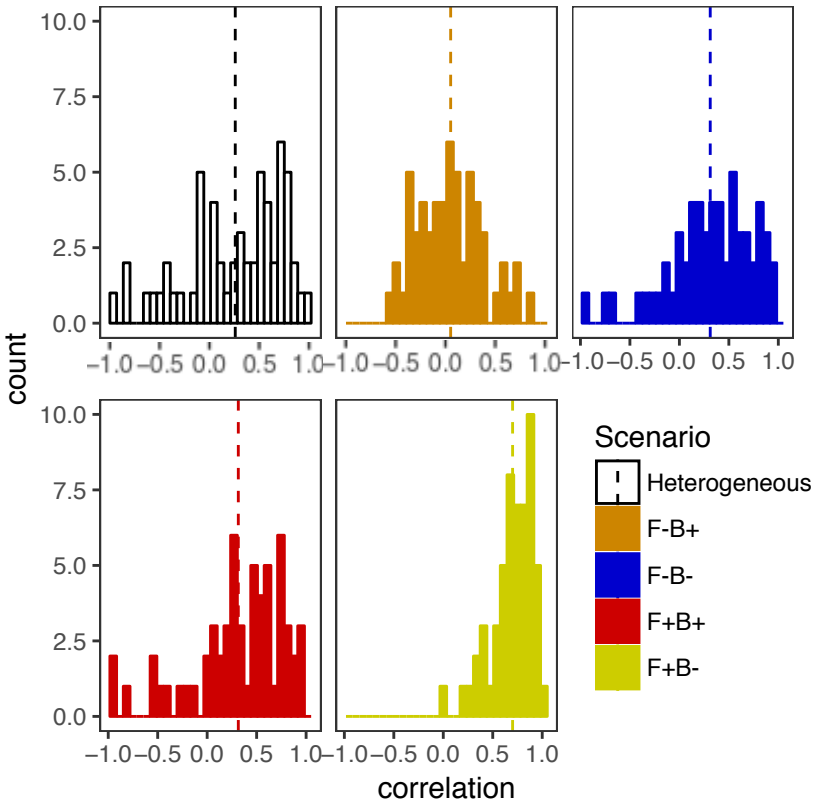

Figure 2.5: Frequency histograms of Pearson correlation coefficients between the number of enzymes taxa which survive to the end of the 6000 day run and their C_t. Each panel corresponds to a different scenario shown elsewhere in the manuscript, with the "counts" in each bar corresponding to a single starting seed (community) under that scenario. Vertical lines denote the mean correlation coefficient for the scenario.

bacteria (and thus higher C demands per unit biomass), we predicted that if fungi have a negative CUE temperature response, they would be weaker competitors at higher temperature than bacterial taxa, reducing their C demand and mitigating the warming effect on SOC stocks. While this contrasts with the premise that fungi should have a higher CUE (259) due to their higher CN ratio (302), it is consistent with a growing body of literature indicating that substrate quality—rather than the F:B ratio correlated with it—is the underlying driver of differences in CUE between soils (91; 179; 261; 275). Despite the low nutrient content of the daily inputs to the model (92:0.26:0.02 C:N:P), microbes did not show evidence for nutrient limitation as biomass CN and CP ratios were lower than are typical for soil communities (299) (4.1 and 36.7 vs. 7.6 and 42.4, respectively). Thus C was limiting, which could have further disfavored the highly C-demanding fungi when their C_t was negative. The lower CUE (and increased sensitivity to warming) for fungi compared to bacteria under a given scenario was also not driven by increased metabolic costs for enzyme production in fungi, as median biomass-weighted enzyme counts were statistically indistinguishable from those in bacteria.

The litter C pool decreased when fungal CUE increased with temperature (Fig. 2.6), correlating with a smaller microbial biomass pool when bacterial CUE also decreased with temperature. By contrast, the LOM and MBC responses to warming were similar when only the C_t of bacteria was changed, indicating that it is the fungal warming response which really drives changes in litter decomposition in DEMENT. This result is interesting because no *a priori* differences in decomposition or uptake potential were imposed on the two groups, and fungal and bacterial richness was

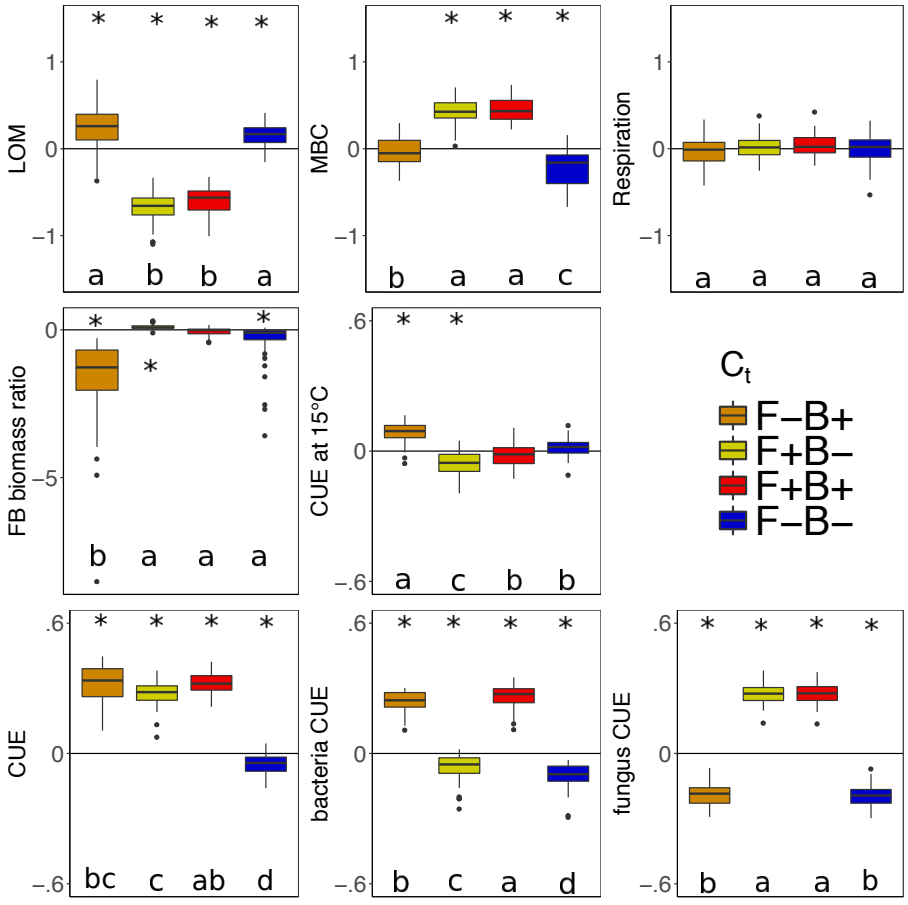

Figure 2.6: Effect of 5°C of warming on components of the litter C cycle when bacteria and fungi show dissimilar (F-B+ (orange), F+B- (yellow)) or similar (F+B+ (red), F-B- (blue)) CUE responses to temperature. Values above the zero line indicate warming increased the value (log ratio positive), and values below indicate a decrease with warming. Boxplots denote 1st to 3rd quartiles with the median. Asterisks denote significant warming effect at $P < 0.0001$ after correcting for multiple comparisons using the Bonferoni method. Letters denote warmed scenarios which are significantly different from one-another by the same criteria.

initially equivalent. Warming decreased the enzyme costs when fungal C_t was positive but bacterial C_t was negative, and decreased them under the opposing scenario, as evidenced by an increase in C_r in the former and decrease in the latter. Nonetheless, as long as both bacterial and fungal CUE did not both decrease their CUE with temperature, community level CUE remained higher at 20°C than it was at 15°C.

Empirical evidence for high-level differences in the temperature sensitivity of CUE in bacteria and fungi is currently mixed, but indicate CUE temperature response for fungi is unlikely to be more positive than that for bacteria. (304) did not find a correlation between the lipid-based fungal:bacterial ratio and Q_{10} of CUE over a range of soils. However, we (chapter 1) and our colleagues (194) have found that fungi tend to show a stronger negative CUE response with warming than do bacteria when examining them in isolation in the lab. This is consistent with the observation that fungal CUE decreases more strongly with warming than bacterial CUE does when C_t is restricted to negative values (Fig. 2.6). It is also consistent with the premise that bacterial growth benefits more from elevated temperature than does fungal growth in some soils (216). Greater empirical insight into the taxonomic drivers of the temperature sensitivity of CUE will assist with constraining the parameterization and projections of microbially-explicit decomposition models such as DEMENT.

2.4.5 Comparison to empirical warming studies

Litter decomposition is typically observed to accelerate under warming (174). However, both the chemical composition of the litter and the identity of the living plant community at the site of decomposition are important for the magnitude of this response (56; 289). Consistent with these empirical studies—but inconsistent

with a previous publication using DEMENT (8)—we found that litter decomposition was accelerated by warming in seven of ten scenarios. The range of losses and gains of litter C we observed with warming (-62% (scenario C) to +42% (scenario A_i)) approximates the -65% to +36% change observed in field experiments (174), with the upper limit only being exceeded when C_t is constrained to negative values. Likewise, values for simulated litter respiration response (-5 to +6%) fell within those observed for soil respiration in the field (-48 to +178%), and responses for microbial biomass C were also within the observed range (-25 to +58% vs -47 to +86%) (174). Our modeled responses to warming thus suggest that one possible explanation for differences in terrestrial C pool responses to warming may be diverse temperature sensitivities of underlying decomposer communities. Nonetheless, a number of additional factors must be taken into consideration when interpreting our results in the context of global climate change, including soil mineral-mediated modulation of substrate supply (58; 246), plant-microbe feedbacks (187; 258; 271), and temporal variation in temperature.

While we explored how different relationships between temperature sensitivity of CUE and enzyme count or taxonomic affiliation affects the C cycle, empirical support for these scenarios is lacking. By including additional dimensions to the warming response we showed that species effectively sort to make communities with differing impacts on litter decomposition. Following up on the direction and magnitude of these underlying metabolic scenarios in the soil and litter can help us better constrain our model results on reality. New and emerging work indicates that the temperature sensitivity of CUE is weakly negatively correlated with the temperature sensitivity

of extracellular enzyme activity, and with bacterial—but not fungal—biomass on the community level (304). However, different kinds of bacteria and fungi are able to show positive, negative, or no temperature sensitivity of CUE (Chapter 1), and so high-level assumptions about how these groups respond are unlikely to resolve uncertainties about the magnitude of soil C loss under warming.

2.5 Conclusions

Our results indicate that accounting for heterogeneous temperature response increases uncertainty regarding future litter C stocks, but only when C_t does not differ from zero on average. However, by combining simulations, empirical studies, and literature searches, we can conclude that microbes with high enzyme costs are likely to have larger increases in intrinsic CUE with temperature; that taxa can sort on a CUE temperature response axis; and that fungi are more likely to increase CUE with warming than bacteria. The simulations meeting each or all of these criteria lead to loss of litter C under warming, indicating that litter is likely to become a net atmospheric C source in a warmer world. We encourage models functioning on larger scales to explore the effect of including heterogeneity in the temperature response of CUE in order to determine the robustness of our conclusions to other model structures. However, ultimately increased integration of the growing body of literature on the temperature sensitivity of CUE must be explored for root causes of heterogeneity in temperature sensitivity of CUE in taxa under *in situ* conditions.

Table 2.2: Median (or median-standardized interquartile range (IQRm)) output values for various DEMENT model runs, marked according to warming effect (+/-) and model structure effects (letters) determined using Bonferoni-corrected post-hoc tests following linear mixed effect models. Symbols: "+" warming increased value; "-" warming decreased value). Letters: differences between warmed scenarios. All heated scenarios were compared to values in the "control" column to determine the warming effect. Only values within boxes defined by vertical lines were evaluated for significance differences of warming scenario, as different seeds needed to be excluded for failing to constrain litter accumulation in the two boxes. NA indicates that fungi died out completely in many instances (i.e. median fungal biomass of zero), so the parameter output could not be determined. The number in brackets denotes the median excluding the scenarios where all the fungi died out.

	NON-HEATED	CUE heterogeneity		CUE-Enzyme relationship		Fungi and bacteria differ			
Fig. 1 scenario	NA	A	B	C	D	E	F	G	H
C_t ($^oC^{-1}$)	NA	0	-0.022 to 0.022	-0.022 to 0.022	-0.022 to 0.022	-0.022 to 0 (F) 0 to 0.022 (B)	-0.022 to 0 (B) 0 to 0.022 (F)	0 to 0.022	-0.022 to 0
enz_cost/ C_t relationship	NA	ind	ind	pos	neg	ind	ind	ind	ind
LOM IQRm	0.2	0.14	0.28	0.33	0.15	0.39	0.29	0.23	0.3
MBC IQRm	0.16	0.16	0.25	0.02	0.24	0.14	0.16	0.15	0.19
Surviving taxa	9.5	11a	8b	13a+	7b-	12a	5c-	9b	8b-
Enzyme count	16	16b	20.5b	34.5a+	10.8c-	17.5a	20.5a+	19a	18a
Shannon's H	1.81	2.01a	1.58b-	2.11a+	1.31b-	1.93a	1.21c-	1.61a	1.64a-
MBC (mg cm^{-3})	20.9	21.0b	30.5a+	15.6c-	29.3a+	20.3b	33.0a+	32.3a+	17.2c-
LOM (mg cm^{-3})	583.2	496.0b-	361.5c-	220.1d-	603.2a	746.0a+	300b-	334.6b-	706.5a+
CUE at 15°C	0.23	0.23b	0.23b	0.19c-	0.25a+	0.25a+	0.22c-	0.23b	0.23b
CUE at 20°C	NA	0.23c	0.32a+	0.28b+	0.29b+	0.32bc+	0.31c+	0.32ab+	0.22d-
FB biomass ratio	0.86	0.84b	0.81b-	0.00c-	0.88a	0.12b-	0.96a+	0.85a	0.73a-
Respiration (mg cm^{-3} day^{-1})	0.93	0.94b	0.96ab	0.99a+	0.88c-	0.91a	0.94a	0.96a	0.94a
FB richness ratio	0.45	0.48a	0.44a	0.00b-	0.50a	0.14c-	0.67a+	0.44b	0.40b
CUE bacteria	0.27	0.27b	0.26c-	0.18d-	0.36a+	0.35b+	0.26c-	0.36a+	0.25d-
CUE fungus	0.22	0.23c	0.31a+	NA(0.28)b+	0.28b+	NA(0.18)b-	0.30a+	0.29a+	0.18b-

CHAPTER 3

HEAVY AND WET: EVALUATING THE VALIDITY AND IMPLICATIONS OF ASSUMPTIONS MADE WHEN MEASURING GROWTH EFFICIENCY USING ^{18}O WATER

3.1 Abstract

How microbes allocate carbon to growth vs. respiration plays a central role in determining the ability of soil to retain carbon. This carbon use efficiency (CUE) is increasingly measured using the ^{18}O-H_2O method, in which heavy oxygen incorporated into DNA is used to estimate growth. Here we evaluated the validity of some of the assumptions of this method using a literature search, and then tested how violating them affected estimates of the growth component of CUE in soil. We found that the ^{18}O method is consistently sensitive to assumptions made about oxygen sources to DNA, but that the effect of other assumptions depends on the microbial community present. We provide an example for how the tools developed here may be used with observed CUE values, and demonstrate that the original conclusions drawn from the data remain robust in the face of methodological bias. Our results lay the foundation for a better understanding of the consequences to the ^{18}O method underlying assumptions. Future studies can use the approach developed here to identify how different incubation conditions and/or treatments might bias its CUE

estimates and how trustworthy their results are. Further wet-lab work dissecting the assumptions of the ^{18}O method in soil will help justify the scenarios under which it is reasonable to trust its results.

3.2 Introduction

Carbon use efficiency (CUE) - or the fraction of carbon taken up by a cell and retained in biomass - is a central determinant of soil organic matter longevity. Across a wide range of complexities, models of the carbon cycle have shown that the degree to which soil organic matter is lost in a warmer world is contingent on CUE (12; 91; 167; 258). For many years, the study of CUE was limited to looking at one substrate type at a time, as a single heavy-labeled carbon source was added to the soil. Under this method, heavy carbon is partitioned by the cell into respiration and biomass, and CUE can be calculated as the fraction of heavy carbon collected from biomass compared to the sum collected from biomass and CO_2 respiration. However, this method is believed to overestimate "true" efficiency by measuring the uptake of simple labile compounds, and not their integration into biomass (95; 105). ^{13}C methods may also overestimate CUE if the target compound preferentially enters anabolic pathways while non-labeled substrates are used to generate ATP (100; 160). Finally, ^{13}C methods measure substrate use efficiency on a specific compound, and do not capture the repertoire of substrates microbes are faced with in natural environments such as soil.

Due to these known biases there has been a recent push towards using substrate-agnostic growth-based measures of biomass increment, such as ^{18}O-H_2O incorpo-

ration into DNA. This method provides more realistic and reproducible measures of CUE than the other dominant methods (95). To complete this assay, ^{18}O-H_2O is added at 5-50% of the total soil moisture and the soil is incubated in a sealed container for 12-72 hours (95; 263). At the end of the incubation, a gas sample is taken to measure the dissimilatory carbon losses, and the incubated soil is extracted for DNA. The amount of ^{18}O incorporated into the DNA is then determined using Isotope-Ratio Mass Spectrometry (IRMS), and converted into new DNA produced assuming 31% of DNA is oxygen. This DNA "growth" is then converted into microbial biomass carbon produced using either a sample-specific (95; 221; 284) or a cross-sample average ratio between total DNA yield and chloroform fumigation-extractable microbial biomass carbon (262). CUE can then be calculated as for the ^{13}C and ^{14}C labeled methods.

For the ^{18}O-H_2O method to provide an accurate estimate of CUE, a number of assumptions must be made. These include extracellular water being the sole source of oxygen in DNA; unbiased DNA and microbial biomass carbon extraction, and the actively growing community being representative of the total community (Fig. 3.1). Here we explore the validity of these assumptions, the effects of violating them, and the subsequent consequences for the conclusions made. We focus primarily on how the sensitivity of conclusions changes as a function of the fungal:bacterial DNA ratio of soil, both because proxies for this value are often determined during routine soil analyses, and because relevant physiological differences between these two groups are relatively well studied.

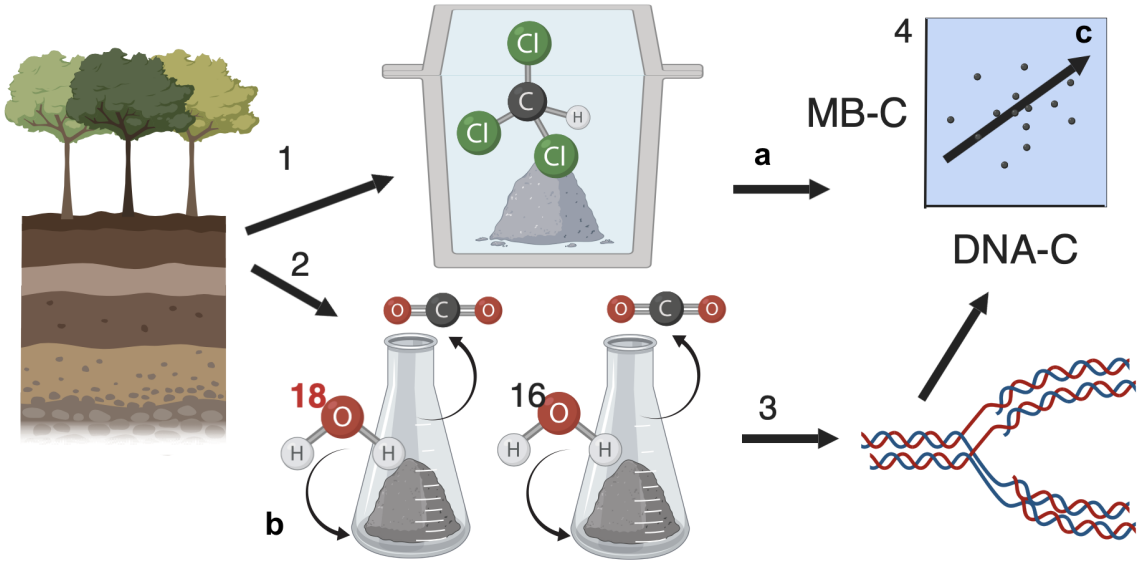

Figure 3.1: The ^{18}O-H_2O method of evaluating microbial growth in units of carbon (numbers), and the assumptions made (letters). 1. Soil collected from the environment is subject to chloroform fumigation extraction to determine total microbial biomass carbon. All taxa are assumed to have their biomass extracted with equal and complete efficiency (a). 2. A subfraction of the soil is incubated with ^{18}O-H_2O, which is assumed to be incorporated into new DNA (3) to comprise a fraction of the oxygens equal to its abundance as a fraction of total soil water (b). 4. The DNA is extracted and quantified, so that a relationship between the DNA and microbial biomass carbon content of the community can be established. It is assumed that this community-level MBC:DNA ratio is representative of the community which grew during the incubation with ^{18}O-H_2O, such that the new DNA growth can be converted to new microbial biomass carbon (c). Image made in BioRender.

3.3 Methods

We generated models to simulate the effects of inefficient DNA and MBC extraction, the active community not representing the total community, alternative oxygen sources to DNA, and differential growth rates between bacteria and fungi on measured MBC accumulation. All analyses were completed in R v3.4.0 (232), and results were plotted using ggplot2 (291). Other packages used for the analysis included: plyr (292), Shiny (45), and ggpubr (128).

3.3.1 Model development

First, we explored the existing literature for reported values regarding each parameter corresponding to the underlying assumptions that could impact CUE estimates (Table 1). Second, we generated a Shiny app (45) to interactively explore the effect of violating the assumptions of microbial growth measurements over a range of fungal:bacterial ratios. It is available at: `https://gracepold.shinyapps.io/18OSimulations/` until 25 hours/month server time have been used, and also as supplementary file S1. These simulations were run either assuming identical growth rates for bacteria and fungi (which were generated as a function of the fungal:bacterial DNA ratio), or that bacteria and fungi formed groups with distinct growth rates. Within each of these scenarios, we evaluated subsets where just DNA was extracted inefficiently, where MBC was extracted inefficiently, or where both were incompletely extracted. This app was additionally used for error checking the code used in subsequent steps, as predicted responses and test cases could be readily screened than when embedded in sensitivity analyses.

Next, we completed a sensitivity analysis by running simulations where a single parameter was changed to the minimum or maximum value observed in the literature (supplementary file S1 and 3.1), while keeping all the remaining parameters at a best-estimate value. Since "true" MBC differed between simulations, we divided the resultant "apparent" or "observed" microbial biomass carbon by the true microbial biomass carbon in order to standardize results. Sensitivity values were subsequently recorded as per Allison *et al.* (12; 105):

$$Sensitivity = \frac{|log10(highoutput) - log10(lowoutput)|}{|log10(highparameter) - log10(lowparameter)|} \tag{3.1}$$

where *high output* is the ratio of the true CUE to the observed CUE under the high parameter value, and *low output* is the ratio of the observed CUE under the low parameter value. Simulation parameters and the underlying assumptions can be found in Table 3.1, and references are available as a part of our Shiny app.

3.3.2 Empirical validation

We used a soil microbial diversity manipulation experiment to explore how removing fungi from inocula impacts estimates of CUE under a range of methodological errors. Briefly, microbial communities were extracted from temperate deciduous forest soil and either the complete ("fungi + bacteria") or less than 0.8uM fraction ("filtered"; "bacteria only") was used to inoculate an artificial soil matrix. This matrix consisted of 70% acid-washed sand, 20% muffled and acid-washed silt, and 10% calcium chloride-treated bentonite clay, initially amended with mixed deciduous leaf litter DOC, 2X roller media (266), VL55 minerals and yeast extract. The commu-

nities were grown for four months, with weekly additions of 0.5mg g soil^{-1} cellobiose and 0.05mg g soil^{-1} ammonium nitrate solutions as sources of carbon and nitrogen, respectively, for the first three months.

CUE was then measured by adding ^{18}O-H_2O to 20% of the final water present to subsamples of the soil. Samples were prepared identically, only using ^{16}O-H_2O, as controls for background heavy oxygen incorporation. The samples were then placed in sealed tubes for 24 hours and the CO_2 produced during this time measured using an IRGA. The soil samples were stored at -80C until DNA extraction using the Qiiagen Powersoil HTP kit. The resultant DNA was quantified using PicoGreen (Invitrogen), and its ^{18}O enrichment was measured using IRMS at the UC Davis Stable Isotope Facility. CUE was calculated as per (262). The abundance of total bacteria and total fungi was assessed by real-time quantitative PCR (qPCR) using 16S rrNA primers (199) and ITS primers (87), respectively. The abundance in each soil sample was based on increasing fluorescence intensity of the SYBR Green dye during amplification. Preceding qPCR assay an inhibition test was performed by running serial dilutions of DNA extractions and no amplification inhibition was detected. The qPCR assay was carried out in a 15 μl reaction volume containing 2 ng of DNA, 7.5 μl of SYBR green (QuantiFast SYBR Green PCR Master Mix) and 1 uM of each primer. Two independent qPCR assay were performed for each gene. The qPCR efficiencies for both genes ranged between 85 and 105%. 16S qPCR conditions were: 15 minutes at 95°C; 40x 15s @ 94°C, 30s @ 55°C, 30s @72°C; and a melting curve. ITS qPCR conditions were: 15 minutes at 95°C; 40x 15s @ 94°C, 30s @ 46°C, 30s @ 72°C; and a melting curve. These values were corrected to a genome counts

basis using median values from (172) for ITS copies and from (61) for bacterial 16S ribosomal RNA operon copy number.

Table 3.1: Values used to parameterize simulations of microbial biomass carbon growth during ^{18}O-H_2O addition to soil

Definition	**Parameter**	**value**	**minimum**	**maximum**	**Reference**
Metabolically active fraction bacteria	activeFractionB	0.1	0.01	1	(161; 210; 287)
Metabolically active fraction of fungi	activeFractionF	0.1	0.01	1	NA
Fraction of DNA oxygen from extracellular water	DNAbias	0.7	0.3	1	(1; 95; 118; 144; 145; 166)
Bacterial DNA extraction efficiency	DNAexteffB	0.5	0.06	0.5	(85), personal obs
Fungal DNA extraction efficiency	DNAexteffF	0.33	0.04	0.5	(85), personal obs
Bacterial growth rate (daily multiplier)	GRbact	0.167	0.003	3.4	(34; 98; 140; 239; 261)
Fungal growth rate (daily multiplier)	GRfun	0.0088	0.0001	0.8	(34; 78; 239; 261), Eric Morrison, pers. comm.
MBC:DNA ratio of bacteria	MBCDNAratB	13.22	3.6	37	(22; 50; 51; 146; 178; 196; 228; 261)
MBC:DNA ratio of fungi	MBCDNAratF	1070	90	3300	(16; 103; 146; 196; 157)
Bacterial MBC extraction efficiency	MBCexteffB	0.32	0.1	0.51	(69; 122; 123; 274)
Fungal MBC extraction efficiency	MBCexteffF	0.33	0.21	0.45	(69; 123; 183; 274)
Bacterial 16S copies per genome	rrNpergenome	2.25	1	15	(61; 268)
Fungal ITS copies per genome	ITSpergenome	82	14	1442	(172)

3.3.3 Shiny app and theoretical sensitivity simulations

Each simulation was set up under a series of biologically-plausible scenarios. Fungal:bacterial ratio and total community size are presented in terms of DNA, as this is the unit of growth measurement for the ^{18}O method. Definitions for parameters are found in Table 3.1, and for variables defined in the equations below in Table 3.2. Values without subscripts denote true MBC, DNA, and MBC:DNA ratios, while values with subscripts denote observed values were DNA (d), MBC (c), or both (dc) to be extracted inefficiently:

A community of size *totalDNA* was generated as a function of the fungal fraction of the total DNA pool (*FBratio*), where 30 was used as an arbitrary multiplier to determine the amount of DNA, and 3 as an additive factor to ensure that bacteria-only (FBratio of zero) still had DNA.

$$totalDNA = 30 * FBratio + 3 \tag{3.2}$$

The corresponding amount of microbial biomass carbon (*MBC*) is calculated as the sum of the biomass carbon of bacteria and fungi, which are the products of their DNA and MBC:DNA ratios.

$$MBC = FBratio * totalDNA * MBCDNAratF + (1 - FBratio) * totalDNA * MBCDNAratB \tag{3.3}$$

Since the MBC:DNA ratio of bacteria (*MBCDNAratB*) is generally larger in fast-growing and well-fed cells (50; 51), we also added the option to allow this ratio to vary

Table 3.2: Variables defined in the microbial biomass carbon calculations

Parameter	Description	units
totalDNA	The true total mass of the DNA pool in the soil	ug g^{-1} soil
FBratio	Fungal fraction of total DNA pool	dimensionless
MBC	The true total mass of the microbial biomass carbon pool in the soil	ug g^{-1} soil
MBCc	The apparent total mass of the microbial biomass carbon pool in the soil, given inefficient microbial biomass carbon extraction	ug g^{-1} soil
totalDNAd	The apparent total size of the true DNA pool in the soil, given a DNA extraction inefficiency	ug g^{-1} soil
MBCDNA	True microbial biomass carbon to DNA mass ratio of starting community; Used to convert the DNA growth increment into microbial biomass carbon growth.	dimensionless
MBCDNAc	Apparent microbial biomass carbon to DNA mass ratio of starting community, given that microbial biomass carbon is not completely extracted; Used to convert the DNA growth increment into microbial biomass carbon growth.	dimensionless
MBCDNAd	Apparent microbial biomass carbon to DNA mass ratio of starting community, given that DNA is not completely extracted; Used to convert the DNA growth increment into microbial biomass carbon growth.	dimensionless
MBCDNAdc	Apparent microbial biomass carbon to DNA mass ratio of starting community, given that both DNA and microbial biomass carbon are not completely extracted; Used to convert the DNA growth increment into microbial biomass carbon growth.	dimensionless
GRmean	Growth rate for simulations when bacteria and fungi are assumed to grow at the same community-level mean	day^{-1}
TrueMBCsame	The true new microbial biomass carbon produced during the CUE incubation, assuming bacteria and fungi grow at the same rate (GRmean)	ug C day^{-1}
MBCsamed	The apparent new microbial biomass carbon produced during the CUE incubation, given that not all the DNA is extracted from the growing community and assuming that bacteria and fungi grow at the same rate (GRmean)	ug C day^{-1}
MBCsamec	The apparent new microbial biomass carbon produced during the CUE incubation, given that not all the microbial biomass carbon is extracted from the growing community and assuming that bacteria and fungi grow at the same rate (GRmean)	ug C day^{-1}
MBCsamedc	The apparent new microbial biomass carbon produced during the CUE incubation, given that not all the DNA and microbial biomass carbon are extracted from the growing community and assuming that bacteria and fungi grow at the same rate (GRmean)	ug C day^{-1}
DNAbias	The fraction of new oxygen in DNA which comes from extracellular water (i.e. the 18O-water added) rather than other sources	dimensionless
TrueMBCdiff	The true new microbial biomass carbon produced during the CUE incubation assuming bacteria and fungi grow at different rates	ug C day^{-1}
MBCdiffd	The apparent new microbial biomass carbon produced during the CUE incubation assuming bacteria and fungi grow at different rates, given that not all the DNA is extracted from the growing community	ug C day^{-1}
MBCdiffc	The true new microbial biomass carbon produced during the CUE incubation assuming bacteria and fungi grow at different rates, given that not all the microbial biomass carbon is extracted from the growing community	ug C day^{-1}
MBCdiffdc	The true new microbial biomass carbon produced during the CUE incubation assuming bacteria and fungi grow at different rates, given that not all the DNA and microbial biomass carbon are extracted from the microbial community	ug C day^{-1}

as a function of bacterial growth rate. This was done by scaling the ratio between the minimum and maximum *MBCDNAratB* values observed in the literature over the range of bacterial growth rate (*GRbact*) values observed (Table 3.1), and assuming a linear relationship:

$$MBCDNAratB = GRbact * 15.5/0.199 + 4.422111 \tag{3.4}$$

which is the solution of

$$MBCDNAratB = GRbact * \frac{MBCDNAratBmax - MBCDNAratBmin}{GRbactmax - GRbactmin} + MBCDNAratBmin - \frac{MBCDNAratBmax - MBCDNAratBmin}{GRbactmax - GRbactmin} \tag{3.5}$$

The MBC:DNA ratio of the starting community is therefore:

$$MBCDNA = \frac{MBC}{totalDNA} \tag{3.6}$$

However, DNA is not completely extracted from soil microbes, with some evidence for a higher extraction efficiency for bacteria (*DNAexteffB*) than fungi (*DNAexteffF*) (85). Spores may be extracted with even lower efficiency (73), but do not contribute to growth so do not play into our calculations. The observed total DNA observed assuming inefficient DNA extraction ($totalDNA_d$) is then:

$$totalDNA_d = FBratio * totalDNA * DNAexteffF + (1 - FBratio) * totalDNA * DNAexteffB \tag{3.7}$$

The corresponding MBC:DNA ratio assuming inefficient DNA extraction ($MBCDNA_d$) is:

$$MBCDNA_d = \frac{MBC}{totalDNA_d} \tag{3.8}$$

MBC is also inefficiently extracted, with chloroform fumigation extraction capturing the true fungal (*MBCexteffF*) and bacterial (*MBCexteffB*) biomass carbon present with different efficiencies (122). MBC_c represents the total amount of microbial biomass observed after accounting for this chloroform fumigation extraction inefficiency:

$$MBC_c = FBratio * totalDNA * MBCDNAratF * MBCexteffF +$$

$$(1 - FBratio) * totalDNA * MBCDNAratB * MBCexteffB \tag{3.9}$$

And the corresponding MBC:DNA ratio is:

$$MBCDNA_c = \frac{MBC_c}{totalDNA} \tag{3.10}$$

If inefficiencies in both MBC and DNA extraction must be accounted for, then the apparent MBC:DNA ratio ($MBCDNA_{dc}$) is:

$$MBCDNA_{dc} = \frac{MBC_c}{totalDNA_d} \tag{3.11}$$

Steps 4-6 therefore show the MBC:DNA ratios a researcher converting the new DNA produced to MBC would use if they were unaware of extraction biases and did

not account for differences in bacterial and fungal growth rates (below). We assume growth during the incubation is representative of overall community growth. In other words, the community is assumed to be in a steady state and the rate of turnover of a given taxon matches its growth. In turn, the turnover of DNA in the environment is proportionate to its abundance (162). If bacteria and fungi grow at the same rate, then the community-level growth rate (GRmean) can be set to vary as a function of the community composition:

$$GRmean = FBratio * GRfun + GRbact * (1 - FBratio) \tag{3.12}$$

The corresponding true increase in MBC for bacteria and fungi when they are assumed to grow at the same rate (*TrueMBCsame*) is:

$$TrueMBCsame = GRmean * totalDNA * FBratio * MBCDNAratF +$$

$$GRmean * totalDNA * (1 - FBratio) * MBCDNAratB \tag{3.13}$$

However, we may not "see" all this growth because extracellular water is not the sole source of oxygen in DNA. Rather, anywhere from 4-70% of oxygen in DNA may come from metabolic water (145; 144; 166). We refer to this bias towards using extracellular rather than intracellular water as *DNAbias*, which is the fraction of DNA oxygen derived from extracellular water.

Subsequently, if just DNA is extracted inefficiently then the corresponding apparent new MBC produced (MBCsame_d) is:

$$MBCsame_d = DNAbias*(GRmean*totalDNA*FBratio*DNAexteffF*MBCDNA_d + GRmean*totalDNA*(1-FBratio)*DNAexteffB*MBCDNA_d) \quad (3.14)$$

If just MBC is extracted inefficiently, then the corresponding apparent new MBC produced (MBCsame_c) is:

$$MBCsame_c = DNAbias*(GRmean*totalDNA*FBratio*MBCDNA_c + GRmean*totalDNA*(1-FBratio)*MBCDNA_c) \quad (3.15)$$

If both MBC and DNA are extracted inefficiently, then the apparent new MBC produced (MBCsame_dc) is:

$$MBCsame_{dc} = DNAbias*(GRmean*totalDNA*FBratio*DNAexteffF*MBCDNA_{dc} + GRmean*totalDNA*(1-FBratio)*DNAexteffB*MBCDNA_{dc}) \quad (3.16)$$

When bacterial growth rate (*GRbact*) and fungal growth rate (*GRfun*) differ, the true MBC produced (*TrueMBCdiff*) is:

$$TrueMBCdiff = GRfun*totalDNA*FBratio*MBCDNAratF + GRbact*totalDNA*(1-FBratio)*MBCDNAratB \quad (3.17)$$

And the values for the true MBC produced under the various extraction bias scenarios are:

$$MBCdiff_d = DNAbias*(GRfun*totalDNA*FBratio*DNAexteffF*MBCDNA_d+$$
$$GRbact * totalDNA * (1 - FBratio) * DNAexteffB * MBCDNA_d) \quad (3.18)$$

$$MBCdiff_c = DNAbias * (GRfun * totalDNA * FBratio * MBCDNA_c$$
$$+ GRbact * totalDNA * (1 - FBratio) * MBCDNA_c) \quad (3.19)$$

$$MBCdiff_{dc} = DNAbias*(GRfun*totalDNA*FBratio*DNAexteffF*MBCDNA_{dc}$$
$$+ GRbact * totalDNA * (1 - FBratio) * DNAexteffB * MBCDNA_{dc}) \quad (3.20)$$

One of the assumptions of the ^{18}O-CUE method is that the turnover of labeled biomass is negligible over the course of the incubation. Assuming a steady microbial community biomass, the corresponding bulk turnover rates of 0.3 to 7% per day above indicate that this expectation is reasonable. However, the true DNA growth rate is likely to be higher, and the impact on estimates of microbial carbon growth to be mixed. Dormancy estimations vary widely, from 6 to 96% of the community observed as dormant (210; 287). Considering a scenario in which 96% of the community is dormant leads to a 24-fold underestimation of growth rate (0.96/(1-0.96)) due to dilution with the bulk pool, but only minimal underestimation if 6% are. Furthermore, factors such as predation could decrease apparent growth rate through the inefficient

re-allocation of labeled nucleic acids from primary to secondary consumers, particularly if predators selectively consume community members (107) within a narrow size range (32). Finally, as a result of the "live fast, die young" adage often attributed to copiotrophs, CUE is likely to be particularly underestimated when growth is concentrated in a small but rapidly growing fraction of the population compared to a larger but slower growing fraction. Our simulations accounted for an active community fraction varying from 1 to 99%. Therefore, the true growth rate is calculated as *GRfun* and *GRbact* multiplied by the *activeFraction* to account for dormancy:

$$GRfun = GRfun * activeFractionF \tag{3.21}$$

$$GRbact = GRbact * activeFractionB \tag{3.22}$$

3.3.4 Sensitivity of CUE to fungal removal

We assessed the sensitivity of observed CUE to various methodological assumptions using a few modifications to account for observed fungal:bacterial ratio. Unlike the simulations above, we wished to retain the inter-sample differences in MBC:DNA ratio and growth. Therefore we applied modifying factors to the original data using expected ratios between bacterial and fungal parameters, rather than imposing fixed values for these organism classes as above.

First, we converted the observed fungal:bacterial DNA ratio based on qPCR to a F:B DNA ratio. To do this, we assumed 82 ITS copies per genome (*ITSpergenome*) (Table 3.1) and a median genome size of $5x10^8$ bp for fungi (48; 172), and 2.25 16S copies per genome (*16Spergenome*) and a genome size of $5x10^6$bp for bacteria (48; 61).

To get the true fungal:bacterial DNA ratio *FBratio*, we had to back-calculate from the observed ITS copies *copiesITS* and 16S ribosomal RNA copies *copies16S* from qPCR. We then accounted for inefficiencies in DNA extraction as follows:

$$copiesITS = \frac{\frac{1}{DNAexteffF} * copiesITS}{ITSpergenome} \tag{3.23}$$

$$copies16S = \frac{\frac{1}{DNAexteffB} * copies16S}{rrNpergenome} \tag{3.24}$$

And then convert the 16S and ITS copies to fungal (*FDNA*) and bacterial (*BDNA*) DNA mass per gram of soil as follows:

$$FDNA = \frac{copiesITS * 5 * 10^8 * 650 * 10^6}{6.02214 * 10^{23}} \tag{3.25}$$

$$BDNA = \frac{copies16S * 5x10^6 * 650 * 10^6}{6.02214 * 10^{23}} \tag{3.26}$$

Where 650*10^6 is the molecular weight of the average DNA basepair in μg and 6.02214*10^{23} is Avogadro's constant. So the corresponding extraction-efficiency and marker gene per genome base pair corrected fungus DNA: bacteria DNA ratio (*FBratio*) is:

$$FBratio = \frac{FDNA}{FDNA + BDNA} \tag{3.27}$$

The corresponding corrected total DNA (*totalDNAActual*) in the initial pool (active and inactive) used for MBC:DNA ratio calculation is:

$$totalDNAActual = totalDNA * FBratio * \frac{1}{DNAexteffF} + totalDNA * (1 - FBratio) * \frac{1}{DNAexteffB} \tag{3.28}$$

We can then calculate relative fungal and bacterial contributions to the MBC pool for fungi (*fcont*) and bacteria (*bcont*), the actual amount of MBC (*MBCactual*) and the MBC:DNA ratios for each group as follows:

$$fcont = \frac{MBCDNAratF * MBCexteffF * FBratio}{MBCDNAratF * MBCexteffF * FBratio + MBCDNAratB * MBCexrteffB * (1 - FBratio)} \tag{3.29}$$

$$bcont = 1 - fcont \tag{3.30}$$

$$MBCactual = \frac{fcont * MBCobs}{MBCexteffF} + \frac{bcont * MBCobs}{MBCexteffB} \tag{3.31}$$

$$MBCDNAactual = \frac{MBCactual}{totalDNAActual} \tag{3.32}$$

$$FMBCDNAratio = \frac{\frac{fcont * MBCobs}{MBCexteffF}}{\frac{totalDNA * FBratio}{DNAexteffF}} \tag{3.33}$$

$$BMBCDNAratio = \frac{\frac{bcont * MBCobs}{MBCexteffB}}{\frac{totalDNA * (1 - FBratio)}{DNAexteffB}} \tag{3.34}$$

Now we calculate the *FBratio_active*, which is the fraction of new growth attributed to fungi during the incubation. It is a function of the relative growth rates of bacteria and fungi, as well as their *FBratio* in the starting bulk community and the fraction of the cells which are active, rather than dormant.

$$FBratio\_active = \frac{FBratio * activeFractionF * GRfun}{FBratio * activeFractionF * GRfun + (1 - FBratio) * activeFractionB * GRbact} \quad (3.35)$$

We can then account for DNA extraction (in)efficiency and the use of intracellular water/other sources of DNA oxygen for the growing community:

$$fungGrowthact = \frac{NewDNAobs * FBratio\_active}{DNAbias * DNAexteffF} \quad (3.36)$$

$$bactGrowthact = \frac{NewDNAobs * (1 - FBratio\_active)}{DNAbias * DNAexteffB} \quad (3.37)$$

Finally, we convert these DNA growth to the MBC growth which occurred after applying our methodological bias corrections:

$$MBCgrowthactual = fungalGrowthact * FMBCDNAratio + bactGrowthact * BMBCDNAratio \quad (3.38)$$

And calculate CUE using the observed respiration rate (per day):

$$CUE\_actual = \frac{MBCgrowthActual}{MBCgrowthActual + respiration} \quad (3.39)$$

3.4 Results and Discussion

3.4.1 Growth bias depends on extraction bias and FB ratio

Our Shiny app simulations showed that observed microbial growth deviated most from true microbial growth at intermediate fungal:bacterial ratios, and when fungi

and bacteria grew at different rates (Fig. 3.2). If only bacteria or fungi are present the active community is better represented by the total community and the MBC:DNA ratio of the active community is as well represented as possible in the MBC:DNA ratio of the starting community. We also found that if groups of microbes with distinct MBC:DNA ratios grow at the same growth rate, then the ability of the ^{18}O method to reliably estimate the increase in MBC is insensitive to any differences in the DNA extraction efficiency. This is demonstrated as the observed and actual MBC growth falling on the 1:1 line over all FB ratios, and can be explained by the DNA being underestimated by equivalent amounts in both the total community used for MBC:DNA conversion and the active community extracted. However, misestimating the MBC extraction efficiency leads to incorrect microbial growth values whether or not bacteria and fungi grow at the same rate (Fig. 3.2, center column). While a mathematically simple scenario to explain, this is particularly alarming because CFE extraction efficiency depends on a wide range of experimentally-relevant features. This includes the ratio of intracellular (cytoplasm) to extracellular (membrane, extracellular polysaccharides, proteins) carbon, which is known to differ with community structure and growth rate (69; 122) and edaphic parameters such as soil pH, water and clay contents (5; 251).

3.4.2 CUE estimates are sensitive in the presence of metabolic water

Using a sensitivity analysis and varying one factor at a time, we found that the deviation of observed microbial growth from true growth was most sensitive to metabolic water content across all extraction scenarios (Fig. 3.3); the sensitivity value was 1 throughout. The first uses of the ^{18}O method for CUE assumed that

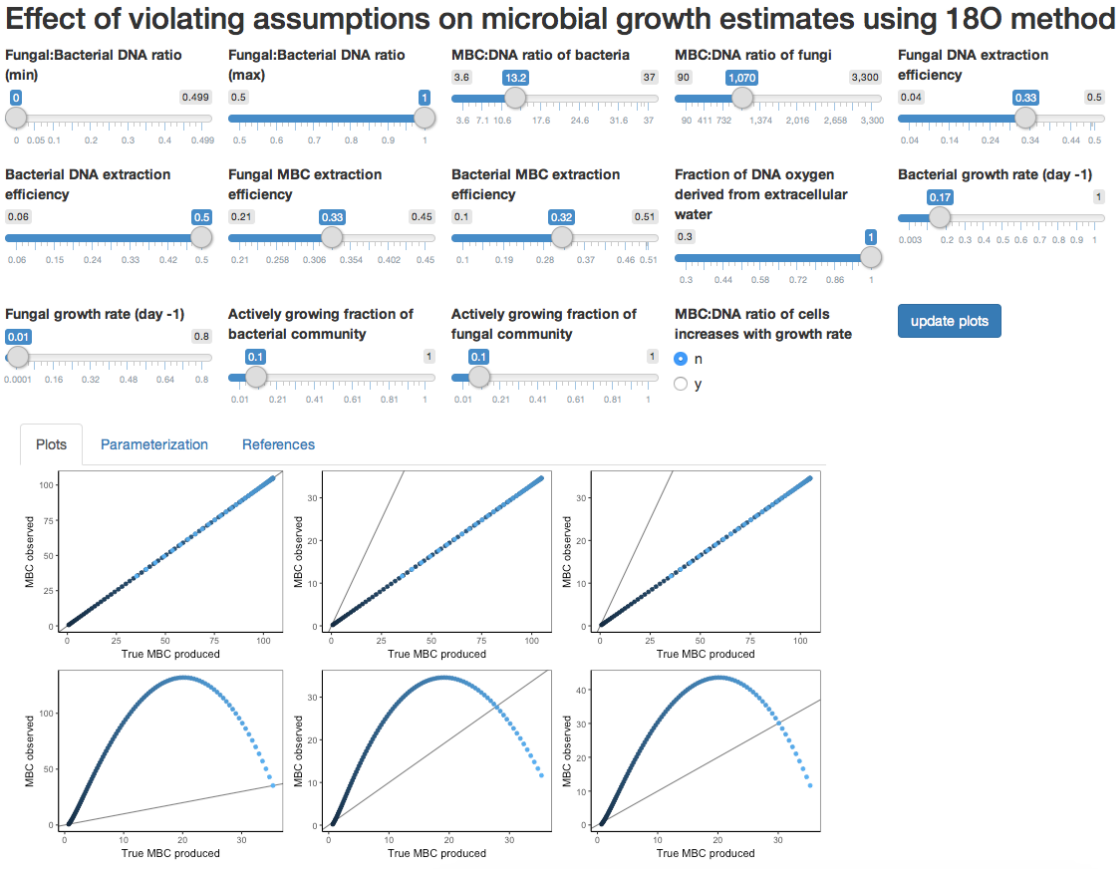

Figure 3.2: Screenshot of Shiny app used to visualize the effect of methodological error on microbial biomass carbon estimates. Each point denotes a community simulated for a different fungal:bacterial DNA ratio, with darker points representing a more bacterial community (in this instance, FB = 0) and lighter blue a more fungally-dominated community (here, FB ratio of 1). The black diagonal denotes the 1:1 line, such that values above the line indicate overestimation of biomass, and those below indicate underestimation. Top row: bacteria and fungi grow at the same rate. Bottom row: bacteria and fungi grow at distinct rates. Left column: DNA extracted inefficiently. Center column: MBC extracted inefficiently. Right column: MBC and DNA both extracted inefficiently.

all DNA oxygen came from extracellular water (262), but it is known that *E. coli* only derives around 30% of its DNA oxygen from intracellular water when grown on rich media in the lab (118; 144). Under the less-than ideal conditions in the soil, the value is likely to be higher - from 70-98% of oxygen from extracellular water - as the contribution of intracellular water to DNA oxygen is lower in slower growing *E. coli* (144) and *B. subtilis* (166). The degree of ^{18}O enrichment in the phosphate backbone also decreases with temperature (31); since growth rate often increases with temperature, this is another mechanism by which growth may be underestimated in the fastest growing communities. On the other hand, the recycling of nucleotides and "cryptic growth" may be more important in slow-growing and nutrient-starved organisms, preferentially hiding growth in these communities. Moreover, we observed the suppression of respiration after addition of ^{18}O H_2O compared to ^{16}O water in three temperate deciduous forest soils (Fig. B.14), which could indicate that ^{18}O-H_2O undersestimates growth by suppressing metabolism. We still lack precise estimates of how important non-extracellular water sources are for DNA oxygen under *in-situ* conditions for bacteria or any conditions for fungi, making them important areas for future research.

3.4.3 Sensitivity of growth to methodological bias depends on heterogeneity in growth rates

With the exception of intracellular water contribution, MBC sensitivity to changes in the other parameters depended on both assumed extraction biases and whether bacteria and fungi grew at same or different rates (Fig. 3.3). In general, estimates were more sensitive to changes in the parameters when bacteria and fungi grew at

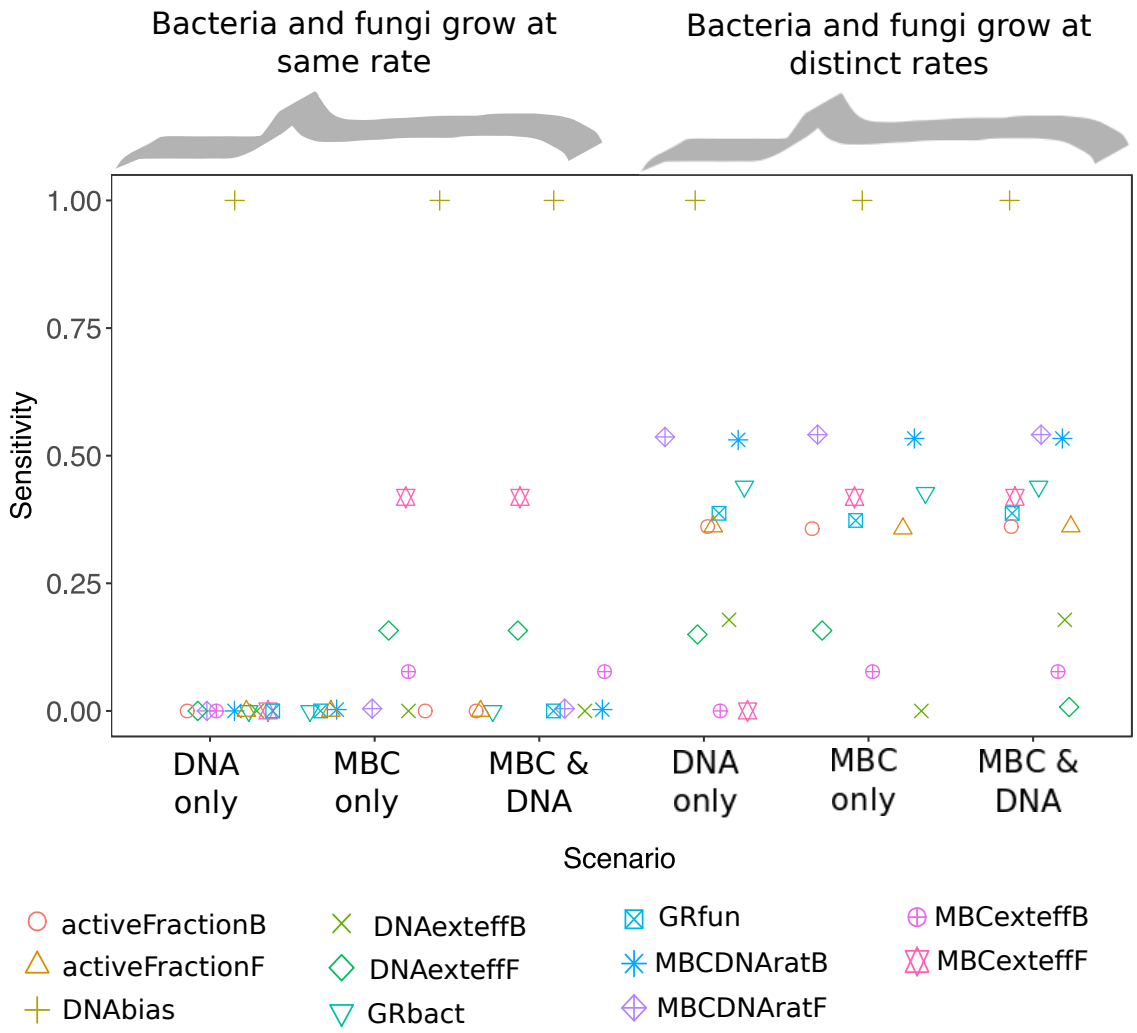

Figure 3.3: Sensitivity of difference between true and observed microbial growth values to violating various assumptions. Left: bacteria and fungi grow at different rates. Right both grow at the population level mean.

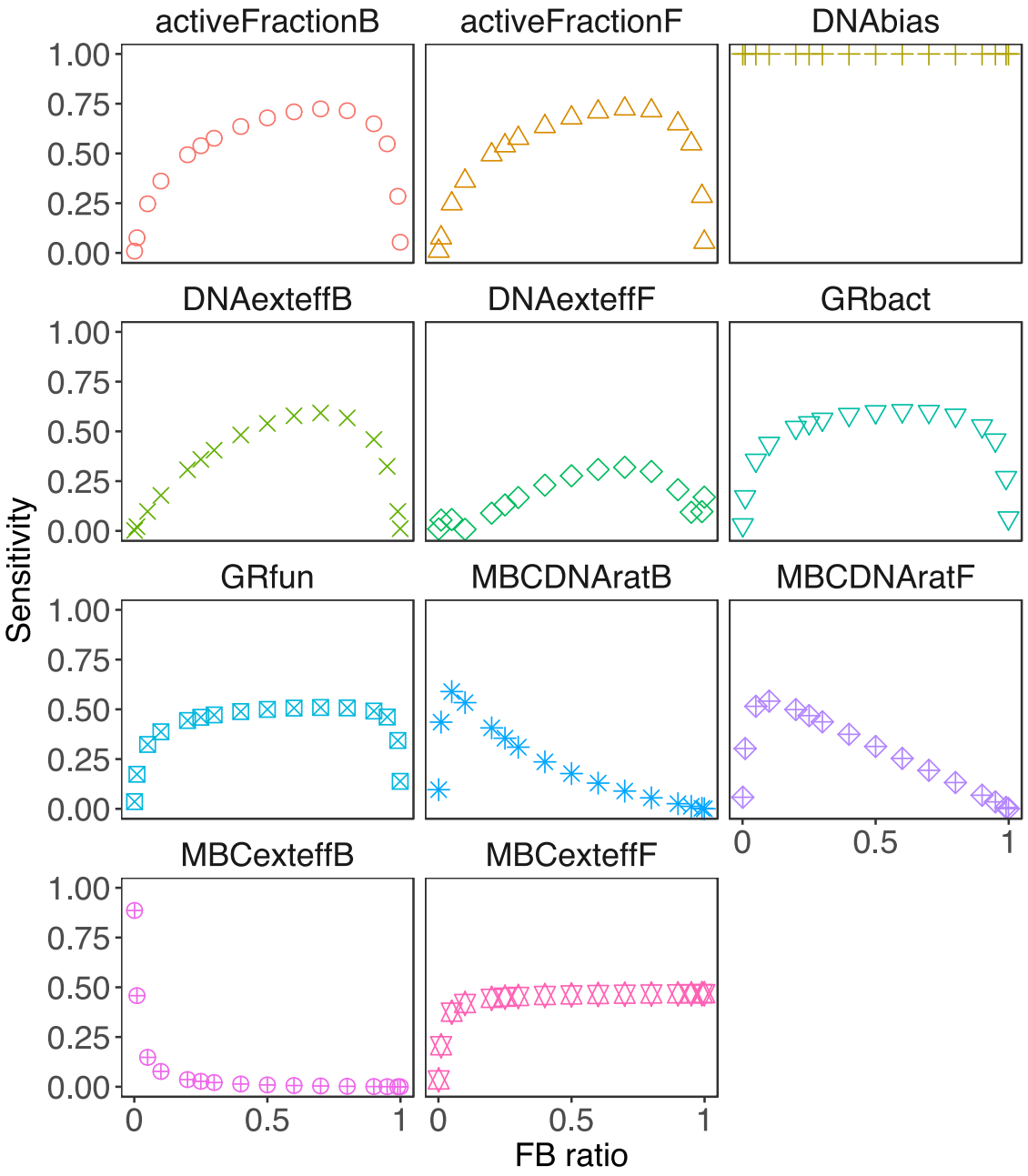

Figure 3.4: Sensitivity of MBC growth estimate error to variation in biological parameters and methodological errors. The plotted scenario assumes that DNA and MBC are both under-extracted, and that fungi and bacteria grow at different rates. Results for the remaining scenarios in Fig. 3.3 can be found in figures B.16,B.15,B.17,**??**, and B.18. Parameters are defined in Table 3.1

different rates rather than some community-level mean, in large part because the MBC:DNA ratio observed for the whole community was no longer representative of the growing population. Fungal MBC:DNA extraction efficiency had a similar effect on how far expected growth deviated from observed growth independent of whether bacteria and fungi grew at the same rate. Errors were also sensitive to bacterial MBC extraction efficiency, but less so. This is because despite slow DNA-based growth in the baseline condition, fungi have a very large MBC:DNA ratio and so contribute disproportionately to the MBC estimate. In a similar thread, errors were less sensitive to fungal DNA extraction efficiency because their growth rate is minimal under baseline conditions. To address this slow growth, researchers sometimes add different amounts of 18O-water to soils or incubate for different periods based on the growth rates of soils (95).

3.4.4 Sensitivity of errors in MBC estimations depend on fungal to bacterial ratio

Fungal to bacterial DNA ratio affected which parameters MBC estimates were most sensitive to, with these sensitivities also differing in their sensitivity to F:B ratio. For instance, MBC error had a sensitivity of approximately 0.5 over all intermediate values of fungal and bacterial growth rate, but decreased precipitously towards zero at FB ratios approaching 0 or 1. By contrast, sensitivity to bacterial DNA extraction efficiency was greatest around a FB ratio of 0.7, and to fungal DNA extraction efficiency at an FB ratio of 0.1-0.2. Sensitivity of MBC extraction efficiency for bacteria was almost zero, except at F:B ratios below 0.1, but almost 1 for fungal MBC extraction efficiency under these same scenarios. Assuming the DNA content

and rrN/ITS copy numbers in table 2, the F:B DNA ratio in both soil metagenomic sequences (225) and qpcr (89; 61) datasets are often less than 10%. As such, many soil samples are within the range of F:B DNA ratios where deviations in CUE estimates are highly sensitive to even small changes in fungal dominance, such that related samples within a study may differ in the kinds of methodological assumptions they are most sensitive to.

3.4.5 Effect of fungal removal on CUE

Fungal:bacterial ratio is one of the oldest and coarsest ways of differentiating microbial communities, with the ratio typically decreasing with depth and increasing with carbon content (23; 89). We found that our conclusions achieved with our simulations regarding the effects of fungal removal on CUE were confirmed by empirically excluding fungi from an artificial soil inocula. This is despite the observation that microcosms with bacteria only or both bacteria and fungi differed in the parameters they were most sensitive to (Fig. 3.6). For instance, bacteria-only microcosms were 2.9x more sensitive to bacterial biomass carbon extraction efficiency, but less than 1% as sensitive to dormancy than were the microcosms with both bacteria and fungi. This led to CUE estimates responding differently to the same assumption in the two community types (Fig. 3.5). The observed, "uncorrected" CUE was on average only 25% as high in communities with fungi excluded than those with fungi for the raw data (Fig. 3.5, solid grey line). No scenarios led CUE in bacteria-only microcosms to approach that of the mixed fungal and bacterial microcosms (ratio = 1; dashed line). This is likely because bacteria dominated in both bacteria-only and mixed microcosms, and was estimated to account for greater than 99% of the DNA. This

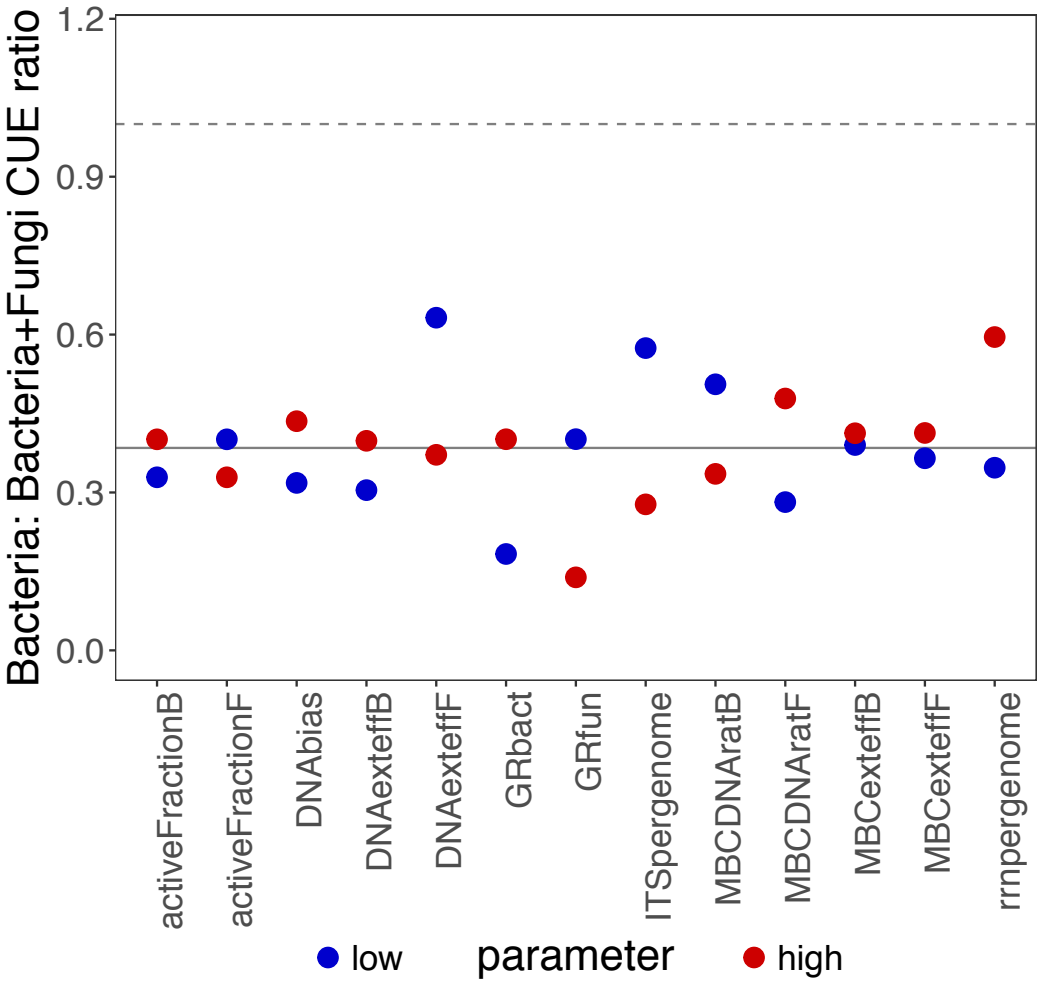

Figure 3.5: Ratio of CUE in artificial soil microcosms inoculated with the "bacterial" ($\leq$0.8um) fraction of soil microbial communities to the value in "complete" soil communities ("bacteria and fungi"). The x-axis denotes which one of the parameters was tested, and dot colour denotes whether the simulated CUE correction was applied at the highest value observed in a literature search, or the lowest. Each value is the median ratio for 6-8 raw replicates of each community type. The grey line denotes the median uncorrected CUE.

imbalance in fungal abundance is much greater than the MBC:DNA ratio for fungi would need to be in order to overcome their much slower growth rates compared to bacteria in our simulations.

Increasing the mean bacterial rrN per genome or decreasing the mean fungal ITS copies per genome increased the ratio of bacteria to bacteria + fungi CUE by decreasing the bacterial contribution to the total DNA pool. However, because fungal DNA was either absent or nearly absent from bacteria-only microcosms, this impacted the mixed community microcosms much more strongly. Since bacteria grow much faster than fungi by default in the model, reducing bacterial contribution to growth in the mixed microcosms enabled the high MBC:DNA ratio fungi to contribute more, and, in turn, increasing estimated MBC increment and CUE. All together, these results indicate that the observation of reduced CUE in communities where fungi were filtered out is not due to a single methodological bias.

Early studies of bacterial vs. fungal CUE proposed that bacteria should be less efficient than fungi because of their lower biomass CN ratio (257). Our results do not dispute that bacteria are less efficient than fungi, as the pattern held even with extreme corrections to CUE. Furthermore, recent work explicitly accounting for differences in bacterial and fungal growth rates and biomasses have found lower CUE in fungal-dominated communities (253). However, our results do illustrate the benefits of sample-specific conversion factors. Microcosms differed in the assumptions their CUE estimates were most sensitive to (Fig. 3.6), and biological differences between samples can alter the degree of methodological correction required. In other words, there are a number of possible methodological biases introduced by the act of using

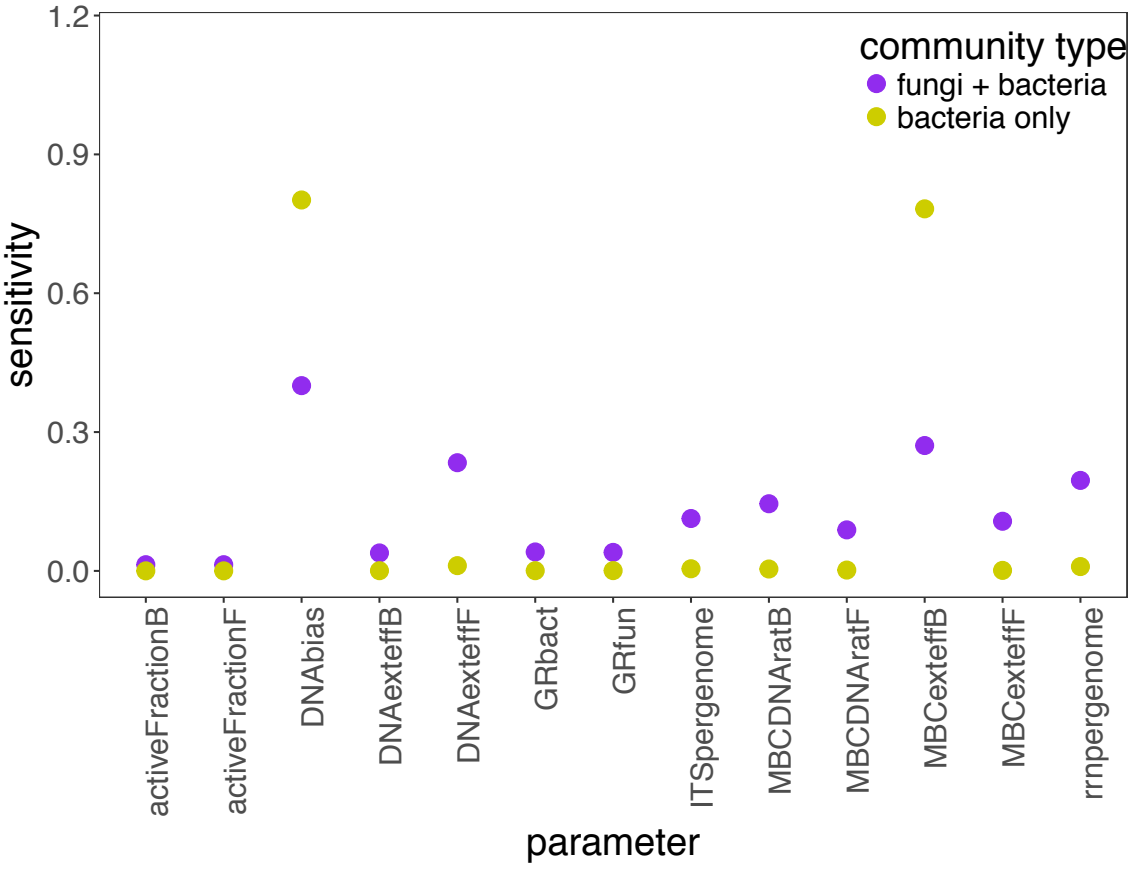

Figure 3.6: Sensitivity analysis of CUE under various methodological biases for microcosms inoculated with a filtered ("bacteria only") or unfiltered ("bacteria and fungi") soil inoculum. Here, sensitivity represents the deviation between the observed and simulated CUE values under the high and low parameter values presented in Table 3.1

a single set of conversion factors for communities with and without fungi. First is that the bacterial communities are dissimilar in composition between the two treatments, with more Gram-positive Actinobacteria in bacteria-only microcosms than bacteria+fungi microcosms. The MBC:DNA ratio of the bacteria-only microcosms was very low, sometimes below 1, indicating that the bacterial biomass carbon was not efficiently extracted. By contrast, observed MBC:DNA ratios of natural soil communities generally fall between 3 and 60 (16; 263), with values as low as 3.6 for bacteria and as high as 3300 for filamentous fungi in the lab (File S1). In addition, the true MBC:DNA ratio of bacteria is lower for small, slow-growing and starving or oligotrophic cells (51; 50; 165). Small cells have a large amount of membrane (which CFE does not effectively capture (69; 122)) relative to cytoplasm (which it does), therefore exacerbating the genuinely lower MBC:DNA ratio. Although we lack empirical evidence for smaller bacterial cells in the absence of fungi, this could explain the apparently low MBC:DNA ratio and necessitate using different extraction efficiencies and MBC:DNA conversions in the two communities. However, we also note that the ^{18}O method of microbial growth determination already requires a number of assumptions to be made, so making additional assumptions should be done with care.

3.4.6 Shortcomings

Many of the values used to parameterize these simulations are based on isolates grown in the lab under ideal conditions. However, microbes are known to grow very differently in the lab compared to in soil. For instance, well-fed bacterial cultures will have lower dormancy and less starvation-induced reductive cell division than

those found in soil (165). Cultivation bias towards fast-growing organisms only exacerbates this, as the (CFE-measureable) cytoplasm:(CFE-ignored) cell membrane ratio will be greater in the copiotrophic organisms we tend to study in the lab (228). The DNA:MBC ratio has been observed to be higher in small, slow-growing cells in communities extracted from soil (50), but to remain constant over a wide range of growth rates in *E. coli* (77; 147). Given how poorly-defined this relationship is, we did not include it as a component in our simulations, although the sensitivity of biomass increment estimates to this parameter indicate that - should such a pattern exist - it should have been accounted for. Furthermore, we note that the contribution of intracellular water to DNA oxygen was 70% for fast compared to 4% in slow-growing bacterial culture on rich media. Therefore, it is likely important to account for intersample differences in the contribution of ^{18}O-H_2O to DNA water as a function of growth rate. However, in the absence of knowledge about where bacterial and fungal growth in soil fit on this intracellular water spectrum, we did not include this parameter in our simulations. Finally, determining the true contribution of different groups of microbes to the soil DNA pool remains challenging; accurate predictions based on metagenomes are limited by both database biases and the abundance of non-coding DNA in eukaryote genomes, while imperfect primers and differences in ribosomal RNA operon copy number limit the utility of QPCR. As such, correction factors for microbial biomass carbon estimates will always be limited by the accuracy of fungal to bacterial ratios in the present simulation framework.

3.5 Conclusion

CUE is an essential descriptor of soil carbon cycling, with interesting ramifications for both the ecology and biogeochemistry of soil. There is great interest in measuring this parameter, but also a growing awareness of the various shortcomings in its quantification. Here we focused on one method - ^{18}O water incorporation into DNA, arguably the most reproducible (95) - to examine how assumptions about what it actually measures affects the conclusions drawn from its estimation. We evaluated how inefficient biomolecule extraction, deviations in microbial growth rate from the population mean, and heterogeneity in microbial community composition affected how far off observed microbial growth values are from their true values. We found that measurements are particularly sensitive to the use of oxygen sources other than extracellular water, a value which has been shown to change with experimental variables such as temperature and growth rate under controlled conditions in the lab. Despite this and other possible biases affecting the CUE we observed in our lab study, our conclusions regarding reduced CUE following fungal removal held. Nonetheless, our results do not account for the possibility that the biology underlying the observed differences in CUE may necessitate sample-specific correction factors, for instance assuming lower MBC extraction efficiencies in clay-rich or nutrient-poor soils compared to more organic soils. However, a more complete understanding of the constraints on and biological factors driving the importance of the biases proposed here is needed if these sample-specific correction factors are to improve - rather than worsen - the degree of measurement bias in CUE. For the time being, we therefore strongly encourage other studies to use the model script that we developed here as

a springboard for evaluating how robust their own conclusions are to the various ^{18}O-H_2O CUE method assumptions.

CHAPTER 4

CONCLUSIONS AND CONTEXTUALIZATION

4.1 Abstract

The measurement of microbial carbon use efficiency under ecologically relevant conditions and understanding its implications for the global carbon cycle remains challenging. In this dissertation, I critically assessed some of the current assumptions about CUE and its role in the ecology and carbon cycling of soil. However, considerable work remains. In this final concluding chapter, I further contextualize my research within the knowns, unknowns, and experimental failures in the hope that others may learn from my errors.

4.2 (Ir)relevance of liquid and litter studies for understanding soil organic matter turnover in a warmer world

At the beginning of this dissertation, I stated that carbon use efficiency (CUE) was a central driver of soil carbon storage (127). However, it is important to note that millennial-scale stability of soil carbon is primarily a function of soil mineralogy (75; 76). Young soils - such as those the majority of isolates used in this project were derived from - are thought to depend more on inputs as regulators of soil carbon stocks, and be much more susceptible to leaking carbon at elevated temperatures

than older soils (75). Biomass components and byproducts differ in their propensity for stabilization in soil (220; 254), so the identity of compounds produced during initial transformations and the efficiency of subsequent processing are also important for the formation of soil organic matter (SOM) on intermediate time scales (204). Liquid culture studies lack both the physical structure to induce these phenotypes, and the ability to measure the biological stability of these byproducts, however. As such, a robust understanding of the linkage between CUE and soil carbon stability necessitates organomineral interactions to be considered in parallel.

4.2.1 Experiments in artificial soil

In order to make progress towards improving our understanding of this area, we attempted to measure the CUE of bacterial isolates in a controlled artificial soil matrix consisting of sand, silt and clay. To do this, we took liquid cultures and inoculated them into artificial soil, and when they had started to respire, transferred these soil-adapted bacteria into fresh artificial soil. We then captured exponential phase by destructively harvesting tubes of soil at times which correlated with an exponential increase in respiration rate (Appendix D). Our initial study appeared promising, as we were able to detect respiration for five of the ten bacterial isolates when transferred straight from R2A plates to glucose media in the artificial soil (Figure 4.1). However, the variation across replicates was high; more than a quarter of the time points were characterized by a coefficient of variation exceeding 100%.

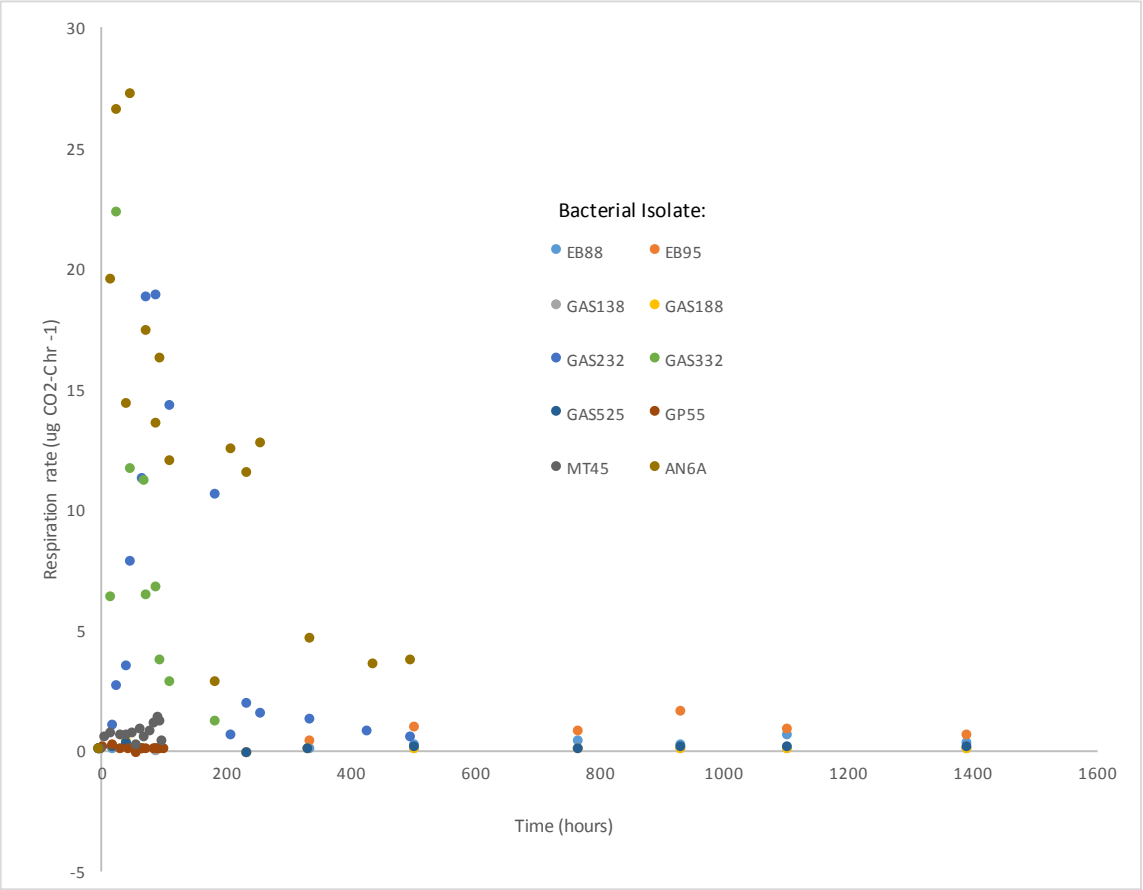

Figure 4.1: Respiration rates for bacterial isolates inoculated into artificial soil. Isolates growing on R2A6 were inoculated into Roller Glucose media which was diluted to an OD of 0.01 (except AN6A, which was accidentally not diluted), and then 1.2mls of this was used inoculate 5g of artificial soil. CO_2 measurements were taken on the stoppered tubes, and the CO_2 produced between measurements was divided by the time passed between consecutive timepoints in order to determine the respiration rate. CO_2 production rates above that of the uninoculated control tubes were not detected for Acidobacterium EB88, Actinobacteria GP55, or the Alphaproteobacteria GAS138, GAS188, and GAS525.

Unfortunately, bacterial growth was too weak and erratic to measure CUE following a second transfer on glucose media to ensure soil acclimation. For instance, despite robust growth at 15°C in liquid glucose media, GAS332 was never observed

to survive transfer to the artificial soil matrix at this same temperature (Appendix D). Likewise, three weeks after inoculation into artificial soil with potato dextrose broth, four of five isolates tested at 20°C did not have respiration rates above the negative control, despite showing respiration in a liquid culture set up in parallel. Only the *Bradyrhizobium* AN6A - an extremely fast grower - was able to grow in the artificial soil in a reproducible manner (Fig. D1, Fig. D2).

One such reason for failed or sporadic growth may be that media supplied to the microbes became strongly sorbed to the surface of the soil, leaving them effectively starved. However, this is unlikely because we were able to recover almost all the carbon added with a dilute potassium sulfate solution during a preliminary trial. Alternatively, the surface charges of the clay may have been damaging to the cells. However, the class of clay we used (bentonite) is thought to be minimally toxic to *Bacillus subtilis* compared to other minerals (176). We found only weak evidence for toxicity, which manifested itself as a large but non-significant decrease in respiration in the presence of clay but not the other soil components (Fig. 4.2). That we managed to get growth at all in the presence of the artificial soil could indicate that moisture limitation could play a role in restricting the growth of taxa in the soil, or that they need the additional organic nutrients provided in this experiment to tolerate the soil environment. The effect of soil component addition on respiration and growth is also likely to have a pH component, as the pH optimum of this organism is 5.5 (range =3-9), and the soil (7.6), silt (9.0), and clay (8.0) have high pH. The soil also has a strong buffering capacity, and needs 1M MES buffer to keep its pH; it is likely this originates from the clay fraction, as it was the only soil component able to resist pH

change in the presence of $100mu$M g^{-1} clay hydrochloric acid. As a result, the four isolates we extracted and characterized from the microcosms had both higher pH optima (6.5-7) and maximum (11) than the GAS332 we could not grow in the soil. Therefore, the combination of low temperature and high pH may have additively stressed GAS332, preventing it from growing sufficiently in the artificial soil at 15°C.

A follow-up experiment using these bacteria pre-selected on the artificial soil provided evidence that isolates can grow on the artificial soil. In this experiment, bacteria were taken straight from a plate with complex media and mixed into artificial soil pre-ammended with leaf litter DOC, yeast extract, vitamins and minerals, cellobiose, and ammonium nitrate. The tubes were then provided a weekly addition of ammonium-nitrate and cellobiose as sources of carbon and nitrogen. Of the four isolates tried (BS19, BS40, BS60, and BS71), two were still showing strong CO_2 production after 70 days. Nonetheless, while this study demonstrated that bacteria can grow in isolation in the artificial soil matrix when provided a mixture of substrates, we are yet to test whether these isolates can do so when fed the defined media we used in our liquid CUE measurements. The DOC and yeast extract initially provided may have all been consumed in the two cases where the bacteria ceased to grow, indicating that pH is not the only challenge with the translating the liquid culture studies into soil.

Despite their challenges, soil-based CUE measurements with isolates remain necessary for advancing our understanding of CUE, and in particular how the presence of a soil matrix might affect how microbial CUE responds to temperature. To attain this goal, it is likely we would need to compromise and move from attempting to

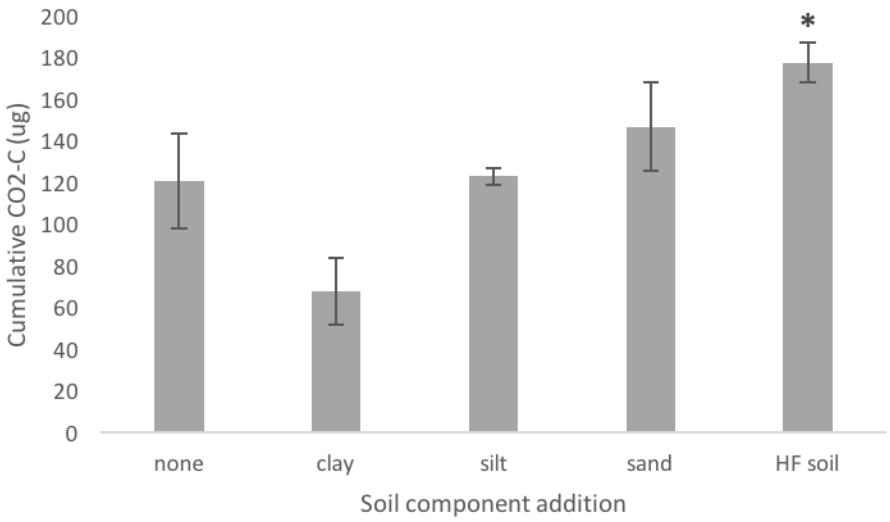

Figure 4.2: Cumulative respiration of Burkholderia GAS332 in liquid culture with the addition of 0.5g soil component per 5mls glucose Roller medium. Tubes were inoculated in a pair-wise manner (one colony split between each treatment for each replicate) and incubated at 15°C. This isolate can grow well at 15°C in liquid culture, but not the artificial soil, indicating that the soil environment contributes some additional stress which we wished to parse out. A paired t-test was used to assess whether soil component addition (or ashed Harvard Forest (HF) mineral soil with the organic matter removed) suppressed cumulative respiration. Differences in respiration may be driven in part by changes in pH, with clay raising the pH of the media to 7.5 and silt to 6.5; sand and HF soil did not cause pH to deviate far from the media-only value of 5.5, which is the pH optimum of the isolate.

measure CUE on defined media during exponential phase to doing so on a mature population grown in the presence of additional organic nutrients the artificial soil. In light of the methodological deficiencies of the ^{18}O method highlighted in this dissertation, it may be the case that the ^{18}O method is better suited for these kinds of isolate-based studies than the natural soil communities it is commonly used for at present. Nonetheless, this approach still would have only allowed an assessment of CUE effects on short-term SOM formation in the presence of "bare" minerals, and not the longer-term stabilization processes responsible for earth-climate feedbacks.

4.2.2 Limitations of modeling

The modeling approach used here is likewise limited in its applicability to soils in that it simulates microbes decomposing leaf litter, and therefore neglects to consider organomineral interactions (75; 137) and plant-microbe feedbacks known to be important for longer-term soil carbon trajectories (258; 265). This includes not only processes such as sorption which regulate the quantity and quality of substrates available to the decomposer community (288), but also spatiotemporal heterogeneity in enzyme turnover and oxygen availability (97; 273). We attempted to model the recycling of organic matter in a mineral soil, following the sorption-desorption kinetics equations implemented in MEND (288) and feeding the mineral soil solely on leached monomers from the litter or organic horizon model. However, we found that the microbes in the litter model were too efficient at taking up the monomers they produced, and the mineral soil communities ended up being starved out. Increasing the fraction leached to 100% of the monomers left over after uptake by enzyme producers did not remedy this, and decreasing the uptake efficiency of the organic

model taxa just caused them to starve out. A possible remedy would be to couple these modifications with a decrease in enzyme and uptake transporter production costs in the organic model, but tweaking the parameters like that became beyond the scope of this project. Furthermore, given that other models much better suited for modeling mineral soils already exist (273; 288; 295), it may be more fruitful to feed leached outputs from litter DEMENT into one of these other models rather than trying to generate a vertically-explicit DEMENT.

Another challenge with modeling is that the strong costs of extracellular enzyme production assumed to contribute to low CUE in DEMENT did not play out in our own data. We discussed at length why it is unsurprising that we missed this tradeoff in our empirical data in chapter 1. However, we have both theoretical calculations for the metabolic costs for producing these enzymes and additional empirical evidence demonstrating that extracellular enzyme production does not always suppress CUE. For instance, CUE decreased with substrate quality (t-test for glucose vs. cellobiose $p<0.01$) only in GAS479 (Fig. 4.3). This is important because GAS479 is the only isolate whose genome encodes a cellobiose phosphorylase and a 6-phospho-beta-glucosidase, but lacks a betaglucosidase, indicating it must obligately take up cellobiose in a manner which reduces the ATP investment required for its use. One explanation for the lack of enzyme costs might be that the catalytic efficiency in liquid is very high and the turnover (degradation) of the enzyme is slow, such that extracellular enzyme production is too small of a fraction of metabolism to detect a cost under assay conditions. However, this pattern would not have been observed unless GAS479 also did not make use of its cellobiose uptake machinery. It is challenging

to determine whether extracellular enzyme production is indeed a substantial cost to growth efficiency, however, due to the presence of numerous confounding factors (180).

If indeed exoenzyme production is cheap, then this indicates that there could be substantially greater loss of litter carbon pools under warming than the current implementation of DEMENT would believe. As my own study demonstrated, how extracellular enzyme costs tradeoff with CUE temperature response is essential to predicting the degree to which litter carbon will be lost. Yet we lack empiricial evidence for how enzyme production may be linked with other relevant, non-CUE traits either. For instance, increased growth rate requires an increased rate of substrate supply. Organisms with high ribosomal RNA operon copies are able to sustain higher growth rates in rich media than those with fewer (66), which indicates that high growth rate and low efficiency may be associated with increased genomic allocation to the acquisition of resources. However, this does not appear to be the case: in fact, both the number and genomic density (genes per MBp) of proteins with signal peptides (required to be targeted to the membrane or outside the cell) actually shows a weak negative correlation with the rrN (and log rrN) for the public bacterial genomes sequenced by IMG (pearson correlation = -0.24 for log rrN, or -0.22 for rrN; p¡0.01). The number of predicted transmembrane domains does, however, show a positive correlation with rrN, indicating that uptake rather than hydrolysis may limit growth. Together these results indicate that it is uptake costs rather than extracellular enzyme activity we should be focusing on the costs of in future iterations of DEMENT.

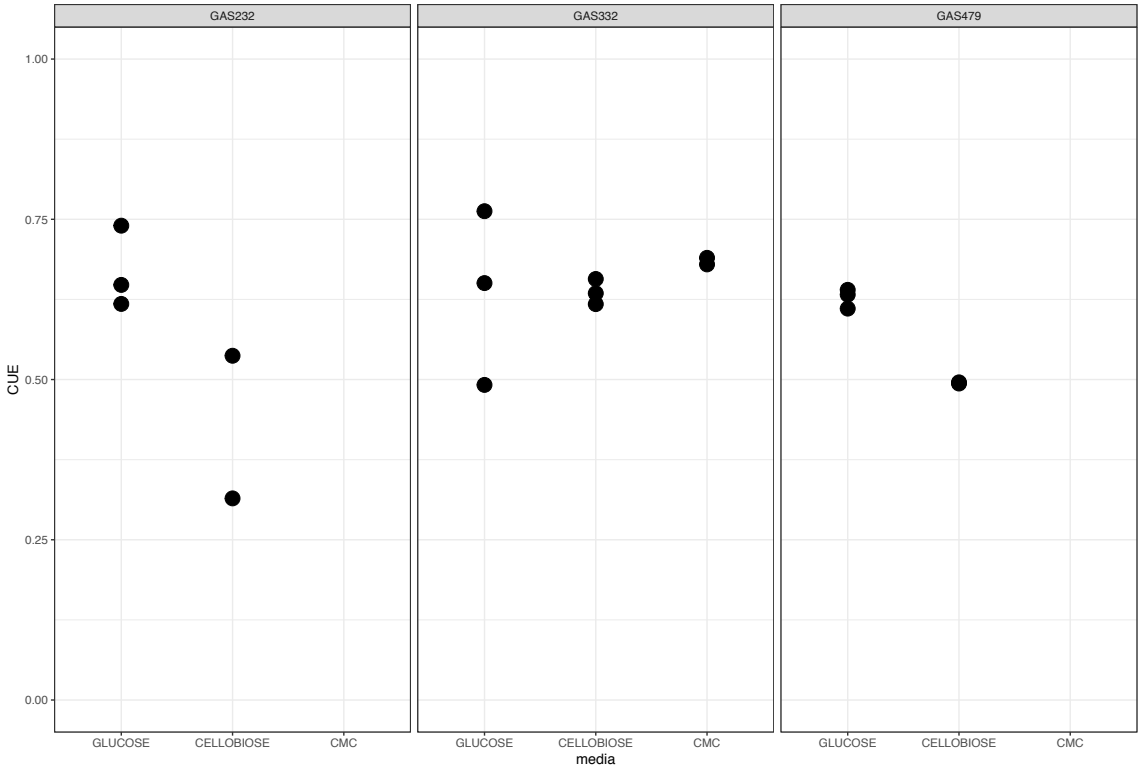

Figure 4.3: Effect of increasing substrate complexity on CUE. Bacteria were grown for CUE as in chapter 1, with 2-3 replicates per condition (missing data indicates bacteria did not grow on that media). GAS479 is a Firmicutes selected because it has the genomic potential to take up cellobiose as a dimer and phosphorylate it inside the cell, whereas GAS332 (Betaproteobacteria) and GAS232 (Acidobacteria) were selected to represent isolates with different growth rates who were predicted based on their genomes to be able to grow on all three substrates.

4.3 Predicting efficiency from genomes

Although using comparative genomics is technically much simpler to complete then transcriptomics, the candidate markers of CUE it identifies may have little to do with differences in the CUE of taxa. Examining genomes enables identification of functional potential, but cannot tell us anything about the degree to which those genes are expressed during our CUE measurements. Indeed, many of the markers of CUE identified may have just been present in genomes of more or less efficient taxa by chance. In other words, I identified correlates of CUE without knowledge of them as being drivers of CUE. In the context of identifying markers of high CUE in mixed communities, the lack of causation is relatively unimportant. But for the grander question of understanding why some organisms are more efficient than others, the approach falls short.

I naiively originally intended to calculate the organism-specific energy yield for the three defined media types using the tools available in KBASE. This is based in the proposition that while copiotrophs may optimize ATP hydrolysis to fuel costly protein biosynthesis, oligotrophs optimize biomass (therefore the optimization functions are expected to differ between trophic strategies). Given the overall aim of my project to identify markers and methods which can be extended to additional organisms, I elected to use the readily-scalable KBASE platform for this purpose. KBASE depends on the SEED subsystem annotations, which are manually-curated families of proteins with known functions that are connected by (metabolic) reactions. These annotations are based on a core set of well-defined model organisms, and should be extendable to other organisms. However, metabolic models often

fail to grow in the absence of gapfilling, even under conditions the corresponding organism is known to survive under (80). This was true for all twelve of my isolate genomes I tried to build metabolic models for, which prevented calculations of metabolic complexity and energetic yield to be made. One approach has been to neglect the strong incongruence between physiology and genome-scale models (242). Alternatively, Edirisinghe and colleagues (2016) developed a core metabolic modeling tool which defines growth costs on the ability to produce a core set of metabolites, overcoming the gapfilling problem. As a result of this simplification, the authors were able to get "growth" of 70% of organisms without gapfilling, compared to the much lower values typically observed using the "full" model. In contrast to "full" metabolic models where biomass production (yield) is optimized during flux balance analysis, these core metabolic models are run with ATP hydrolysis as the the objective function (growth rate). This indicates that a copiotrophic ecological strategy is imposed on the bacteria during modeling, which contraindicates use of the method in my exploratory analysis. Furthermore, the underlying calculations of yield are based on *E. coli* metabolic precursor calculations; since I also wanted to determine organism-specific amino acid costs, this means that using KBASE in this manner to predict organism-specific amino acid biosynthesis costs wouldn't have gotten me any further than the Kaleta *et al.* (2013) approach I ended up using. Nonetheless, metabolic modeling methods are improving all the time, such that correlations between metabolic complexity, organism-specific protein production costs, and CUE will be more readily tested in the near future.

4.4 Biases in CUE measurements

4.4.1 EPS and extracellular products

For my dissertation, I used optical density as a metric of biomass, and later converted these measurements into biomass using a conversion factor. This was a practical necessity given the large volumes of culture needed to attain sufficient biomass for sampling, but may lead to a few possible biases in biomass estimates. One concern is failure to account for extracellular product formation, which may vary throughout the growth curve and differ between media. We measured CUE during exponential phase, as this is supposed to be the only reproducible phase of growth for a given set of conditions (245). Furthermore, extracellular products are produced primarily during decelleration and stationary phases (200; 250), so should not interfere with assays. While for the isolates assayed, we were able to confirm that extracellular enzyme production was not substantial over the course of CUE, EPS production did visibly occur for one isolate during exponential phase (EB95). This was apparent as a white cloud which appeared upon centrifugation in small volumes and made the media so viscous that the tiny bacterial cells were unable to form a pellet.

Although polysaccharides tend to have absorption peaks in the UV-range, biologically-feasible levels of EPS-like compounds absorb sufficiently at the "cell-detecting" wavelength of 600nm to interfere with biomass measurements (Fig. 4.4). By increasing the cell volume by up to 7 times (21), EPS may induce Rayleigh scattering and make optical density measurements unreliable. Unfortunately, there are no good quantitive ways to separate cells from EPS to directly quantify this effect. For instance,

microscopy can provide a reasonable estimate of the volume taken up by EPS, but its water content and carbon content differs from cells. Ultracentrifugation (27) is not practical due to tube size constraints which mean it would take 60 runs and 750 tubes per isolate. EDTA - which strips the EPS of the cations stabilizing it on the cell surface - may only capture a third of the EPS at best and still requires pelleting with the cells (42). And the most vigorous methods such as sulfuric acid digestion or ethanol co-precipitation also lyse cells (235). Therefore, using the argument that exponential phase should be reproducible (so cells captured at any point along exponential phase should have the same composition and behaviour as cells at any other point), we decided that the best approach was to try and co-precipitate the EPS and the cells and quantify them together. However, the OD:MBC conversion factors derived for our own cultures were not realistic, as the mass per OD was exceptionally low for oligotrophs and higher than expected for faster-growing cells, leading to no relationship between biomass and respiration in approximately 75% of our CUE calculations. We think this has to do with inadequate pelleting because the organisms we know have small cells (EB95, GAS188, GAS474, GP187) had very low MBC:OD conversions, independent of EPS production; this occurred despite pelleting cells at the top speed the bottles and centrifuge rotor were able to attain, and increasing the duration of the spin to four times longer than for the larger cells. Therefore, we used the published *E. coli* values in our calculations, even though these are not optimized for our OD setup.

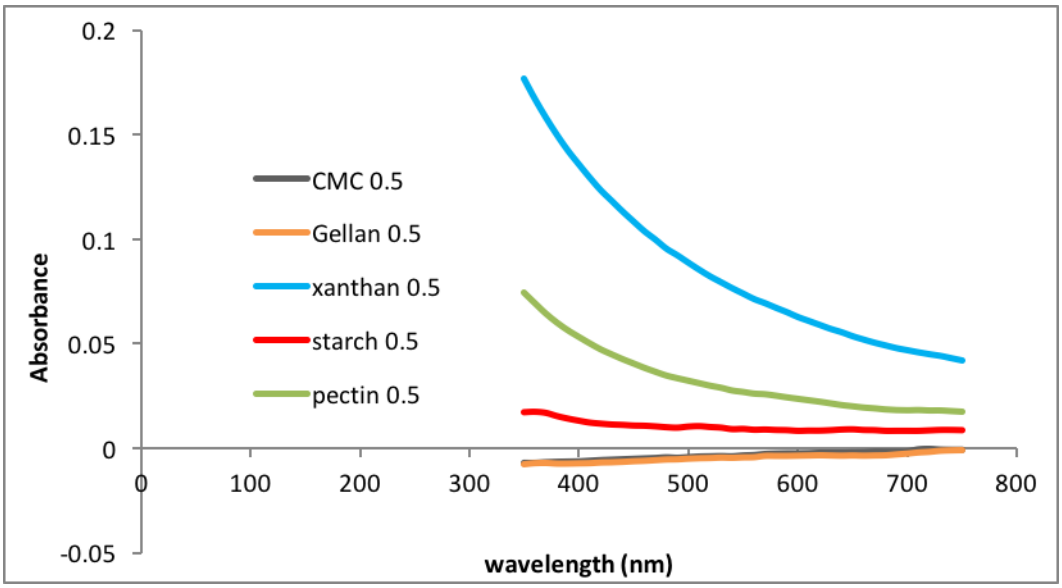

Figure 4.4: Absorption spectra for 0.5g/L of polysaccharides in water, which is equivalent to the upper limit of EPS produced by Acidobacteria in (134). At 600nm, xanthan gum gave an OD of 0.079 and pectin an OD of 0.033 under the conditions used for CUE measurements (i.e. using balch tubes and the tube spectrophotometer)

4.4.2 Taxon selection and cultivation bias

A central issue with extrapolating from the present isolate physiology to whole soil communities is the limited number of organisms studied, and the bias in selecting organisms for study. Specifically, there is an inherent cultivation bias, such that the more rapidly growing members of soil communities are overrepresented in our culture collection. Furthermore, isolates in our culture collection must be capable of growth in monoculture, which is not always true for those with symbiotic relationships. Additionally, the isolates used in this study must be able to grow to appreciable ODs in liquid media - which not all our isolates are - and to appreciable OD's without the addition of high levels of organic nitrogen. The OD requirement limited the number of Actinobacteria we were able to include in our analysis, as we found that - even with the addition of detergents, polysaccharides (113), or changing of ion concentration (74) - they retained aggregated growth in liquid culture. Therefore, our results are biased against organisms which have close interactions with other organisms in soil and those who are incapable of dispersed planktonic growth.

4.4.3 Assay conditions

Assay conditions were selected based on a compromise between maximizing the range of organisms which could grow with the need to not deviate too far from the soil conditions we ultimately intend to infer physiology in. For instance, although the mean annual temperature is approximately 8°C in the "ancestral environment" of the bacterial isolates we used, and reaches 25°C more than occasionally only in experimentally warmed plots, we assayed CUE at 15-25°C because growth was either too slow or absent at 8°C. Furthermore, the optimum growth temperature of

all isolates is between 20-30°C, with final biomass generally being higher at the lower temperature and growth rate greater at the higher temperature. We also used a pH of 6 rather than the soil pH of 3.7-4.5 because many of our isolates are unable to grow at such a low pH. Likewise, we decided not to shake our cultures during growth and instead to vortex vigorously between measurements, as GP187 was unable to grow with shaking and MT45 tended to form aggregates more. Finally, we measured CUE during exponential phase, which bacteria will only very rarely experience in soil (150). Despite the rarity of these "optimum" conditions in the field, the "hotspots" where they are attained have a disproportionate impact on soil-level processes and so it is possible that soil-level gas exchange can be adequately predicted just by looking at these small areas (211). Therefore, while the spatiotemporal frequency of our liquid culture assay conditions may be low in soils, they may disproportionately drive average values.

4.5 Conclusion

CUE is high but variable in soil bacteria, which confirms patterns seen when comparing mixed communities across ecosystems (181), but contrasts with the homogeneous value typically used in modeling studies (288; 295). Although heterogeneity in CUE has been observed to exist in communities, it is more commonly associated with substrate quality (258; 261; 275; 295) and/or high-level differences between bacteria and fungi (258; 261), rather than the consequence of species sorting selecting for bacteria with favourable trait combinations. By contrast, we found that this species-level heterogeneity is important for predicting the fate of litter car-

bon stocks in a warmer world, such that physiologically-diverse communities lead to more substantial carbon losses than homogeneous ones. Future work must explore the possibility that effect traits other than extracellular enzyme production may be linked with CUE temperature response if the results from this modeling is to go from the theoretical to the practical domain. Furthermore, we still lack a set of simplified marker traits for bacteria which may be highly sensitive to warming, which will limit the degree to which our results can be scaled. Nonetheless, we hope that together our lab- and modeling work has contributed additional constraints on how bacteria and communities are responding to the global climate crisis.

APPENDIX A

SUPPLEMENTARY TABLES

Table A.1: Regression coefficients for a phylogenetic generalized least squares model fit to CUE at a given substrate and temperature range versus ribosomal RNA operon copy number or the maximum growth rate observed across all assay conditions. Slopes are shown when the p-value is less than 0.1 (.), 0.05 (*), or 0.01 (**). Metabolic pathway count corresponds to the number of MAPLE (KEGG metabolic) pathways with $> 80\%$ completeness. CUE for EEA production corresponds to the theoretical fraction of carbon from glucose expected to be retained in the extracellular enzymes produced by the organism, rather than being burned to produce the ATP needed to make the corresponding amino acids de novo and then polymerize them into the proteins.

	CUE vs. GRmax	CUE vs. rrN	CUE vs. $\log_2$ rrN	Metabolic pathway count	CUE for EEA production
15-20°C glucose	-	-	-	-0.069 .	-
20-25°C glucose	-	-	-	-	-
15-25°C glucose	-	-	-	-	-2.71*
15-20°C pyruvate	-	-	-	-	NA
20-25°C pyruvate	-	-	-	-0.021 .	NA
15-25°C pyruvate	-	-0.068 .	-	-0.010*	NA
15-20°C succinate	-	-	-	-	NA
20-25°C succinate	-	-	-	-0.051 **	NA
15-25°C succinate	-	-	-	-0.022*	NA
15-20°C PDB	-	-0.071 .	-	-	NA
20-25°C PDB	-	-	-	-	NA
15-25°C PDB	-	-	-	-	NA

Table A.2: Genomic markers of CUE identified in exploratory and complete glucose datasets and confirmed by their presence as correlates of efficiency in the microcosms dataset or for at least two of the three remaining substrates in the liquid culture assays. Markers are included when the slopes were either both positive or both negative for the two datasets at an alpha of 0.05.

validation method	Temperature	corelation	KO
microcosms	15	negative	K09474 - acid phosphatase (class A)
			K01625 - 2-dehydro-3-deoxyphosphogluconate aldolase / (4S)-4-hydroxy-2-oxoglutarate aldolase
	25	negative	K00809 - deoxyhypusine synthase
		positive	K02167 - TetR/AcrR family transcriptional regulator, transcriptional repressor of bet genes
			K09815 - zinc transport system substrate-binding protein
other substrates	15	negative	K01733 - threonine synthase
			K07095 - uncharacterized protein
			K14441 - ribosomal protein S12 methylthiotransferase
		positive	K01752 - L-serine dehydratase
			K02016 - iron complex transport system substrate-binding protein
			K02072 - D-methionine transport system permease protein
			K03786 - 3-dehydroquinate dehydratase II
			K03825 - putative acetyltransferase
			K05596 - LysR family transcriptional regulator, chromosome initiation inhibitor
			K09780 - Uncharacterized protein
			K12256 - putrescine—pyruvate transaminase
	20	negative	K14441 - ribosomal protein S12 methylthiotransferase
		positive	K03442 - small conductance mechanosensitive channel
	25	positive	K00864 - glycerol kinase
			K02013 - iron complex transport system ATP-binding protein
			K02015 - iron complex transport system permease protein
			K02342 - DNA polymerase III subunit epsilon
			K05846 - osmoprotectant transport system permease protein

Table A.3: Genomic markers of the temperature sensitivity (Q10) of CUE identified in exploratory and complete glucose datasets and confirmed by their presence as correlates of efficiency in the microcosms dataset or for at least two of the three remaining substrates in the liquid culture assays. Markers are included when the slopes were either both positive or both negative for the two datasets at an alpha of 0.05, and model residuals met the assumptions of the pgls method.

validation method	temperature range	correlation	KO
microcosms	15-20	negative	K01638 - malate synthase [EC:2.3.3.9]
			K07222 - putative flavoprotein involved in K+ transport
			K02536 - UDP-3-O-[3-hydroxymyristoyl] glucosamine N-acyltransferase [EC:2.3.1.191]
			K03560 - biopolymer transport protein TolR
		positive	K06168 - tRNA-2-methylthio-N6-dimethylallyladenosine synthase [EC:2.8.4.3]
			K07023 - putative hydrolases of HD superfamily
			K08191 - MFS transporter, ACS family, hexuronate transporter
			K09747 - uncharacterized protein
			K11085 - ATP-binding cassette, subfamily B, bacterial MsbA [EC:3.6.3.-]
	15-25	negative	K01638 - malate synthase [EC:2.3.3.9]
			K02283 - pilus assembly protein CpaF
			K00389 - putative membrane protein
	20-25	negative	K00508 - linoleoyl-CoA desaturase [EC:1.14.19.3]
			K01858 - myo-inositol-1-phosphate synthase [EC:5.5.1.4]
			K09764 - uncharacterized protein
		positive	K02049 - NitT/TauT family transport system ATP-binding protein
			K07240 - chromate transporter
other substrates	15-20	positive	K08151 - MFS transporter, DHA1 family, tetracycline resistance protein
	20-25		K03417 - methylisocitrate lyase [EC:4.1.3.30]
			K19294 - alginate O-acetyltransferase complex protein AlgI

Table A.4: Effect of changing the reference CUE and enzyme costs against CUE on the stability and concievability of DEMENT outputs under three warming scenarios. *CUE_ref* is the CUE at 15°C, prior to calculating enzyme costs. *CUE_temp* describes whether CUE is const[ant] or var[iable] between taxa. *CUE_enz* is the maximum cost against CUE for enzyme production (with transporter costs parameterized the same). Stable is the fraction of runs where the microbial community constrained litter accumulation until the end. The median MBC, SOC:MBC ratio, and SOC in days 6000-10000 are shown, along with the biomass-weighted CUE of the active community at the end of this time. CN, CP, and NP refer to median elemental ratios of microbial biomass. Italicized values are those not deemed to be within the range of biologically plausible values.

CUE_ref	*CUE_temp*	Temperature	*CUE_enz*	stable	MedianMBC	Median SOC:MBC	Median SOC	CUEfinal	CN	CP	NP
	const	H	-0.1	0.71	57	*3.4*	198	0.44	4.5	49	9.3
0.58	NA	C	-0.1	0.97	67	*2.3*	142	0.41	4.6	43	9.3
	var	H	-0.1	0.86	107	*1.4*	144	0.53	4.7	43	9
	const	H	-0.1	0.98	36	9.2	331	0.32	4.5	43	9.4
0.48	NA	C	-0.1	0.93	37	7.6	241	0.31	4.3	39	9.1
	var	H	-0.1	0.9	70	*2.1*	137	0.42	4.6	42	9.3
	const	H	-0.2	0.64	20	54	*1041*	0.23	4.5	41	9.2
0.48	NA	C	-0.2	0.81	18	*131*	687	0.15	3.6	35	9.5
	var	H	-0.2	0.97	34	19	325	0.26	3.9	37	9.3
	const	H	-0.1	0.95	20	32	637	0.23	4.4	39	9
0.38	NA	C	-0.1	0.95	20	33	492	0.22	3.8	37	9.3
	var	H	-0.1	0.98	38	7.2	219	0.32	4.1	38	9.2

Table A.5: Median (or median-standardized interquartile range (IQRm)) output values for DEMENT model runs where C_t was either always positive, or always negative, marked according to warming effect (+/-) and model structure effects (letters) determined using Bonferoni-corrected post-hoc tests following linear mixed effect models. Symbols: "+" warming increased value; "-" warming decreased value). Letters: differences between warmed scenarios.

Fig. 1 scenario	A_i	G	A_{ii}	H
C_t ($^oC^{-1}$)	-0.011	-0.022 to 0	+0.011	0 to 0.011
LOM IQRm	0.29	0.23	0.21	0.30
SOM IQRm	0.26	0.15	0.21	0.19
Surviving taxa	11a+	9b	10a	8b
Enzyme count	16.5b	19a	15b-	18a
Shannon's H	1.92a	1.61a	1.86ac	1.64bc-
MBC (mg cm^{-3})	26.5b+	32.3a+	13.6d-	17.2c-
LOM (mg cm^{-3})	411.5c-	334.6d-	841.8a+	706.5b+
CUE at 15°C	0.23bc	0.23c	0.24a+	0.23b
CUE at 20°C	0.29b+	0.32a+	0.19d-	0.22c-
FB biomass ratio	0.85a	0.81ac	0.73bc	0.68b
Respiration (mg cm^{-3} day^{-1})	0.94c	0.96ac	0.90b	0.94abc
FB richness ratio	0.51a	0.46ac	0.40bc	0.43ac
CUE bacteria	0.27b	0.36a+	0.27b	0.25c-
CUE fungus	0.22c	0.29a+	0.23b+	0.18d-

APPENDIX B

SUPPLEMENTARY FIGURES

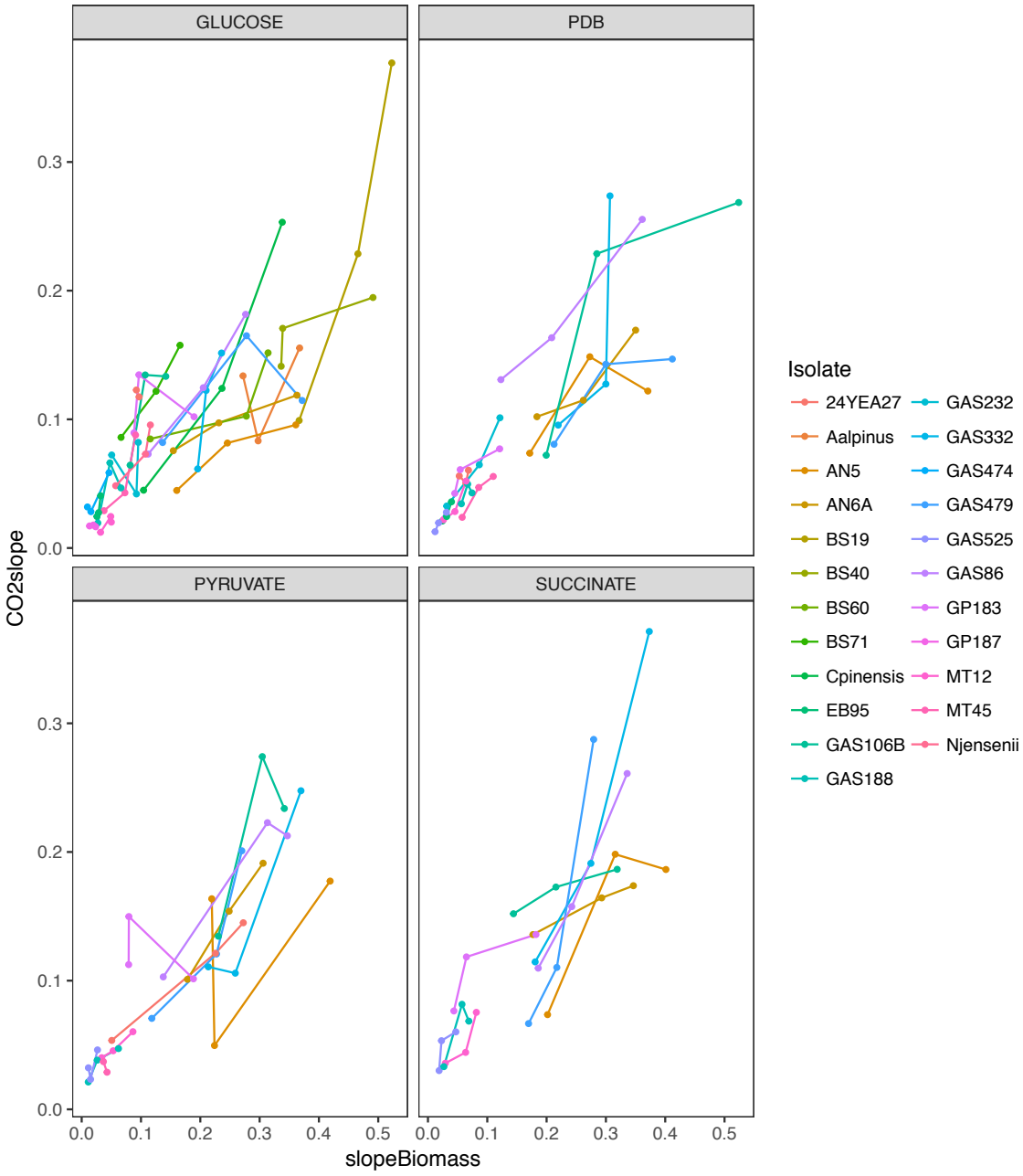

Figure B.1: Responses of mass-specific respiration and growth rate to changes in substrate and temperature. Lines are coloured by isolate, such that a point represents the mean respiration rate and growth rate for a given temperature and substrate for an isolate. Lines are drawn to ease visualizing points corresponding to a given isolate, and do not imply statistical support for the relationship depicted.

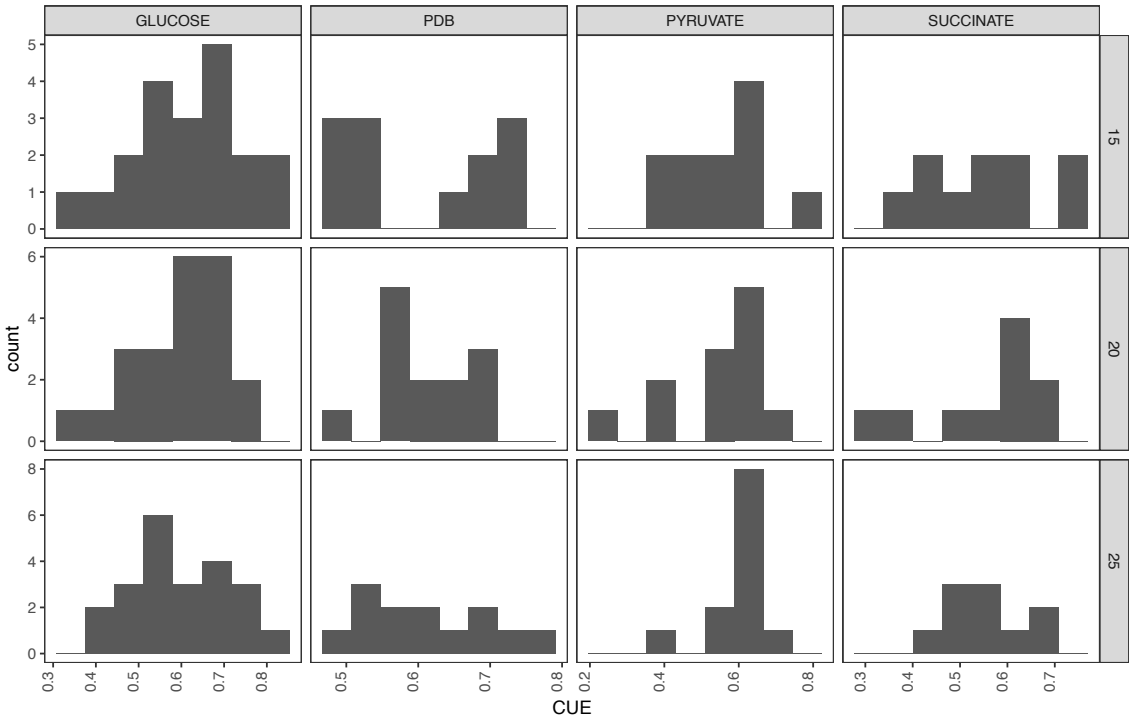

Figure B.2: Frequency histograms of CUE of isolates grown on the four media at three temperatures. Each count is the average of all replicates for a given isolate under that assay condition.

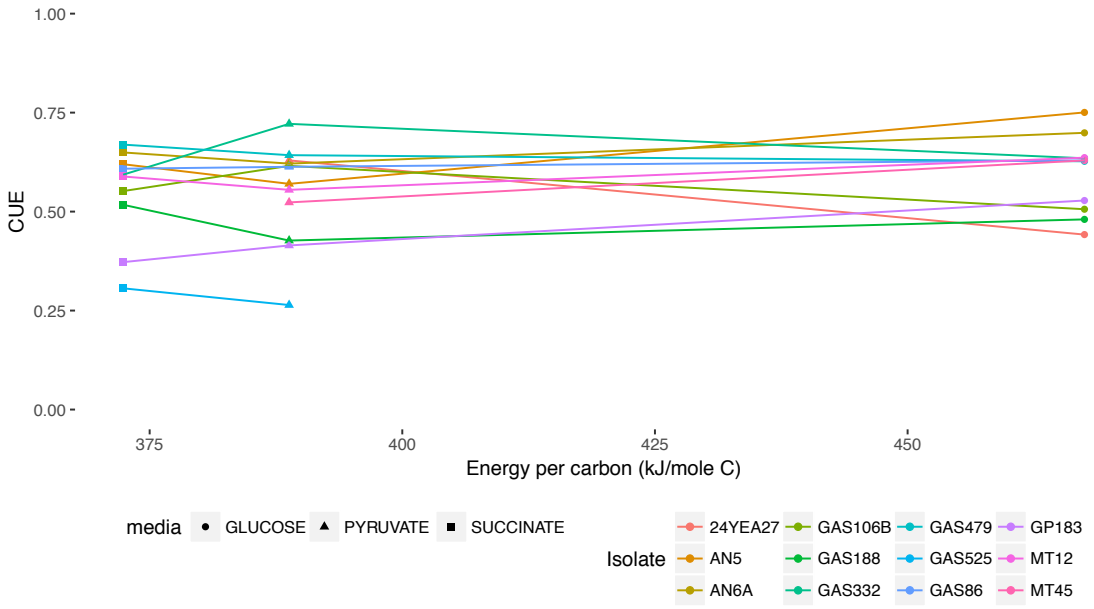

Figure B.3: Effect of carbon quality on CUE. Each line denotes values for a different isolate. The x-axis is the heat of combustion of the substrate in kilojoules per mole divided by the number of carbon atoms in a mole of the substrate. Only cultures grown at 20°C are plotted

(1) (1).pdf

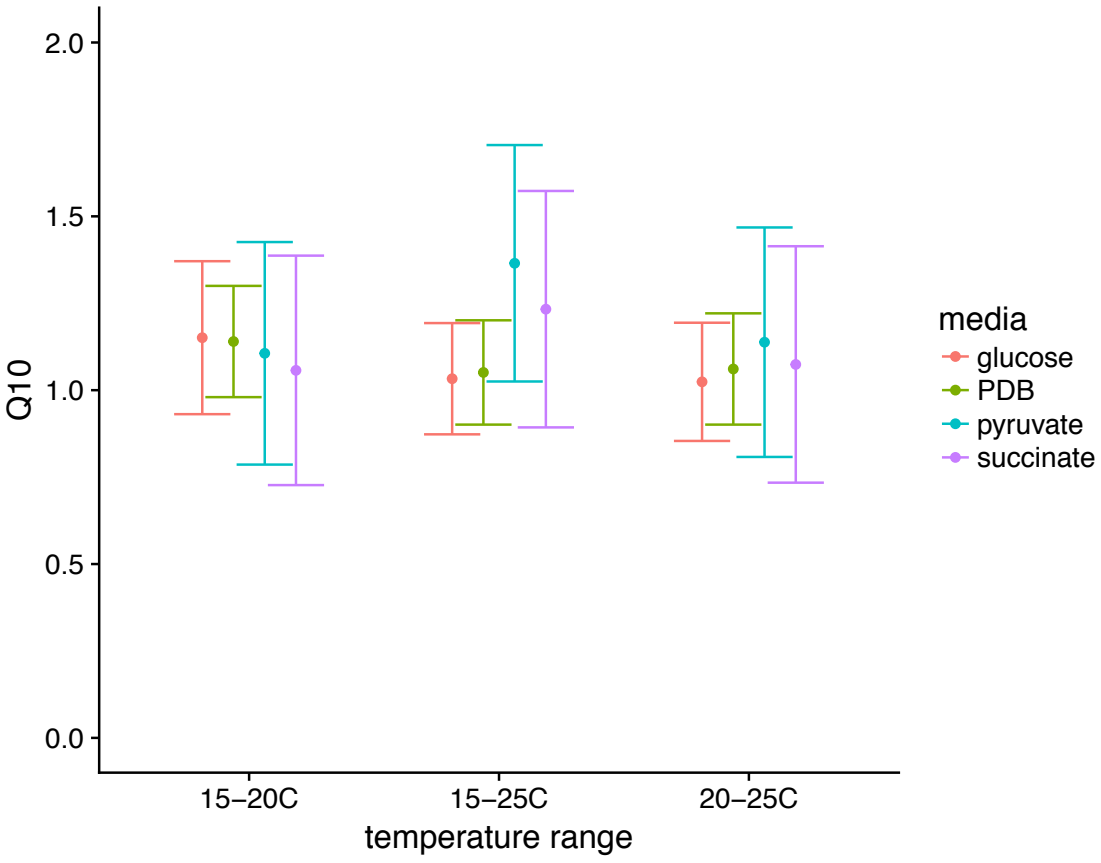

Figure B.4: Phylogenetically-weighted mean temperature sensitivity of CUE for the four substrates and three temperature ranges used in this study, reported with 95% confidence intervals. Reported means and confidence intervals are the posterior estimates resulting from running an animal model in MCMCglmm.

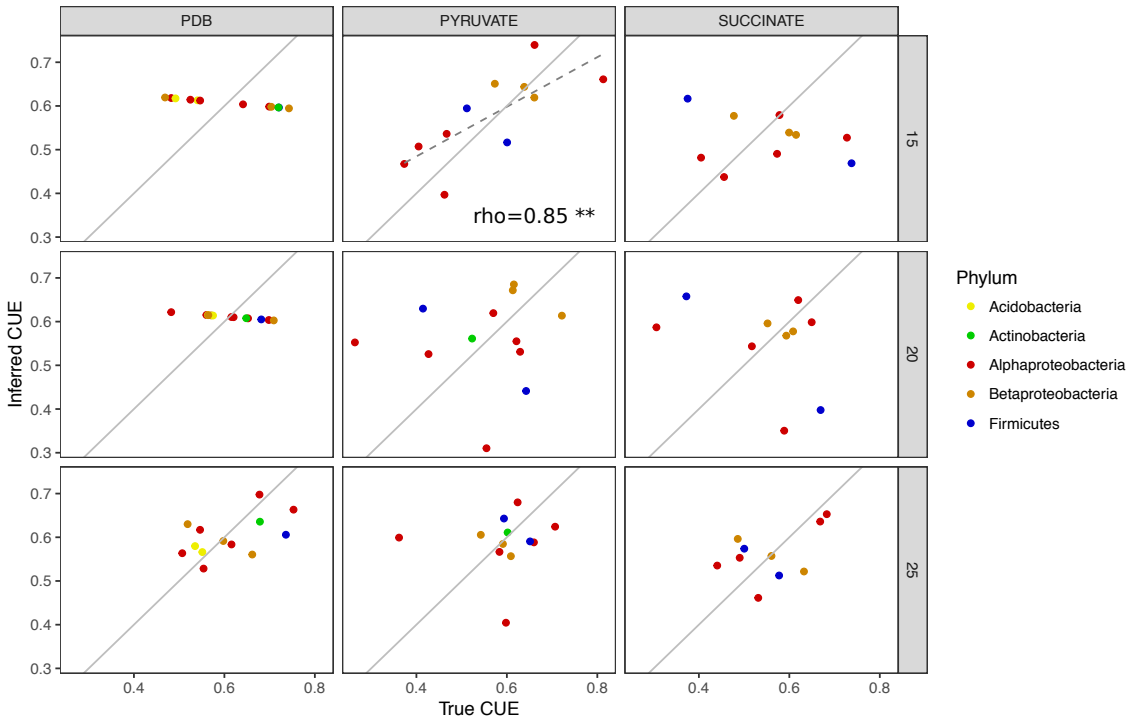

Figure B.5: Plot of observed mean CUE for each isolate and incubation condition vs. the predicted mean CUE based on phylogenetic reconstruction using ancestral reconstruction techniques. Each point represents an isolate, the x-axis the observed mean CUE, and the y-axis the mean CUE predicted for the isolate based on ancestral reconstruction. The 1:1 line, indicating perfect agreement between predicted and observed CUE, is drawn in solid grey, and the correlation for significant relationships between observed and predicted mean CUE for each isolate is drawn as a dashed line alongside the Pearson and Spearman correlation coefficients (** $P < 0.01$,* $P < 0.05$)

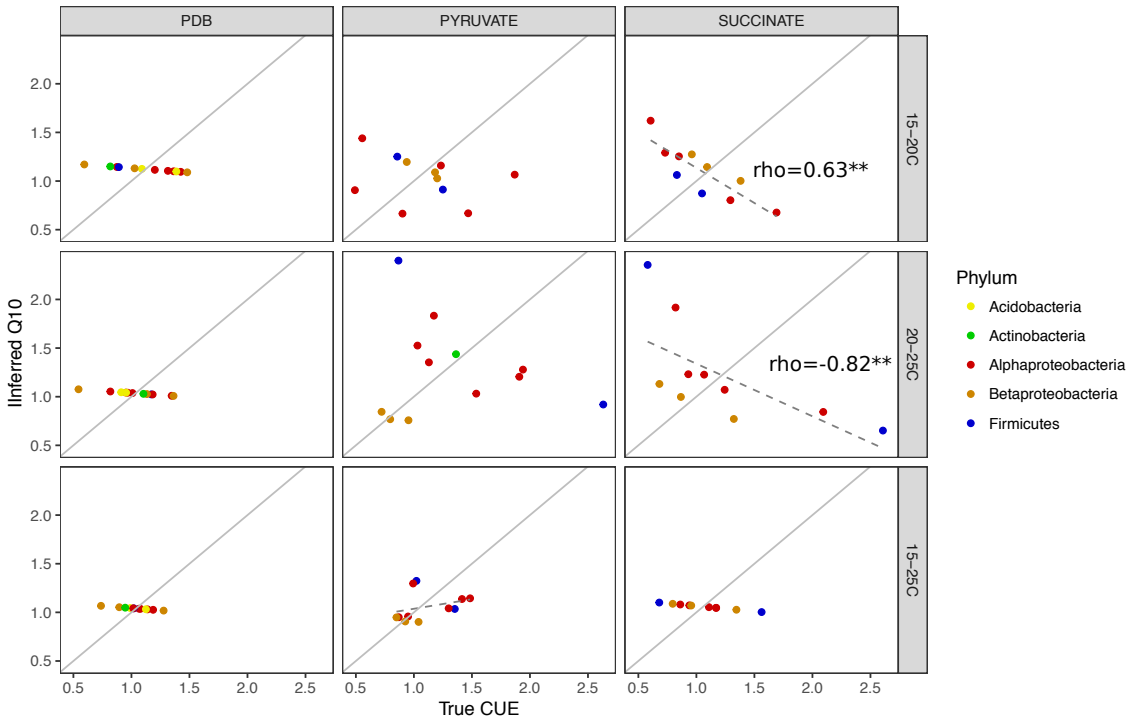

Figure B.6: Plot of observed mean CUE Q_{10} for each isolate and incubation condition vs. the predicted mean CUE Q_{10} based on phylogenetic reconstruction using ancestral reconstruction techniques. Each point represents an isolate, the x-axis the observed mean Q_{10}, and the y-axis the mean Q_{10} predicted for the isolate based on ancestral reconstruction. The 1:1 line, indicating perfect agreement between predicted and observed Q_{10}, is drawn in solid grey, and the correlation for significant relationships between observed and predicted mean Q_{10} for each isolate is drawn as a dashed line alongside the Pearson and Spearman correlation coefficients (** $P < 0.01$,* $P < 0.05$)

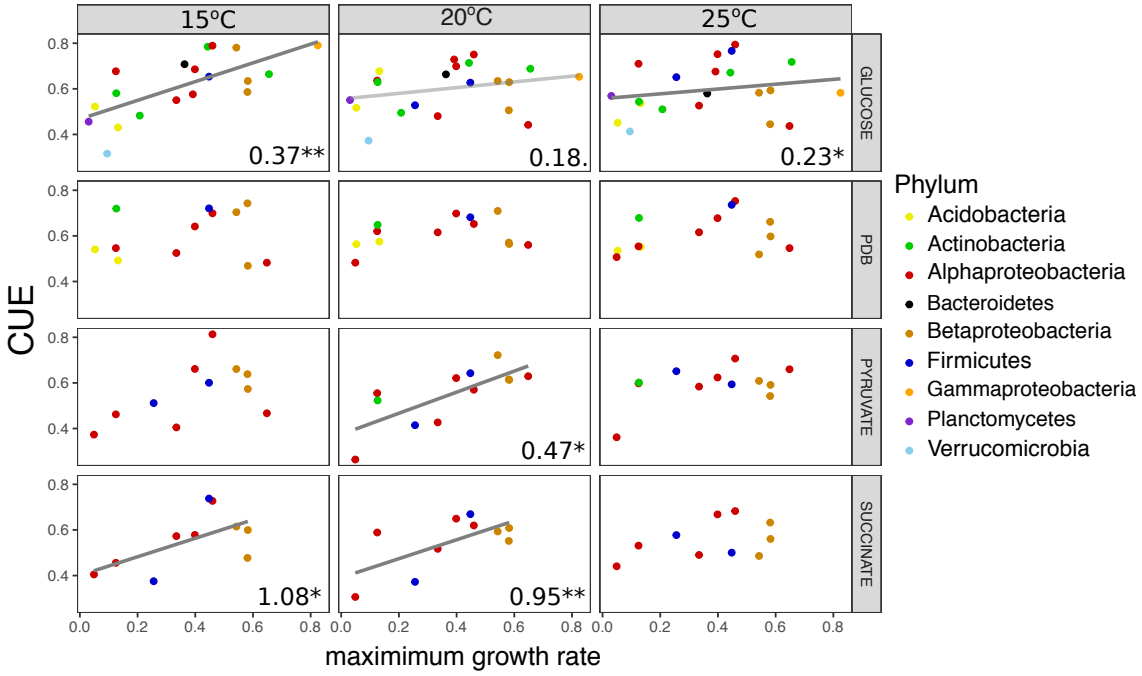

Figure B.7: Correlation between CUE and maximum growth rate of taxa across the four media and three temperatures assayed. PGLS slopes are drawn, with numbers on each panel denoting the slope and its significance (** $P < 0.01$;* $P < 0.05$; . $P < 0.1$)

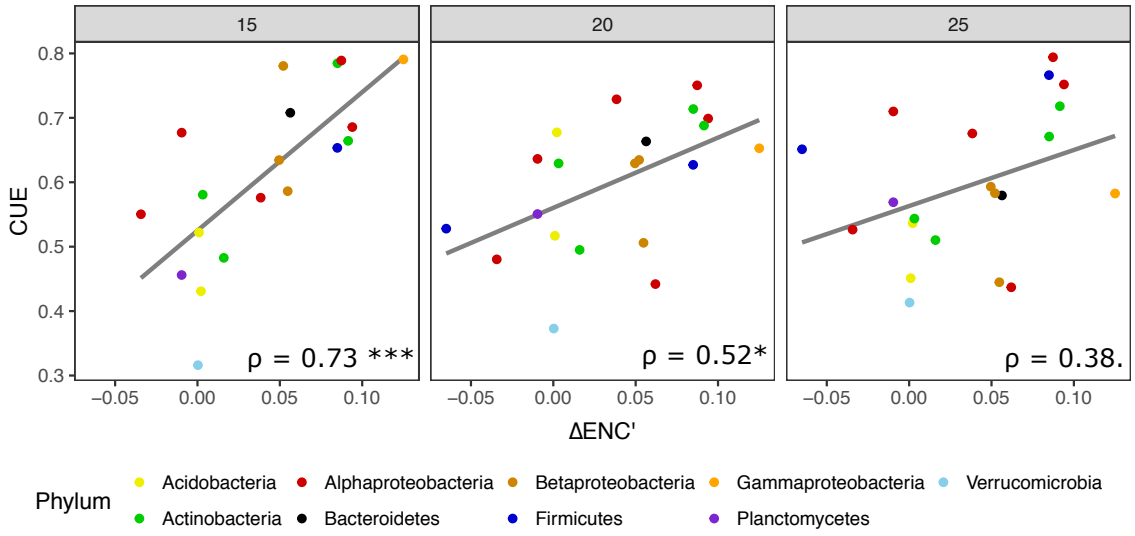

Figure B.8: Correlations between CUE and codon bias (as per (283)) for bacterial isolates grown on glucose. Spearman correlation coefficients (not corrected for phylogenetic correlation) are included, along with the p-value (*** $P < 0.001$;* $P < 0.05$; . $P < 0.1$)

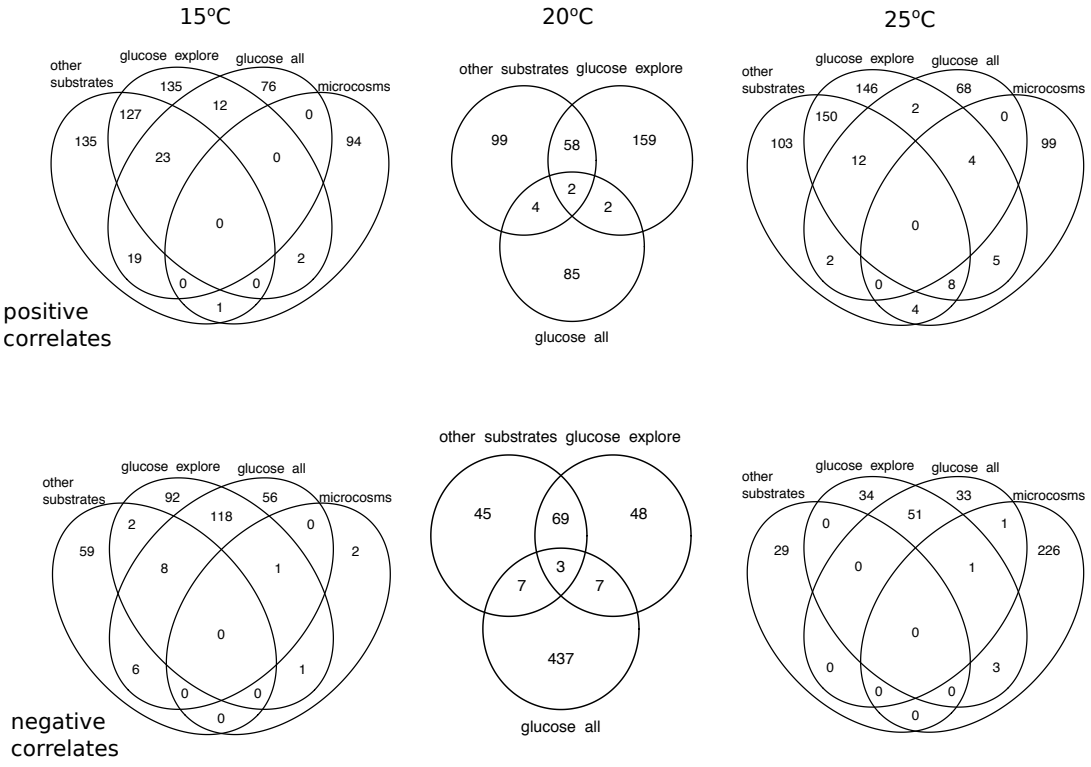

Figure B.9: Venn diagrams of numbers of individual KO markers for which their genomic density is positively or negatively correlated with CUE. In all instances, "glucose explore" is considered to consist of the proposed markers of efficiency, while the remaining three datasets are considered as "validating" datasets. Sample sizes (number of isolates or microcosms) for each analysis are as follows: other substrates (10-13); glucose explore (13); glucose all (22); microcosms (10).

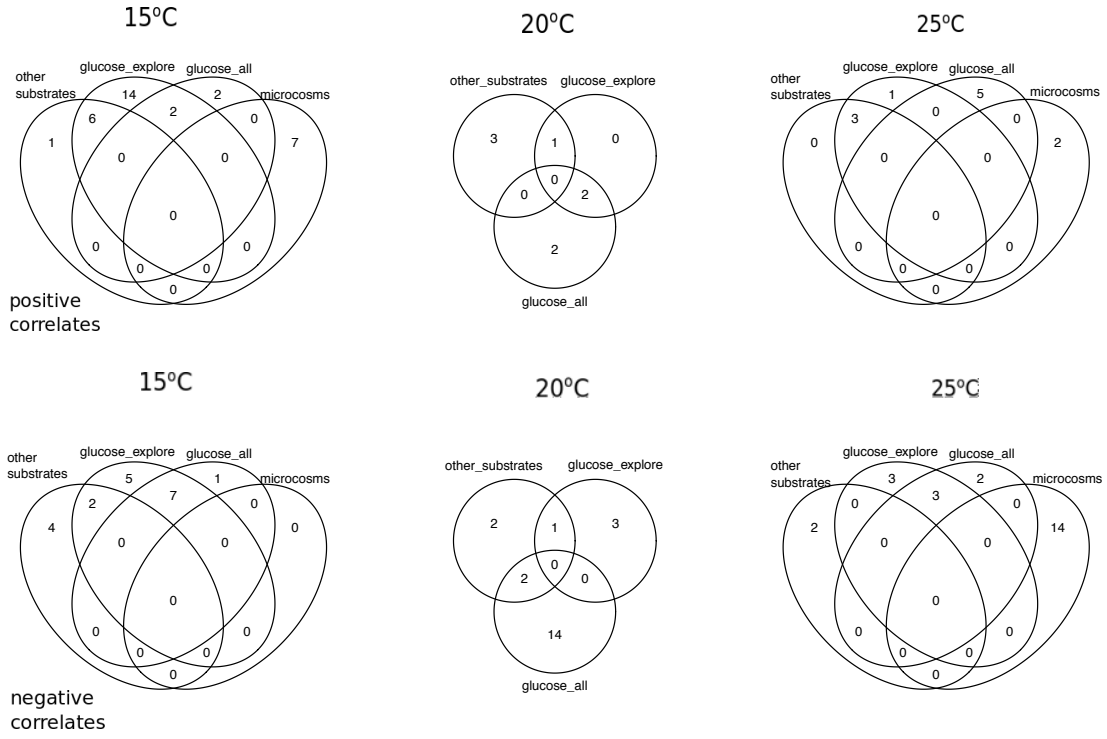

Figure B.10: Venn diagrams of numbers of KO pathway markers for which their genomic density is positively or negatively correlated with CUE. In all instances, "glucose explore" is considered to consist of the proposed markers of efficiency, while the remaining three datasets are considered as "validating" datasets. Sample sizes (number of isolates or microcosms) for each analysis are as follows: other substrates (10-13); glucose explore (13); glucose all (22); microcosms (10).

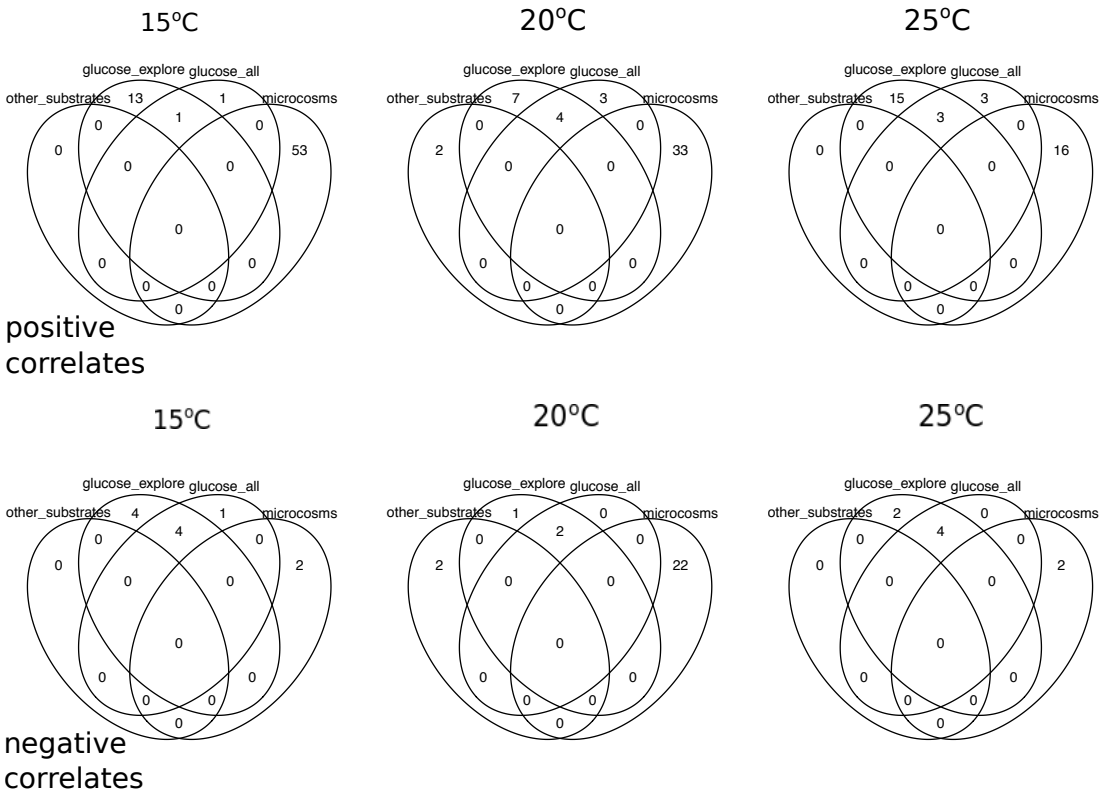

Figure B.11: Venn diagrams of numbers of KO pathway markers for which their genomic density is positively or negatively correlated with the temperature sensitivity (Q10) of CUE. In all instances, "glucose explore" is considered to consist of the proposed markers of efficiency, while the remaining three datasets are considered as "validating" datasets. Sample sizes (number of isolates or microcosms) for each analysis are as follows: other substrates (10-13); glucose explore (13); glucose all (22); microcosms (10).

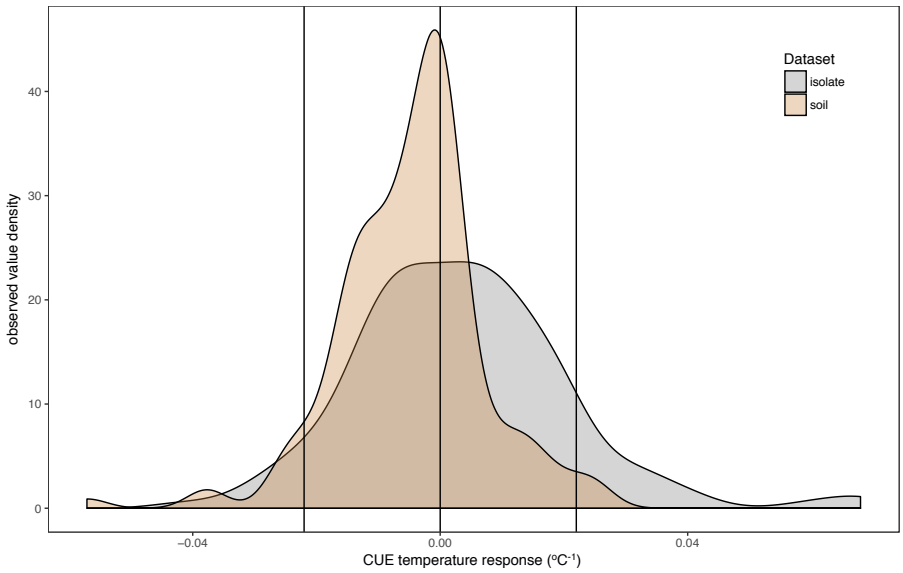

Figure B.12: Density plot of observed CUE temperature response for 23 soil bacterial isolates grown between 15 and 25°C on four different liquid media types in the lab (n=160 datapoints, grey), and for soil microbial communities grown with various different substrates and temperatures based on a literature search (n=141 datapoints, brown). Vertical lines are placed at 0 (no change in CUE with temperature) as well as the +/-0.022 $^{o}C^{-1}$ upper and lower limits used in the present study. Contributing datapoints are primarily derived from (230)

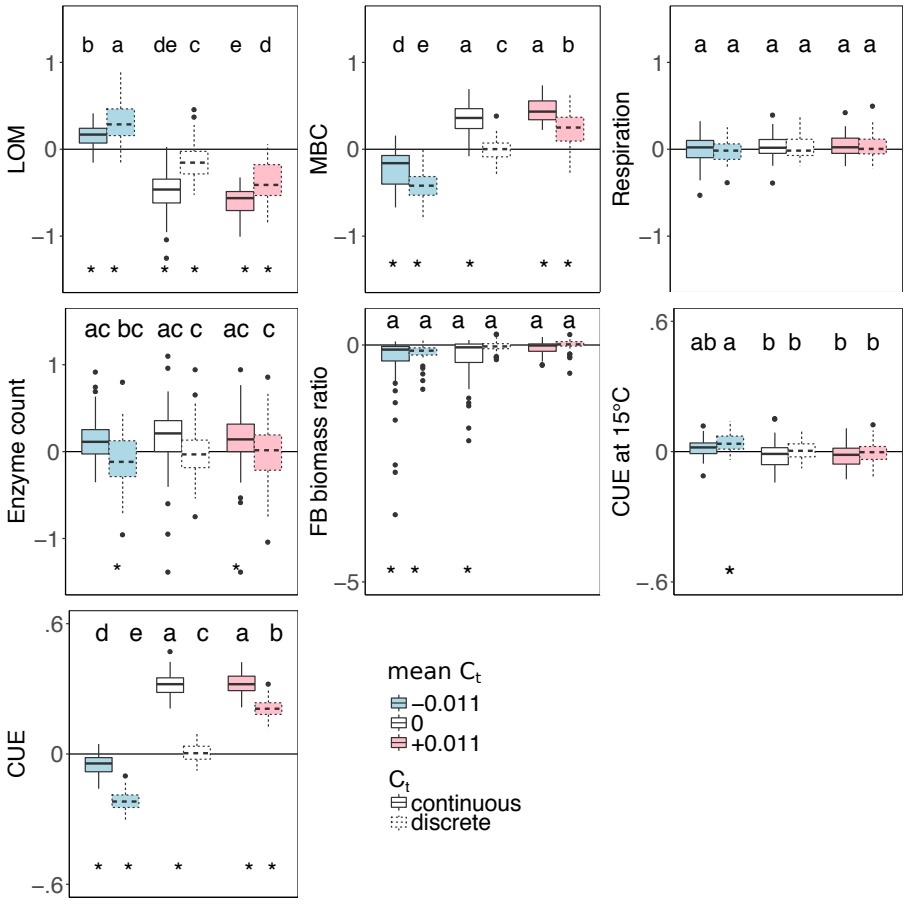

Figure B.13: Effect of 5°C warming on C stocks and flows in simulations, reported as the natural log of the ratio of the values in heated compared to control conditions. Here, the CUE temperature response is allowed to vary (heterogeneous) or is fixed (homogeneous) at the mean cross-taxon value as in Fig.3, but the variability is either constrained to all negative values (mean of -0.011 $^oC^{-1}$; range -0.022 to 0^oC^{-1}), or all positive values (mean of 0.011 $^oC^{-1}$; range 0 to 0.022^oC^{-1})

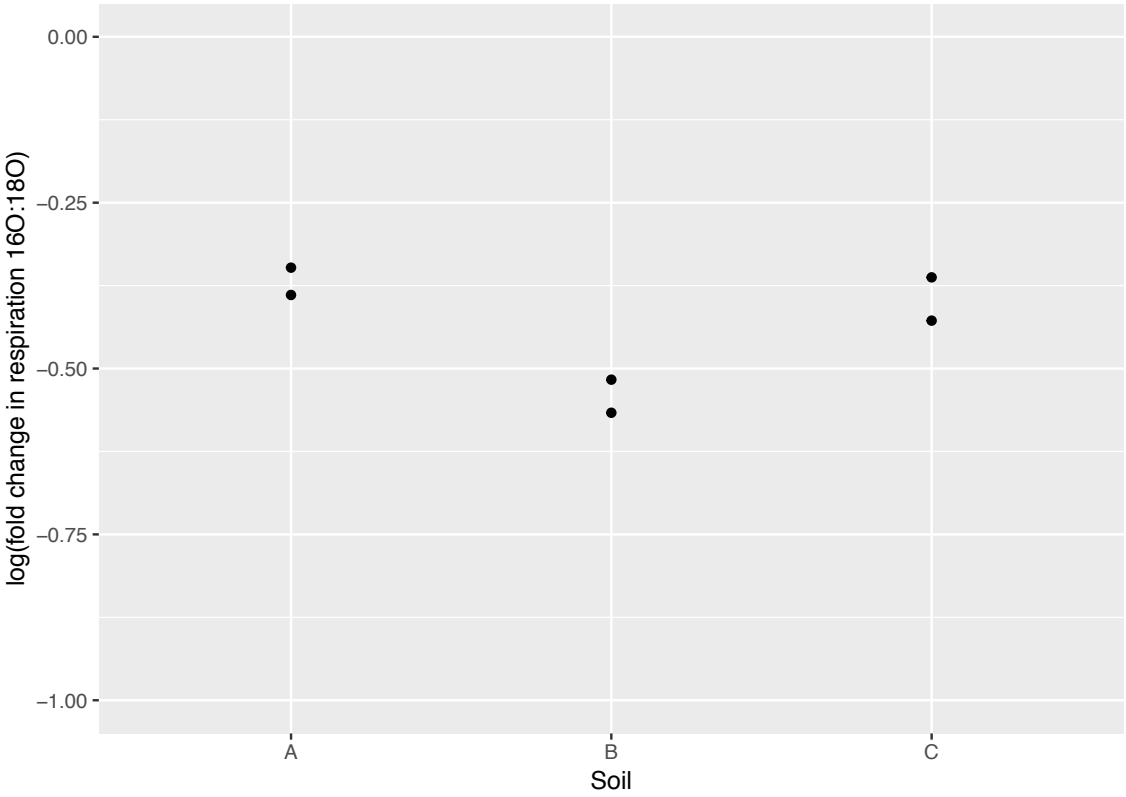

Figure B.14: Respiration suppression after addition of 96 at% ^{18}O-water compared to ^{16}O-water.

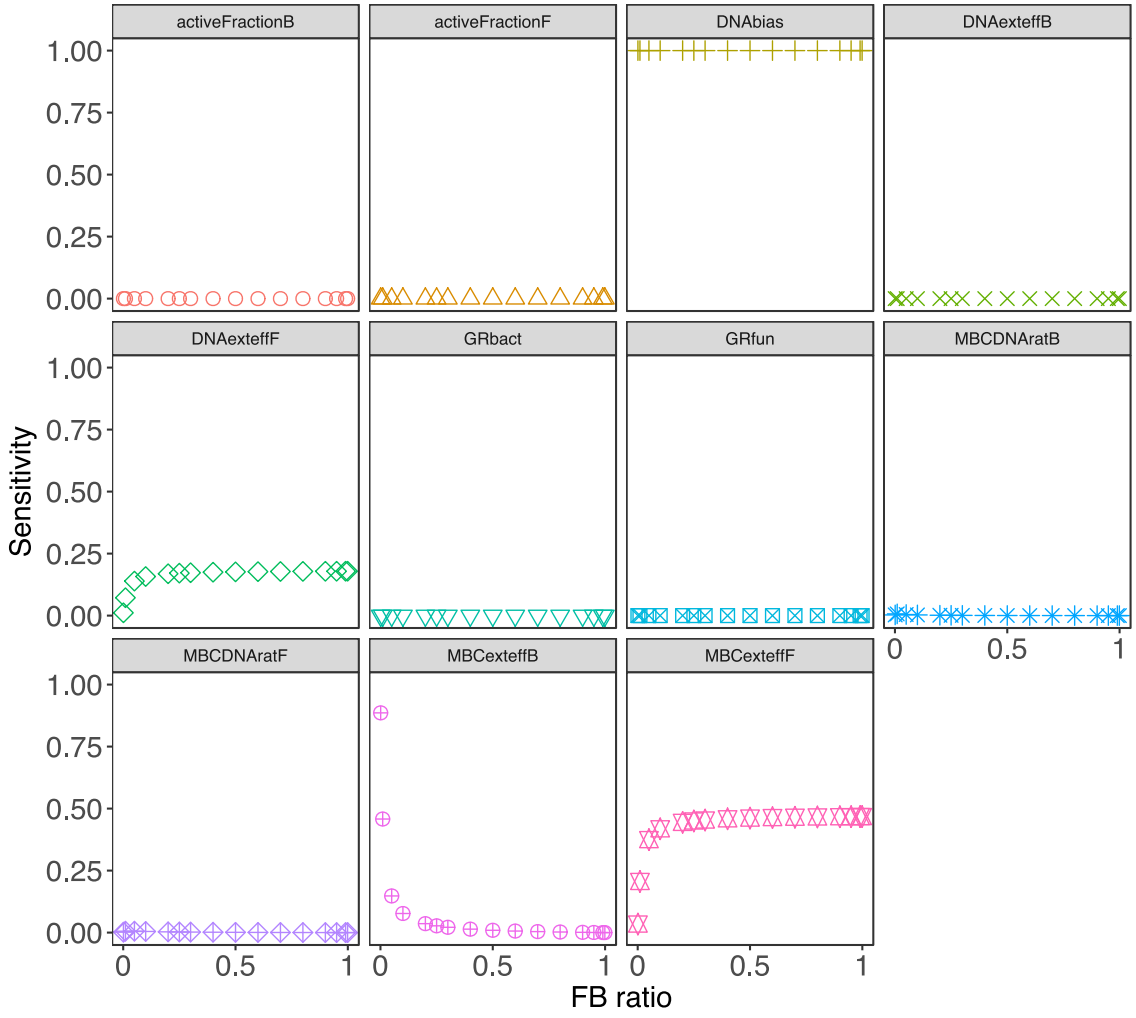

Figure B.15: Sensitivity of MBC growth estimate error to variation in biological parameters and methodological errors. The plotted scenario assumes MBC is under-extracted, and that fungi and bacteria grow at different rates.

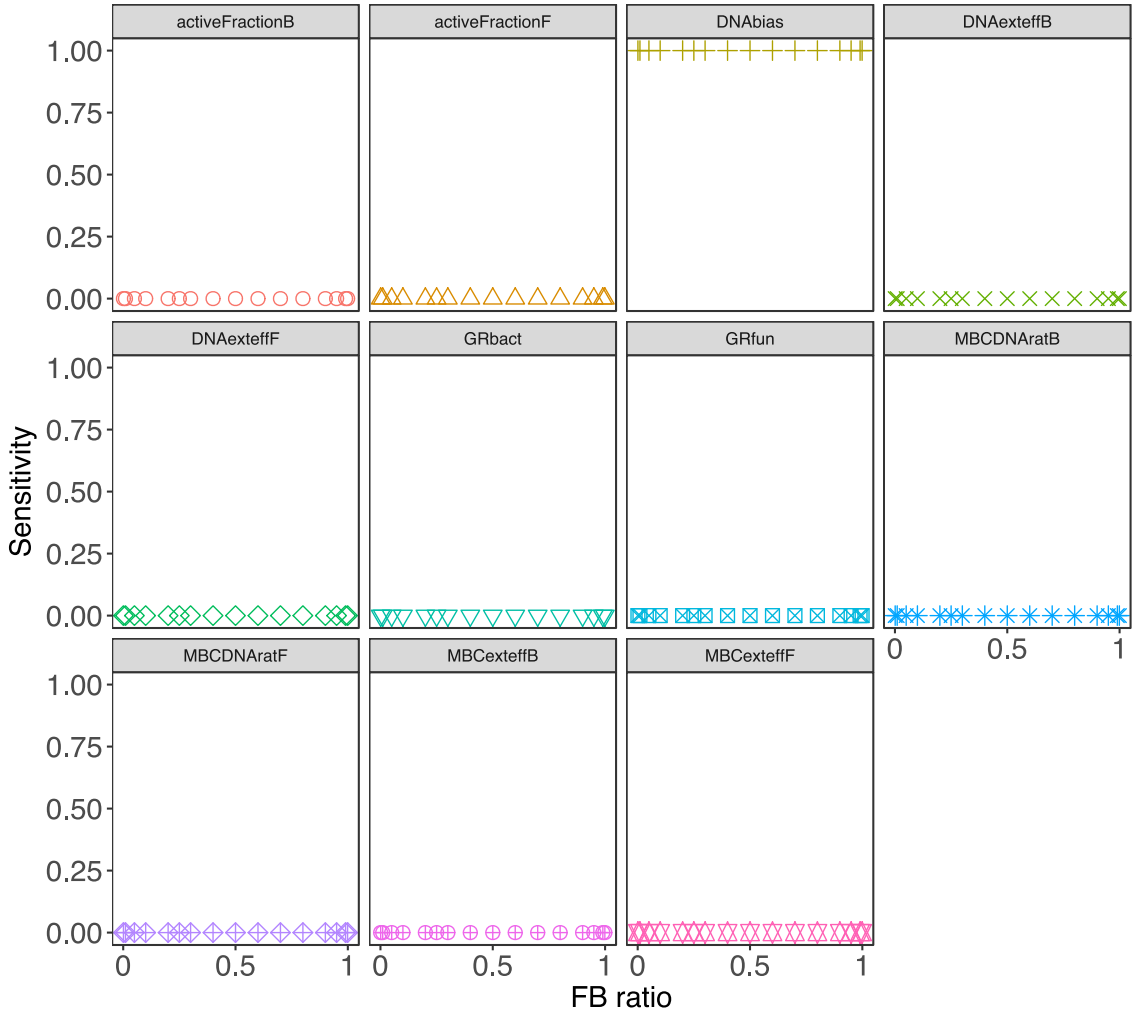

Figure B.16: Sensitivity of MBC growth estimate error to variation in biological parameters and methodological errors. The plotted scenario assumes that DNA is under-extracted, and that fungi and bacteria grow at the same rate.

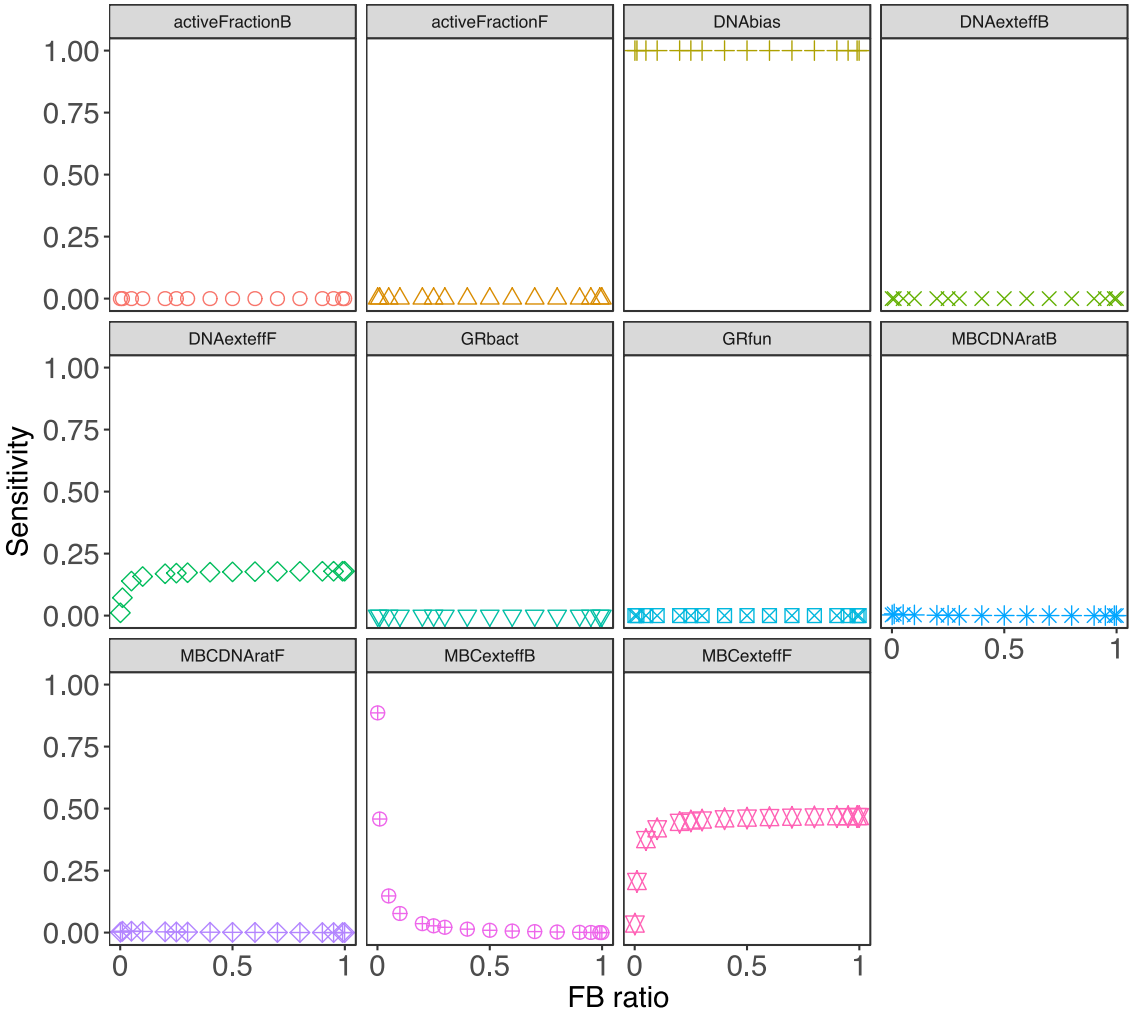

Figure B.17: Sensitivity of MBC growth estimate error to variation in biological parameters and methodological errors. The plotted scenario assumes that DNA and MBC are both under-extracted, and that fungi and bacteria grow at the same rate.

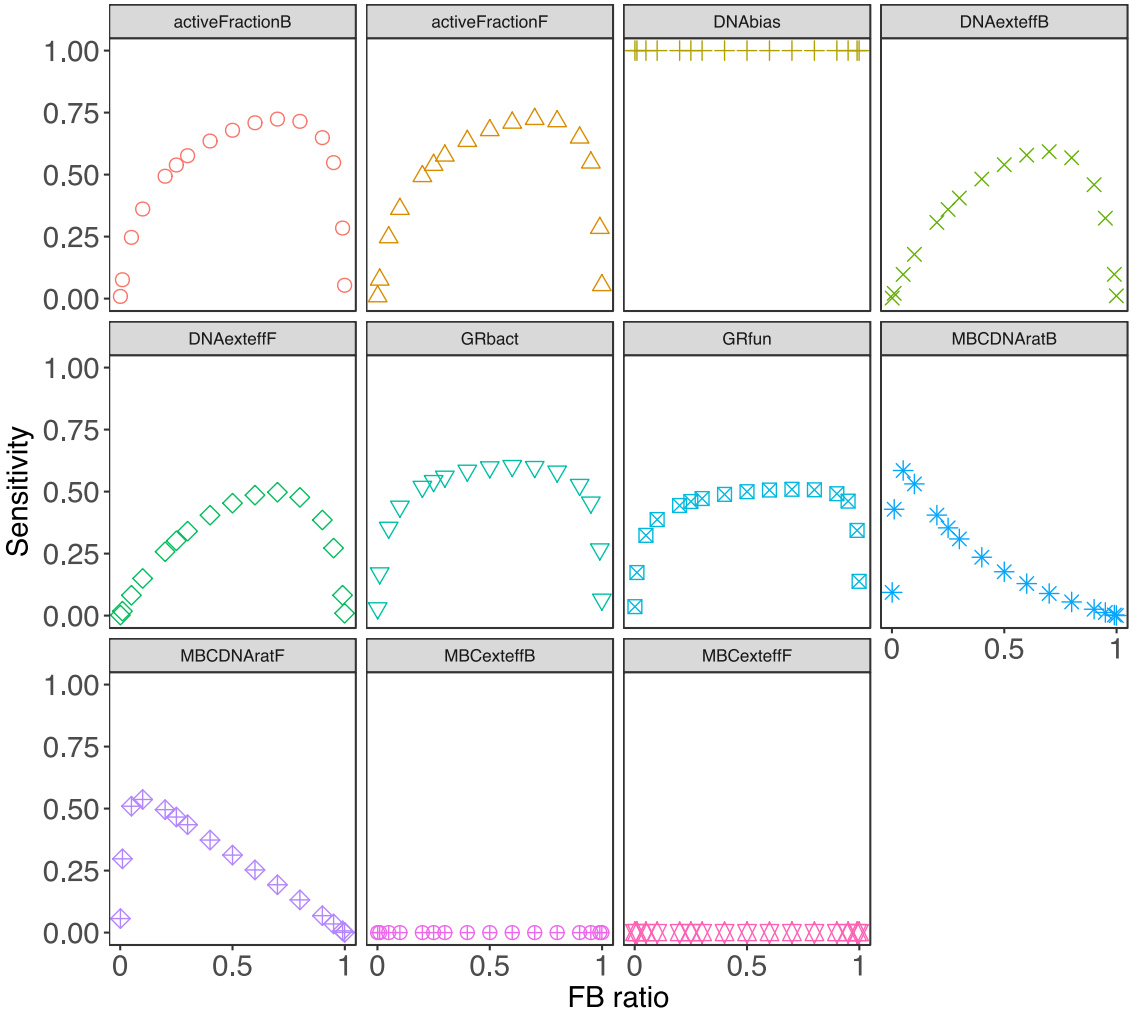

Figure B.18: Sensitivity of MBC growth estimate error to variation in biological parameters and methodological errors. The plotted scenario assumes that MBC is under-extracted, and that fungi and bacteria grow at different rates.

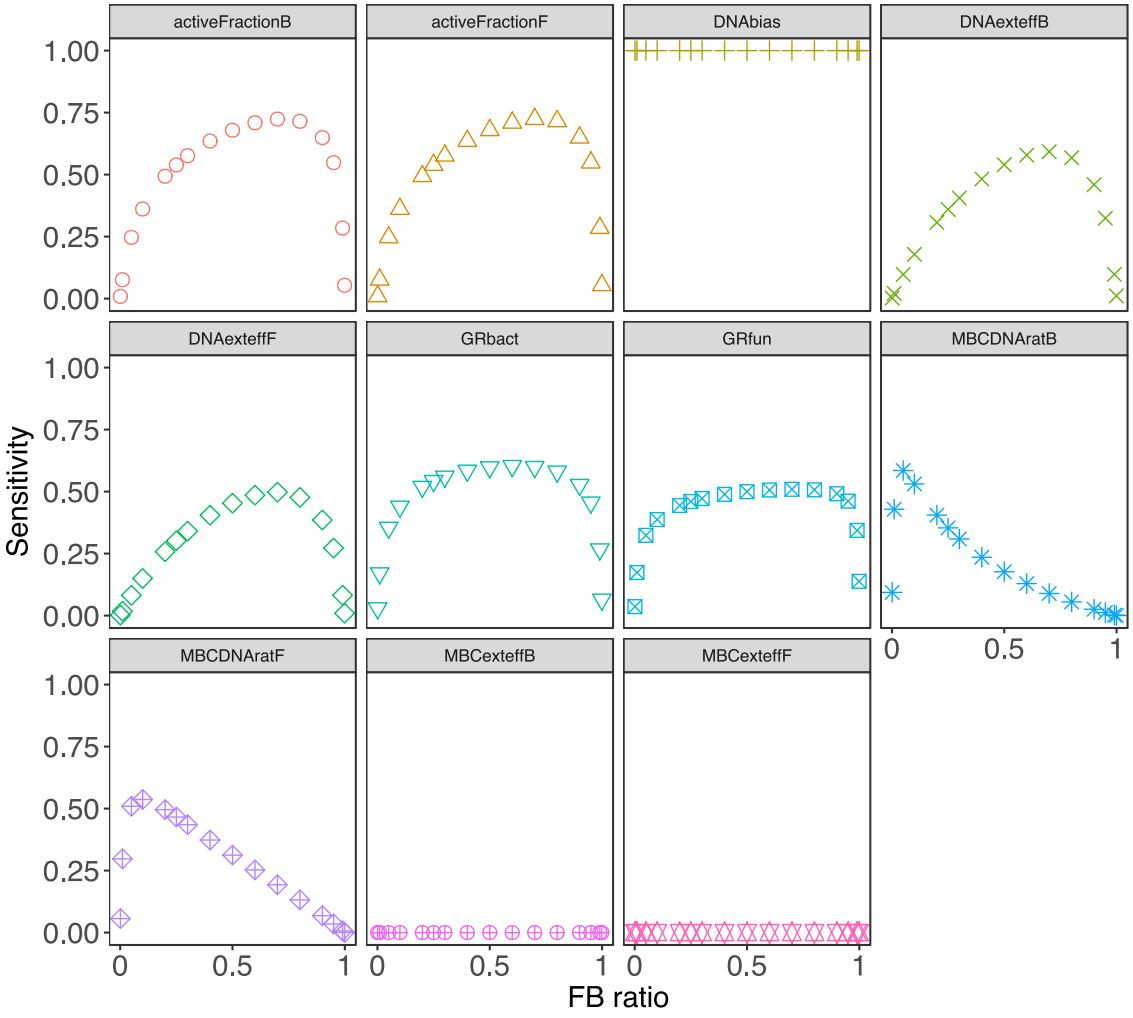

Figure B.19: Sensitivity of MBC growth estimate error to variation in biological parameters and methodological errors. The plotted scenario assumes that DNA is under-extracted, and that fungi and bacteria grow at different rates.

APPENDIX C

SUPPLEMENTARY METHODS FOR CHAPTER 2

C.1 Media preparation

PDB media contained 10g/L alpha glucose, 4g/L potato infusion extract (Sigma 52424), and 8.53g/L of the buffer MES monohydrate. To prevent oxidation, the media was sterile filtered through a 0.22um PES filter rather than being autoclaved. Glucose, pyruvate, and succinate media consisted of a salts base (0.2g KH_2PO_4, 0.25g NH_4Cl, 0.5g KCl, 0.15g $CaCl_2$*$2H_2O$, 0.2905g $MgCl_2$, 0.284g Na_2SO_4, 1mls SL10) buffered with 10mM MES. After autoclaving, sterile-filtered glucose, sodium pyruvate, or sodium succinate were added at 1g carbon L^{-1}, and media was supplemented with 0.05% yeast extract and 2mls VL55 vitamins. This small amount of yeast extract was added since preliminary studies showed some isolates failed to grow beyond the first transfer unless it was supplied, but that isolates were unable to grow to detectable levels on this media base unless additional carbon was supplied. As such, we assume growth is representative of growth on glucose, pyruvate, or succinate alone. The heats of combustion for these substrates was extracted from the NIST Chemistry WebBook (169).

Freezer stocks of bacterial isolates in 20% glycerol were streaked onto pH 6 R2A media and incubated in the dark at 20°C until colonies appeared (2-21 days), and

then transferred to assay conditions. In order to minimize batch effects, we used distinct freezer stocks of each isolate where possible. Approximately 1ul of colony was transferred to triplicate tubes of 200μl pH 6 10mM MES buffer, and 10μl of this was used to inoculate 190μl of potato dextrose broth, glucose, pyruvate, or succinate media in a 96-well plate. Plates were incubated at 15, 20, or 25°C and actively-growing cultures were transferred at least two more times under these conditions in order to: 1. allow acclimation to assay conditions; 2. ensure dilution of carbon transferred with original media; and 3. minimize bias in OD measurements due to aggregation of cells (143). 50-100μl of the final transfer was subsequently pipetted into 7mls of the same media; when this culture reached exponential phase (based on final OD), 0.5-1ml was injected into a sealed stoppered 27ml Balch tube containing 5mls of the same media. At all steps, media was brought to the incubation temperature prior to inoculation.

The optical density and respiration rate of cultures were monitored throughout exponential phase using a Spectronic-20 spectrophotometer at 600nm and a Quantek instruments model 906 CO_2 analyzer, respectively. Prior to each read, tubes were vortexed vigorously to ensure solution and headspace CO_2 were in equilibrium. At least three distinct experiments starting with a new freezer stock restreak were completed for each isolate and condition assayed. A conversion factor of 130 μg carbon $OD^{-1}ml^{-1}$ was used to calculate microbial biomass carbon throughout the growth curve (BioNumber 109836). This constant conversion factor was used due to consistent challenges we faced in quantitatively pelleting the large volumes of small, exponentially-growing cells for our own isolates.

C.2 Measuring extracellular enzyme activity

To determine microbial extracellular enzyme potential, isolates were brought to exponential phase in glucose media at 20°C and then frozen at -20°C for up to two months prior to assays. We assayed for phosphatase (AP), N-acetylglucosaminidase (NAG), beta-glucosidase (BG), alpha-glucosidase (AG), cellobiohydrolase (CBH), and beta-xylosidase (BX) using 225μl of 1000uM MUB-linked substrate and 225μl of culture. We modified the typical protocol used by our lab (225) to account for the anticipated lower activity of isolates compared to soil. Plates were incubated at 20°C for 2.5 hours and the difference between the initial and final fluorescence read at an excitation/emission wavelength pair of 360/445nm was used to determine enzyme activity OD^{-1} hr^{-1} when compared to a standard curve prepared from 4-methylumbeliferone. Activity reported is the mean of the sums of enzyme activity across three technical replicates of 3-8 biological replicates of each isolate.

C.3 Phylogeny construction

A phylogeny was generated for all isolates using a conserved suite of single copy genes (152). Protein sequences for each isolate were downloaded from IMG, and the sequences of relevant genes were extracted using psi-BLAST (14) against the relevant reference sequences from the conserved domains database (CDD) (182). Genes were aligned across species using T-COFFEE (202), and concatenated using FASconCAT-G (148). ProtTest (2) was used to determine the optimum evolutionary model for each protein (LG; (156), and then RaxML was used to build the tree via the Trex-online website using default settings (substitution model = PROTCAT, substitution

matrix = DAYHOFF, hill-climbing algorithm, and bootstrap with 100 starting trees) (36; 264). The tree was subsequently uploaded into ITOL (164) for visual inspection and annotation.

C.4 Data analysis

In order to determine the shape of the temperature response of CUE in a given isolate, we fit curves linear (CUE=slope*Temperature+intercept) and parabolic (CUE=slope_{i}*temperature^2+ slope_{ii}*temperature+intercept) with respect to temperature. Equations were selected when $P < 0.05$ for the model fit, and an ANOVA comparing the two models was significant at $P < 0.05$, indicating one was significantly better than the other.

C.4.0.1 Genome sequencing, assembly, and annotation

gDNA was extracted from bacteria newly presented here using the Qiagen genomic DNA reagents kit and tips, and submitted to the UMass Med Deep Sequencing Core (BS isolates and 24-YEA-27) or Joint Genome Institute (all others) for sequencing using PacBio. Genomes sequenced at UMass were assembled using sprai version 0.9.9.23 (http://zombie.cb.k.u-tokyo.ac.jp/sprai/index.html) and Canu version 1.5 (142) using default settings. Assembly quality was verified based on scaffold count and on genome completeness and contamination using CheckM (212) within the DOE's KBASE platform (18). The eukaryotic KEGG ortholog pathways categorized under the level B category "Cellular community - eukaryotes", and under the

level A categories "Organismal Systems" and "Human Diseases" were excluded from consideration as markers.

Initially we tried to build more specific metabolic models for our isolates using the RAST subsystems in KBASE (18), but abandoned them after models failed to grow with minor gapfilling under conditions the corresponding bacteria are observed to grow robustly under. Instead, we took a more conservative approach and used the number of MAPLE pathways (17) with greater than 80% completeness, as per Muscarella and Lennon (2018).

TrSSP (191) was also used for annotating transporters in our bacterial genomes. However, we excluded its results from our analysis for 1. failing to predict any amino acid uptake transporters for most Gram positive isolates, and 2. predicting twice as many transporters per genome as the previously-reported "highs" of 18% (173).

C.5 Protein production costs

While in phosphate limited media, transcriptional costs limit fitness, in N-limited media translational costs do (125). We anticipate that our defined media is N-limited (soil bacterial NP ratio = 7:1 (53); media NP = 3.18:1), and so calculated the total extracellular enzyme cost as a function of amino acid biosynthesis and translation. Amino acid production requires diversion of substrate otherwise used for energy production into anabolic processes, and therefore generates competition between energy and carbon demands. Over evolutionary time, bacteria may get around this by using amino acids which are "cheaper" to produce, either because they are made from metabolites much of the ATP potential has already been extracted from, or

because only minimal ATP investment is needed to convert them from these central metabolic byproducts. We used the amino acid biosynthesis costs presented in Kaleta *et al.* (2013) for *E. coli*, assuming glucose as the substrate and 4.2 ATP consumed per peptide bond formed (126). Assuming 26 ATP are produced per six glucose carbons, we calculate the theoretical carbon assimilation efficiency for each protein as the ratio of carbon in the protein to the carbon in the protein plus CO_2 respired making the ATP required to make the protein. The "per protein CUE" for each protein was then weighted by its expected relative expression to get a whole exoenzyme production cost.

We lack expression data for our organisms during CUE measurements, so we used gene codon usage bias (GCB; (190) to infer relative expression. GCB assumes that more highly-expressed genes show a more restricted codon usage pattern than those which are less-expressed, as more highly-expressed genes are under stronger selection to match the available tRNA pool of the cell. Instead of calculating the codon usage bias for all genes compared to all others, it takes a user assigned set of genes, calculates the codon usage bias for all other genes against those, and then iteratively selects the set of genes which gives the maximum codon usage bias, indicating it is the most expressed. The GCB then gives a proxy for relative expression level based on the degree to which codon bias deviates from that used in the genes proposed to be the most highly expressed. We used all ribosomal proteins as our initial reference set for calculations, and excluded genes with fewer than 80 codons from calculations because codon bias is unreliable (82). The GCB can give negative numbers because it is a log ratio of codon biases for the gene of interest vs. the highly expressed reference

set. Therefore we added one to all values before multiplying the per enzyme costs and re-calculating the average. Fasta manipulations were completed using bioStrings (209), and codon bias calculations using coRdon (82) in R v3.4.0 (232).

C.6 Microcosm CUE measurements

CUE in the microcosms was measured by adding ^{18}O-H_2O to 20% of the final water present to subsamples of the soil. Samples were prepared identically, only using ^{16}O-H_2O, as controls for background heavy oxygen incorporation. The samples were then placed in sealed tubes for 24 hours and the CO_2 produced during this time measured using an IRGA. The soil samples were stored at -80C until DNA extraction using the Qiiagen Powersoil HTP kit. The resultant DNA was quantified using PicoGreen (Invitrogen), and its ^{18}O enrichment was measured using IRMS at the UC Davis Stable Isotope Facility. CUE was calculated by converting new DNA to new microbial biomass carbon produced as per (262).

APPENDIX D

SUPPLEMENTARY METHODS AND RESULTS FOR CHAPTER 4

D.1 Measuring isolate CUE in artificial soil

Isolates were streaked from freezer stocks onto R2A-6 media plates. Cultures were grown in triplicate to exponential phase in Roller glucose media and then pelleted in the centrifuge (5000xg, 5 minutes). The cultures were then re-suspended in fresh media to an OD of 0.02, and 1mls of this was used to inoculate 5g of artificial soil (50% water holding capacity). Data from preliminary respiration curves where CO_2 was measured for an extended period were used to estimate when exponential phase was, where the phase of maximum respiration rate was assumed to correspond to the exponential phase. When growth was apparent based on CO_2 production, 1g of wet weight soil was removed and resuspended in 5mls of fresh glucose media. 1ml of this was then used to inoculate 6-10 replicate fresh artificial soil tubes. At each timepoint, a respiration measurement was taken on one tube of each replicate, and the soil contents of that tube were then frozen at -80°C until DNA extraction.

We looked for the three timepoints where the logarithm of hourly CO_2 production rates against time had the greatest slope, and used these samples for estimating microbial biomass carbon and CUE.

DNA was extracted using the Qiagen PowerSoil DNA extraction kit. Qiagen technical support stated that the columns in this kit tend to bind DNA inefficiently at both low and high concentrations of DNA. Since we found low concentrations of DNA, we also tried coarser methods of DNA extraction, including bead-beating with a phosphate buffer. However, the DNA resulting from this extraction was so dirty that the estimated DNA content was 500 times higher than expected based on the number of cells put in. Therefore, we stuck with the original PowerSoil protocol.

Since we know both the genome size and rrN of the isolates inoculated into the artificial soil, we could use either qPCR to estimate ribosomal DNA copies or DNA yield as an estimate of the number cells in the soil. qPCR is more sensitive than total DNA quantification using a Qubit, but also requires additional conversion factors to yield estimates of cells. In both methods, an average microbial biomass carbon per cell estimate can be used to convert the DNA-based cell copy number data into microbial biomass carbon. Although in theory both methods should yield similar estimates of CUE, in practice biomass estimates using qPCR were much higher than those used Qubit (Fig. D2).

D.2 CUE results: AN6A

Example results for the intrinsic rate of increase ("r") and mass-specific respiration rates used to calculate CUE for AN6A can be found in figures D.1 and D.2.

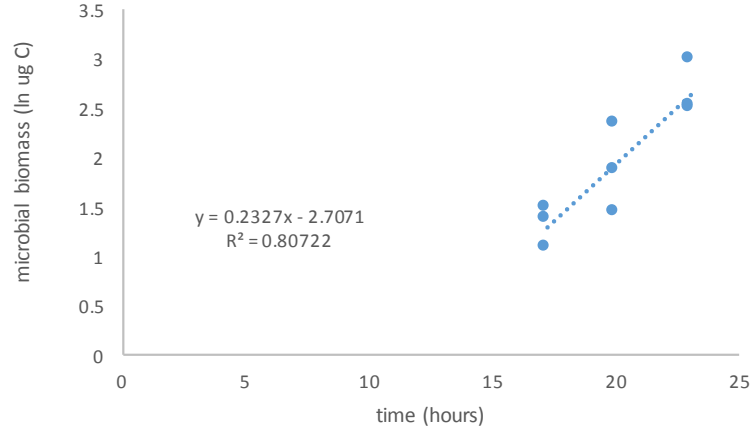

(a) growth

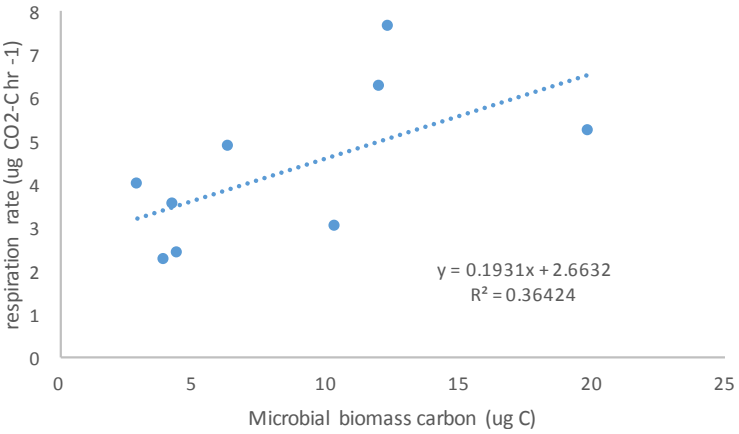

(b) respiration

Figure D.1: Growth (a) and respiration rate (b) of AN6A grown on glucose Roller media in artificial soil at 20°C. Microbial biomass carbon was estimated by converting the DNA yielded from DNA extraction into genome copies, and then into microbial biomass carbon. In this instance, CUE is 0.55 using the slope determined by pooling all three experimental replicates for each timepoint (here), or 0.58, 0.31, and 0.39 when slopes are calculated separately for each replicate.

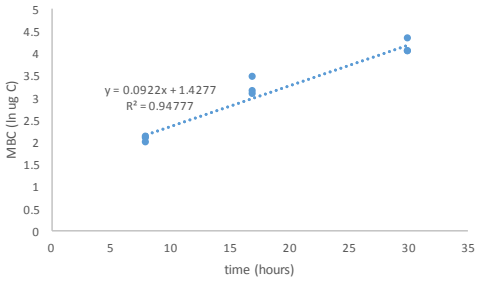

(a)

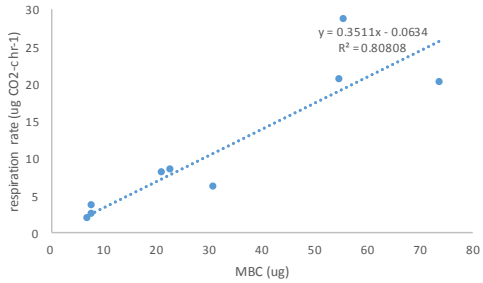

(b)

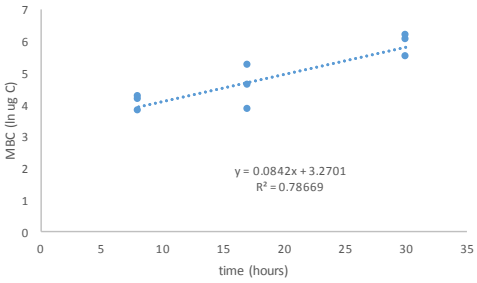

(c)

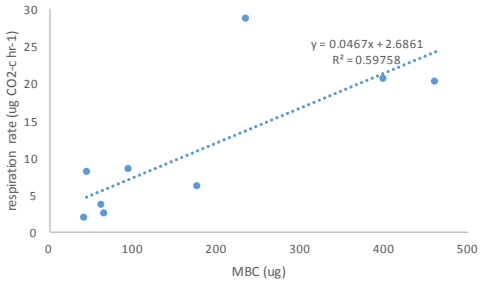

(d)

Figure D.2: Growth (a,c) and respiration rate (b,d) of AN6A grown on glucose Roller media in artificial soil at 15°C, using either qPCR-derived estimates of biomass (a,b), or genomic DNA quantification (c,d). CUE is estimated as 0.21 using the Qubit and 0.64 using qPCR. Values calculated identically for experiments set up at 25°C yielded estimates of 0.34 and 0.82, respectively.

D.3 CUE results: GAS332

Example results for the intrinsic rate of increase ("r") and mass-specific respiration rates used to calculate CUE for GAS332 can be found in figure D.3.

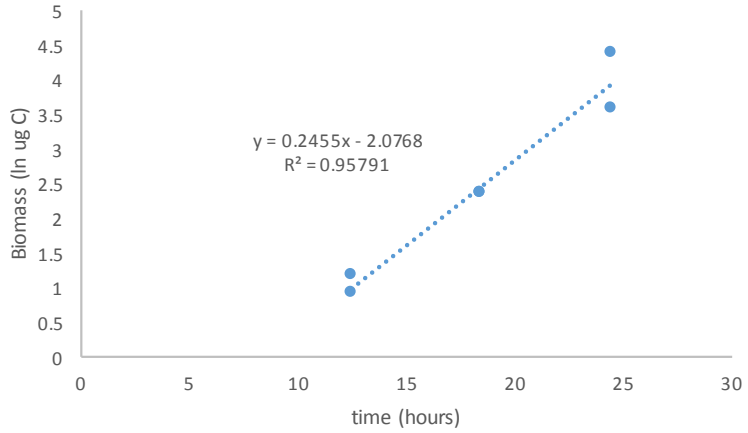

(a) growth

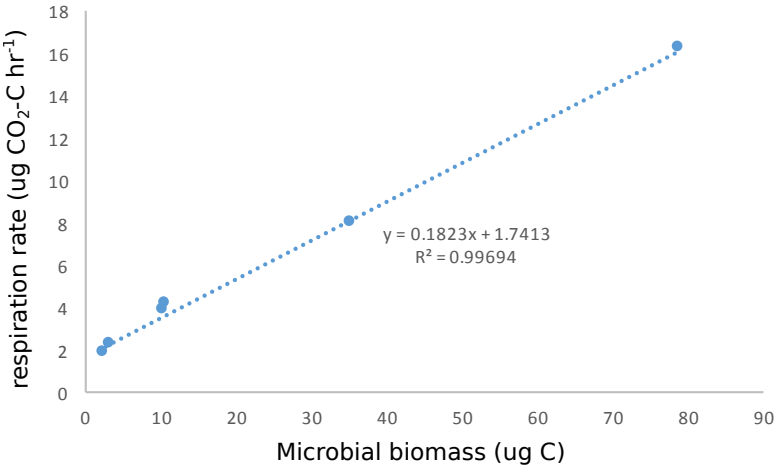

(b) respiration

Figure D.3: Growth (a) and respiration rate (b) of GAS332 grown on glucose Roller media in artificial soil at 25°C. Microbial biomass carbon was estimated by converting the DNA yield into genome copies, and then into microbial biomass carbon. In this instance, CUE is 0.57 when calculated as for the liquid CUE in chapter 1. The corresponding tubes for 15°C did not grow, so no data are provided.

BIBLIOGRAPHY

[1] Aanderud, Zachary T, and Lennon, Jay T. Validation of heavy-water stable isotope probing for the characterization of rapidly responding soil bacteria. *Applied and environmental microbiology* (2011), AEM–02735.

[2] Abascal, Federico, Zardoya, Rafael, and Posada, David. Prottest: selection of best-fit models of protein evolution. *Bioinformatics 21*, 9 (2005), 2104–2105.

[3] Adu, JK, and Oades, JM. Utilization of organic materials in soil aggregates by bacteria and fungi. *Soil Biology and Biochemistry 10*, 2 (1978), 117–122.

[4] Alberts, Bruce, Johnson, Alexander, Lewis, Julian, Morgan, David, Raff, Martin, Roberts, Keith, and Walter, Peter. *Molecular Biology of the Cell*, 6 edition ed. Garland Science, Nov. 2014.

[5] Alessi, Daniel S, Walsh, Dana M, and Fein, Jeremy B. Uncertainties in determining microbial biomass c using the chloroform fumigation–extraction method. *Chemical Geology 280*, 1-2 (2011), 58–64.

[6] Allison, SD. A trait-based approach for modelling microbial litter decomposition. *Ecology letters 15*, 9 (2012), 1058–1070.

[7] Allison, Steven D. Cheaters, diffusion and nutrients constrain decomposition by microbial enzymes in spatially structured environments. *Ecology Letters 8*, 6 (2005), 626–635.

[8] Allison, Steven D. Modeling adaptation of carbon use efficiency in microbial communities. *Frontiers in microbiology 5* (2014), 571.

[9] Allison, Steven D, and Goulden, Michael L. Consequences of drought tolerance traits for microbial decomposition in the dement model. *Soil Biology and Biochemistry 107* (2017), 104–113.

[10] Allison, Steven D, Lu, Lucy, Kent, Alyssa G, and Martiny, Adam C. Extracellular enzyme production and cheating in pseudomonas fluorescens depend on diffusion rates. *Frontiers in microbiology 5* (2014).

[11] Allison, Steven D, Romero-Olivares, Adriana L, Lu, Ying, Taylor, John W, and Treseder, Kathleen K. Temperature sensitivities of extracellular enzyme vmax and km across thermal environments. *Global change biology 24*, 7 (2018), 2884–2897.

[12] Allison, Steven D, Wallenstein, Matthew D, and Bradford, Mark A. Soil-carbon response to warming dependent on microbial physiology. *Nature Geoscience 3*, 5 (2010), 336–340.

[13] Alster, Charlotte J, Weller, Zachary D, and von Fischer, Joseph C. A meta-analysis of temperature sensitivity as a microbial trait. *Global change biology* (2018).

[14] Altschul, Stephen F, Madden, Thomas L, Schäffer, Alejandro A, Zhang, Jinghui, Zhang, Zheng, Miller, Webb, and Lipman, David J. Gapped blast and psi-blast: a new generation of protein database search programs. *Nucleic acids research 25*, 17 (1997), 3389–3402.

[15] Amend, Anthony S, Martiny, Adam C, Allison, Steven D, Berlemont, Renaud, Goulden, Michael L, Lu, Ying, Treseder, Kathleen K, Weihe, Claudia, and Martiny, Jennifer BH. Microbial response to simulated global change is phylogenetically conserved and linked with functional potential. *The ISME journal 10*, 1 (2016), 109–118.

[16] Anderson, Traute-Heidi, and Martens, Rainer. Dna determinations during growth of soil microbial biomasses. *Soil Biology and Biochemistry 57* (2013), 487–495.

[17] Arai, Wataru, Taniguchi, Takeaki, Goto, Susumu, Moriya, Yuki, Uehara, Hideya, Takemoto, Kazuhiro, Ogata, Hiroyuki, and Takami, Hideto. Maple 2.3. 0: an improved system for evaluating the functionomes of genomes and metagenomes. *Bioscience, biotechnology, and biochemistry 82*, 9 (2018), 1515–1517.

[18] Arkin, Adam P, Cottingham, Robert W, Henry, Christopher S, Harris, Nomi L, Stevens, Rick L, Maslov, Sergei, Dehal, Paramvir, Ware, Doreen, Perez, Fernando, Canon, Shane, et al. Kbase: the united states department of energy systems biology knowledgebase. *Nature biotechnology 36*, 7 (2018).

[19] Bachmann, Herwig, Fischlechner, Martin, Rabbers, Iraes, Barfa, Nakul, dos Santos, Filipe Branco, Molenaar, Douwe, and Teusink, Bas. Availability of public goods shapes the evolution of competing metabolic strategies. *Proceedings of the National Academy of Sciences 110*, 35 (2013), 14302–14307.

[20] Bakdash, Jonathan Z, and Marusich, Laura R. Repeated measures correlation. *Frontiers in psychology 8* (2017), 456.

[21] Bakken, Lars R, and Olsen, Rolf A. Buoyant densities and dry-matter contents of microorganisms: conversion of a measured biovolume into biomass. *Applied and Environmental Microbiology 45*, 4 (1983), 1188–1195.

[22] Bakken, Lars Reier, and Olsen, Rolf Arnt. Dna-content of soil bacteria of different cell size. *Soil Biology and Biochemistry 21*, 6 (1989), 789–793.

[23] Baldrian, Petr, Kolařík, Miroslav, Štursová, Martina, Kopeckỳ, Jan, Valášková, Vendula, Větrovskỳ, Tomáš, Žifčáková, Lucia, Šnajdr, Jaroslav, Rídl, Jakub, Vlček, Čestmír, et al. Active and total microbial communities in forest soil are largely different and highly stratified during decomposition. *The ISME journal 6*, 2 (2012), 248.

[24] Ballantyne IV, Ford, and Billings, Sharon A. Model formulation of microbial co 2 production and efficiency can significantly influence short and long term soil c projections. *The ISME journal* (2018), 1.

[25] Barberán, Albert, Velazquez, Hildamarie Caceres, Jones, Stuart, and Fierer, Noah. Hiding in plain sight: Mining bacterial species records for phenotypic trait information. *MSphere 2*, 4 (2017), e00237–17.

[26] Bates, Douglas, Mächler, Martin, Bolker, Ben, and Walker, Steve. Fitting linear mixed-effects models using lme4. *Journal of Statistical Software 67*, 1 (2015), 1–48.

[27] Bendaoud, Meriem, Vinogradov, Evgeny, Balashova, Nataliya V, Kadouri, Daniel E, Kachlany, Scott C, and Kaplan, Jeffrey B. Broad-spectrum biofilm inhibition by kingella kingae exopolysaccharide. *Journal of bacteriology 193*, 15 (2011), 3879–3886.

[28] Berglund, Eva, and Rousk, Johannes. Microbial adaptations to temperature modulates carbon use efficiencies. In *EGU General Assembly Conference Abstracts* (2018), vol. 20, p. 8531.

[29] Blagodatskaya, Evgenia, Blagodatsky, Sergey, Anderson, Traute-Heidi, and Kuzyakov, Yakov. Microbial growth and carbon use efficiency in the rhizosphere and root-free soil. *PloS one 9*, 4 (2014), e93282.

[30] Blagodatskaya, Evgenia, and Kuzyakov, Yakov. Active microorganisms in soil: Critical review of estimation criteria and approaches. *Soil Biology and Biochemistry 67* (Dec. 2013), 192–211.

[31] Blake, Ruth E, Surkov, Aleksandr V, Stout, Lisa M, Li, Hui, Chang, Sae Jung, Jaisi, Deb P, Colman, Albert S, and Liang, Yuhong. Dna thermometry: A universal biothermometer in the 18o/16o ratio of po4 in dna. *American Journal of Science 316*, 9 (2016), 813–838.

[32] Blanc, Cyril, Sy, M, Djigal, D, Brauman, Alain, Normand, P, and Villenave, Cécile. Nutrition on bacteria by bacterial-feeding nematodes and consequences on the structure of soil bacterial community. *European Journal of Soil Biology 42* (2006), S70–S78.

[33] Blankinship, Joseph, Niklaus, Pascal, and Hungate, Bruce. A meta-analysis of responses of soil biota to global change. *Oecologia 165*, 3 (2011), 553–565.

[34] Blazewicz, Steven J, Schwartz, Egbert, and Firestone, Mary K. Growth and death of bacteria and fungi underlie rainfall-induced carbon dioxide pulses from seasonally dried soil. *Ecology 95*, 5 (2014), 1162–1172.

[35] Blomberg, Simon P, Garland, Theodore, and Ives, Anthony R. Testing for phylogenetic signal in comparative data: behavioral traits are more labile. *Evolution 57*, 4 (2003), 717–745.

[36] Boc, Alix, Diallo, Alpha Boubacar, and Makarenkov, Vladimir. T-rex: a web server for inferring, validating and visualizing phylogenetic trees and networks. *Nucleic acids research 40*, W1 (2012), W573–W579.

[37] Boose, Emery. Fisher Meteorological Station at Harvard Forest since 2001. Harvard Forest Data Archive: HF001, doi = doi:10.6073/pasta/04076dfd30b286c6c29301b6345a63f5, howpublished= `http://harvardforest.fas.harvard.edu:8080/exist/apps/datasets/showdata.html?id=hf001`, 2001.

[38] Bosdriesz, Evert, Molenaar, Douwe, Teusink, Bas, and Bruggeman, Frank J. How fast-growing bacteria robustly tune their ribosome concentration to approximate growth-rate maximization. *FEBS journal 282*, 10 (2015), 2029–2044.

[39] Boutte, Cara C, and Crosson, Sean. Bacterial lifestyle shapes stringent response activation. *Trends in microbiology 21*, 4 (2013), 174–180.

[40] Bradford, Mark, Wieder, William, Bonan, Gordon, Noah, Fierer, Raymond, Peter, and Crowther, Thomas. Managing uncertainty in soil carbon feedbacks to climate change. *Nature Climate Change 6*, August 2016 (2016), 751–758.

[41] Bradford, Mark A, Davies, Christian A, Frey, Serita D, Maddox, Thomas R, Melillo, Jerry M, Mohan, Jacqueline E, Reynolds, James F, Treseder, Kathleen K, and Wallenstein, Matthew D. Thermal adaptation of soil microbial respiration to elevated temperature. *Ecology Letters 11*, 12 (2008), 1316–1327.

[42] Brown, Melanie J, and Lester, John N. Comparison of bacterial extracellular polymer extraction methods. *Appl. Environ. Microbiol. 40*, 2 (1980), 179–185.

[43] Caporaso, J Gregory, Kuczynski, Justin, Stombaugh, Jesse, Bittinger, Kyle, Bushman, Frederic D, Costello, Elizabeth K, Fierer, Noah, Pena, Antonio Gonzalez, Goodrich, Julia K, Gordon, Jeffrey I, et al. Qiime allows analysis of high-throughput community sequencing data. *Nature methods 7*, 5 (2010), 335.

[44] Cavicchioli, Ricardo. On the concept of a psychrophile. *The ISME journal 10*, 4 (2016), 793.

[45] Chang, Winston, Cheng, Joe, Allaire, JJ, Xie, Yihui, and McPherson, Jonathan. *shiny: Web Application Framework for R*, 2018. R package version 1.1.0.

[46] Chapman, Samantha K, Newman, Gregory S, Hart, Stephen C, Schweitzer, Jennifer A, and Koch, George W. Leaf litter mixtures alter microbial community development: mechanisms for non-additive effects in litter decomposition. *PLoS One 8*, 4 (2013), e62671.

[47] Chen, I-Min A, Chu, Ken, Palaniappan, Krishna, Pillay, Manoj, Ratner, Anna, Huang, Jinghua, Huntemann, Marcel, Varghese, Neha, White, James R, Seshadri, Rekha, et al. Img/m v. 5.0: an integrated data management and comparative analysis system for microbial genomes and microbiomes. *Nucleic acids research 47*, D1 (2018), D666–D677.

[48] Chen, I-Min A, Markowitz, Victor M, Chu, Ken, Palaniappan, Krishna, Szeto, Ernest, Pillay, Manoj, Ratner, Anna, Huang, Jinghua, Andersen, Evan, Huntemann, Marcel, et al. Img/m: integrated genome and metagenome comparative data analysis system. *Nucleic acids research* (2016), gkw929.

[49] Cheng, Chuankai, O'brien, Edward J, McCloskey, Douglas, Utrilla, Jose, Olson, Connor, LaCroix, Ryan A, Sandberg, Troy E, Feist, Adam M, Palsson, Bernhard O, and King, Zachary A. Laboratory evolution reveals a two-dimensional rate-yield tradeoff in microbial metabolism. *BioRxiv* (2018), 414912.

[50] Christensen, H, Olsen, RA, and Bakken, LR. Flow cytometric measurements of cell volumes and dna contents during culture of indigenous soil bacteria. *Microbial ecology 29*, 1 (1995), 49–62.

[51] Christensen, Henrik, Bakken, Lars R, and Olsen, Rolf A. Soil bacterial dna and biovolume profiles measured by flow-cytometry. *FEMS Microbiology Ecology 11*, 3-4 (1993), 129–140.

[52] Chubukov, Victor, Gerosa, Luca, Kochanowski, Karl, and Sauer, Uwe. Coordination of microbial metabolism. *Nature Reviews Microbiology 12*, 5 (2014), 327–340.

[53] Cleveland, Cory C, and Liptzin, Daniel. C: N: P stoichiometry in soil: is there a "redfield ratio" for the microbial biomass? *Biogeochemistry 85*, 3 (2007), 235–252.

[54] Collins, MD, Dorsch, M, and Stackebrandt, E. Transfer of pimelobacter tumescens to terrabacter gen. nov. as terrabacter tumescens comb. nov. and of pimelobacter jensenii to nocardioides as nocardioides jensenii comb. nov. *International Journal of Systematic and Evolutionary Microbiology 39*, 1 (1989), 1–6.

[55] Conant, Richard T., Steinweg, J. Megan, Haddix, Michelle, Paul, Eldor A., Plante, Alain F., and Six, Johan. Experimental warming shows that decomposition temperature sensitivity increases with soil organic matter recalcitrance. *Ecology 89* (2008), 2384–2391. 9.

[56] Cornelissen, Johannes HC, Van Bodegom, Peter M, Aerts, Rien, Callaghan, Terry V, Van Logtestijn, Richard SP, Alatalo, Juha, Stuart Chapin, F, Gerdol, Renato, Gudmundsson, Jon, Gwynn-Jones, Dylan, et al. Global negative vegetation feedback to climate warming responses of leaf litter decomposition rates in cold biomes. *Ecology letters 10*, 7 (2007), 619–627.

[57] Cottrell, Matthew T., and Kirchman, David L. Transcriptional control in marine copiotrophic and oligotrophic bacteria with streamlined genomes. *Applied and Environmental Microbiology* (2016).

[58] Coward, Elizabeth K, Ohno, Tsutomu, and Sparks, Donald L. Direct evidence for temporal molecular fractionation of dissolved organic matter at the iron oxyhydroxide interface. *Environmental science & technology 53*, 2 (2018), 642–650.

[59] Crowther, Thomas W, Thomas, Stephen M, Maynard, Daniel S, Baldrian, Petr, Covey, Kristofer, Frey, Serita D, van Diepen, Linda TA, and Bradford, Mark A. Biotic interactions mediate soil microbial feedbacks to climate change. *Proceedings of the National Academy of Sciences 112*, 22 (2015), 7033–7038.

[60] De Deken, RH. The crabtree effect: a regulatory system in yeast. *Microbiology 44*, 2 (1966), 149–156.

[61] DeAngelis, Kristen M, Pold, Grace, Topçuoğlu, Begüm D, van Diepen, Linda TA, Varney, Rebecca M, Blanchard, Jeffrey L, Melillo, Jerry, and Frey, Serita D. Long-term forest soil warming alters microbial communities in temperate forest soils. *Frontiers in microbiology 6* (2015), 104.

[62] Dechesne, Arnaud, Wang, Gang, Gülez, Gamze, Or, Dani, and Smets, Barth F. Hydration-controlled bacterial motility and dispersal on surfaces. *Proceedings of the National Academy of Sciences 107*, 32 (2010), 14369–14372.

[63] Del Rio, Tijana Glavina, Abt, Birte, Spring, Stefan, Lapidus, Alla, Nolan, Matt, Tice, Hope, Copeland, Alex, Cheng, Jan-Fang, Chen, Feng, Bruce, David, et al. Complete genome sequence of chitinophaga pinensis type strain (uqm 2034 t). *Standards in genomic sciences 2*, 1 (2010), 87.

[64] Delgado-Baquerizo, Manuel, Oliverio, Angela M, Brewer, Tess E, Benavent-González, Alberto, Eldridge, David J, Bardgett, Richard D, Maestre, Fernando T, Singh, Brajesh K, and Fierer, Noah. A global atlas of the dominant bacteria found in soil. *Science 359*, 6373 (2018), 320–325.

[65] DeSantis, Todd Z, Hugenholtz, Philip, Larsen, Neils, Rojas, Mark, Brodie, Eoin L, Keller, Keith, Huber, Thomas, Dalevi, Daniel, Hu, Ping, and Andersen, Gary L. Greengenes, a chimera-checked 16s rrna gene database and workbench compatible with arb. *Appl. Environ. Microbiol. 72*, 7 (2006), 5069–5072.

[66] Dethlefsen, Les, and Schmidt, Thomas M. Performance of the translational apparatus varies with the ecological strategies of bacteria. *Journal of bacteriology 189*, 8 (2007), 3237–3245.

[67] Deutscher, Josef, Francke, Christof, and Postma, Pieter W. How phosphotransferase system-related protein phosphorylation regulates carbohydrate metabolism in bacteria. *Microbiol. Mol. Biol. Rev. 70*, 4 (2006), 939–1031.

[68] Devêvre, Olivier C, and Horwáth, William R. Decomposition of rice straw and microbial carbon use efficiency under different soil temperatures and moistures. *Soil Biology and Biochemistry 32*, 11-12 (2000), 1773–1785.

[69] Dictor, Marie-Christine, Tessier, Laurent, and Soulas, Guy. Reassessement of the kec coefficient of the fumigation–extraction method in a soil profile. *Soil Biology and Biochemistry 30*, 2 (1998), 119–127.

[70] Dijkstra, Paul, Blankinship, Joseph C, Selmants, Paul C, Hart, Stephen C, Koch, George W, Schwartz, Egbert, and Hungate, Bruce A. Probing carbon flux patterns through soil microbial metabolic networks using parallel position-specific tracer labeling. *Soil Biology and Biochemistry 43*, 1 (2011), 126–132.

[71] Dijkstra, Paul, Dalder, Jacob J, Selmants, Paul C, Hart, Stephen C, Koch, George W, Schwartz, Egbert, and Hungate, Bruce A. Modeling soil metabolic processes using isotopologue pairs of position-specific 13 c-labeled glucose and pyruvate. *Soil Biology and Biochemistry 43*, 9 (2011), 1848–1857.

[72] Dijkstra, Paul, Thomas, Scott C, Heinrich, Paul L, Koch, George W, Schwartz, Egbert, and Hungate, Bruce A. Effect of temperature on metabolic activity of intact microbial communities: evidence for altered metabolic pathway activity but not for increased maintenance respiration and reduced carbon use efficiency. *Soil Biology and Biochemistry 43*, 10 (2011), 2023–2031.

[73] Dineen, SM, Aranda, Rt, Anders, DL, and Robertson, JM. An evaluation of commercial dna extraction kits for the isolation of bacterial spore dna from soil. *Journal of applied microbiology 109*, 6 (2010), 1886–1896.

[74] Dobson, Lynne F, and O'Shea, Daniel G. Antagonistic effect of divalent cations ca 2+ and mg 2+ on the morphological development of streptomyces hygroscopicus var. geldanus. *Applied microbiology and biotechnology 81*, 1 (2008), 119.

[75] Doetterl, S., Berhe, A. A., Arnold, C., Bodé, S., Fiener, P., Finke, P., Fuchslueger, L., Griepentrog, M., Harden, J. W., Nadeu, E., Schnecker, J., Six, J., Trumbore, S., Van Oost, K., Vogel, C., and Boeckx, P. Links among warming, carbon and microbial dynamics mediated by soil mineral weathering. *Nature Geoscience* (2018).

[76] Doetterl, Sebastian, Stevens, Antoine, Six, Johan, Merckx, Roel, Van Oost, Kristof, Pinto, Manuel Casanova, Casanova-Katny, Angélica, Muñoz, Cristina, Boudin, Mathieu, Venegas, Erick Zagal, et al. Soil carbon storage controlled by interactions between geochemistry and climate. *Nature Geoscience 8*, 10 (2015), 780–783.

[77] Donachie, William D. Relationship between cell size and time of initiation of dna replication. *Nature 219*, 5158 (1968), 1077.

[78] Drigo, Barbara, Anderson, Ian C, Kannangara, GSK, Cairney, John WG, and Johnson, David. Rapid incorporation of carbon from ectomycorrhizal mycelial necromass into soil fungal communities. *Soil Biology and Biochemistry 49* (2012), 4–10.

[79] Edgar, Robert C. Search and clustering orders of magnitude faster than BLAST. *Bioinformatics 26*, 19 (Oct. 2010), 2460–2461.

[80] Edirisinghe, Janaka N, Weisenhorn, Pamela, Conrad, Neal, Xia, Fangfang, Overbeek, Ross, Stevens, Rick L, and Henry, Christopher S. Modeling central metabolism and energy biosynthesis across microbial life. *BMC genomics 17*, 1 (2016), 568.

[81] Elbourne, Liam DH, Tetu, Sasha G, Hassan, Karl A, and Paulsen, Ian T. Transportdb 2.0: a database for exploring membrane transporters in sequenced genomes from all domains of life. *Nucleic acids research 45*, D1 (2016), D320–D324.

[82] Elek, Anamaria, Kuzman, Maja, and Vlahovicek, Kristian. *coRdon: Codon Usage Analysis and Prediction of Gene Expressivity*, 2018. R package version 1.0.0.

[83] Evans, Sarah, Martiny, Jennifer BH, and Allison, Steven D. Effects of dispersal and selection on stochastic assembly in microbial communities. *The ISME journal 11*, 1 (2017), 176.

[84] Falkowski, Paul G, Fenchel, Tom, and Delong, Edward F. The microbial engines that drive earth's biogeochemical cycles. *science 320*, 5879 (2008), 1034–1039.

[85] Feinstein, Larry M, Sul, Woo Jun, and Blackwood, Christopher B. Assessment of bias associated with incomplete extraction of microbial dna from soil. *Applied and environmental microbiology 75*, 16 (2009), 5428–5433.

[86] Fierer, Noah, Bradford, Mark A, and Jackson, Robert B. Toward an ecological classification of soil bacteria. *Ecology 88*, 6 (2007), 1354–1364.

[87] Fierer, Noah, Jackson, Jason A, Vilgalys, Rytas, and Jackson, Robert B. Assessment of soil microbial community structure by use of taxon-specific quantitative pcr assays. *Appl. Environ. Microbiol. 71*, 7 (2005), 4117–4120.

[88] Fierer, Noah, and Jackson, Robert B. The diversity and biogeography of soil bacterial communities. *Proceedings of the National Academy of Sciences of the United States of America 103*, 3 (2006), 626–631.

[89] Fierer, Noah, Strickland, Michael S, Liptzin, Daniel, Bradford, Mark A, and Cleveland, Cory C. Global patterns in belowground communities. *Ecology letters 12*, 11 (2009), 1238–1249.

[90] Flamholz, Avi, Noor, Elad, Bar-Even, Arren, Liebermeister, Wolfram, and Milo, Ron. Glycolytic strategy as a tradeoff between energy yield and protein cost. *Proceedings of the National Academy of Sciences* (2013), 201215283.

[91] Frey, Serita D, Lee, Juhwan, Melillo, Jerry M, and Six, Johan. The temperature response of soil microbial efficiency and its feedback to climate. *Nature Climate Change 3*, 4 (2013), 395.

[92] Friedlingstein, Pierre, Meinshausen, Malte, Arora, Vivek K, Jones, Chris D, Anav, Alessandro, Liddicoat, Spencer K, and Knutti, Reto. Uncertainties in cmip5 climate projections due to carbon cycle feedbacks. *Journal of Climate 27*, 2 (2014), 511–526.

[93] Friedman, Jonathan, Higgins, Logan M, and Gore, Jeff. Community structure follows simple assembly rules in microbial microcosms. *Nature ecology & evolution 1*, 5 (2017), 0109.

[94] German, Donovan P, Marcelo, Kathleen RB, Stone, Madeleine M, and Allison, Steven D. The michaelis–menten kinetics of soil extracellular enzymes in response to temperature: a cross-latitudinal study. *Global Change Biology 18*, 4 (2012), 1468–1479.

[95] Geyer, Kevin M, Dijkstra, Paul, Sinsabaugh, Robert, and Frey, Serita D. Clarifying the interpretation of carbon use efficiency in soil through methods comparison. *Soil Biology and Biochemistry 128* (2019), 79–88.

[96] Geyer, Kevin M, Kyker-Snowman, Emily, Grandy, A Stuart, and Frey, Serita D. Microbial carbon use efficiency: accounting for population, community, and ecosystem-scale controls over the fate of metabolized organic matter. *Biogeochemistry 127*, 2-3 (2016), 173–188.

[97] Ghezzehei, Teamrat A, Sulman, Benjamin, Arnold, Chelsea L, Bogie, Nathaniel A, and Berhe, Asmeret Asefaw. On the role of soil water retention characteristic on aerobic microbial respiration. *Biogeosciences 16*, 6 (2019), 1187–1209.

[98] Gibson, Beth, Wilson, Daniel J, Feil, Edward, and Eyre-Walker, Adam. The distribution of bacterial doubling times in the wild. *Proceedings of the Royal Society B: Biological Sciences 285*, 1880 (2018), 20180789.

[99] Goldfarb, Katherine C, Karaoz, Ulas, Hanson, China A, Santee, Clark A, Bradford, Mark A, Treseder, Kathleen K, Wallenstein, Matthew D, and Brodie, Eoin L. Differential growth responses of soil bacterial taxa to carbon substrates of varying chemical recalcitrance. *Frontiers in microbiology 2* (2011), 94.

[100] Gommers, PJF, Van Schie, BJ, Van Dijken, JP, and Kuenen, JG. Biochemical limits to microbial growth yields: an analysis of mixed substrate utilization. *Biotechnology and bioengineering 32*, 1 (1988), 86–94.

[101] Goo, Eunhye, An, Jae Hyung, Kang, Yongsung, and Hwang, Ingyu. Control of bacterial metabolism by quorum sensing. *Trends in microbiology 23*, 9 (2015), 567–576.

[102] Grandy, A Stuart, Strickland, Michael S, Lauber, Christian L, Bradford, Mark A, and Fierer, Noah. The influence of microbial communities, management, and soil texture on soil organic matter chemistry. *Geoderma 150*, 3-4 (2009), 278–286.

[103] Grimmett, IJ, Shipp, KN, Macneil, A, and Bärlocher, F. Does the growth rate hypothesis apply to aquatic hyphomycetes? *fungal ecology 6*, 6 (2013), 493–500.

[104] Gunina, Anna, Dippold, Michaela A, Glaser, Bruno, and Kuzyakov, Yakov. Fate of low molecular weight organic substances in an arable soil: from microbial uptake to utilisation and stabilisation. *Soil Biology and Biochemistry 77* (2014), 304–313.

[105] Hagerty, Shannon B, Allison, Steven D, and Schimel, Joshua P. Evaluating soil microbial carbon use efficiency explicitly as a function of cellular processes: implications for measurements and models. *Biogeochemistry 140*, 3 (2018), 269–283.

[106] Hagerty, Shannon B, Van Groenigen, Kees Jan, Allison, Steven D, Hungate, Bruce A, Schwartz, Egbert, Koch, George W, Kolka, Randall K, and Dijkstra, Paul. Accelerated microbial turnover but constant growth efficiency with warming in soil. *Nature Climate Change 4*, 10 (2014), 903.

[107] Hai-Feng, XIAO, Gen, LI, Da-Ming, LI, Feng, HU, and Hui-Xin, LI. Effect of different bacterial-feeding nematode species on soil bacterial numbers, activity, and community composition. *Pedosphere 24*, 1 (2014), 116–124.

[108] Hall, Edward K, Singer, Gabriel A, Kainz, Martin J, and Lennon, Jay T. Evidence for a temperature acclimation mechanism in bacteria: an empirical test of a membrane-mediated trade-off. *Functional Ecology 24*, 4 (2010), 898–908.

[109] Harmon, Luke J, Weir, Jason T, Brock, Chad D, Glor, Richard E, and Challenger, Wendell. Geiger: investigating evolutionary radiations. *Bioinformatics 24*, 1 (2007), 129–131.

[110] Harrison, David EF. The regulation of respiration rate in growing bacteria. In *Advances in microbial physiology*, vol. 14. Elsevier, 1976, pp. 243–313.

[111] Herron, Patrick M, Stark, John M, Holt, Carson, Hooker, Toby, and Cardon, Zoe G. Microbial growth efficiencies across a soil moisture gradient assessed using 13 c-acetic acid vapor and 15 n-ammonia gas. *Soil Biology and Biochemistry 41*, 6 (2009), 1262–1269.

[112] Himeoka, Yusuke, and Kaneko, Kunihiko. Enzyme oscillation can enhance the thermodynamic efficiency of cellular metabolism: consequence of anti-phase coupling between reaction flux and affinity. *Physical biology 13*, 2 (2016), 026002.

[113] Hobbs, Glyn, Frazer, Catherine M, Gardner, David CJ, Cullum, John A, and Oliver, Stephen G. Dispersed growth of streptomyces in liquid culture. *Applied microbiology and biotechnology 31*, 3 (1989), 272–277.

[114] Hoehler, Tori M., and Jørgensen, Bo Barker. Microbial life under extreme energy limitation. *Nature Reviews Microbiology 11*, 2 (Feb. 2013), 83–94.

[115] Hoeppner, Susanne S., and Dukes, Jeffrey S. Interactive responses of old-field plant growth and composition to warming and precipitation. *Global Change Biology 18*, 5 (2012), 1754–1768.

[116] Huang, Le, Zhang, Han, Wu, Peizhi, Entwistle, Sarah, Li, Xueqiong, Yohe, Tanner, Yi, Haidong, Yang, Zhenglu, and Yin, Yanbin. dbcan-seq: a database of carbohydrate-active enzyme (cazyme) sequence and annotation. *Nucleic acids research 46*, D1 (2017), D516–D521.

[117] Hui, Sheng, Silverman, Josh M, Chen, Stephen S, Erickson, David W, Basan, Markus, Wang, Jilong, Hwa, Terence, and Williamson, James R. Quantitative proteomic analysis reveals a simple strategy of global resource allocation in bacteria. *Molecular systems biology 11*, 2 (2015), 784.

[118] Hungate, Bruce A, Mau, Rebecca L, Schwartz, Egbert, Caporaso, J Gregory, Dijkstra, Paul, van Gestel, Natasja, Koch, Benjamin J, Liu, Cindy M, McHugh, Theresa A, Marks, Jane C, et al. Quantitative microbial ecology through stable isotope probing. *Applied and environmental microbiology* (2015), AEM–02280.

[119] Ihssen, Julian, and Egli, Thomas. Global physiological analysis of carbon- and energy-limited growing escherichia coli confirms a high degree of catabolic flexibility and preparedness for mixed substrate utilization. *Environmental microbiology 7*, 10 (2005), 1568–1581.

[120] IPCC. Climate Change 2013: The Physical Science Basis. Contribution of Working Group I to the Fifth Assessment Report of the Intergovernmental Panel on Climate Change (IPCC). Tech. rep., Cambridge University Press, Cambridge, United Kingdom and New York, NY, USA, 2013.

[121] Jacob, François, and Monod, Jacques. Genetic regulatory mechanisms in the synthesis of proteins. *Journal of molecular biology 3*, 3 (1961), 318–356.

[122] Jenkinson, DS. The effects of biocidal treatments on metabolism in soil—iv. the decomposition of fumigated organisms in soil. *Soil Biology and Biochemistry 8*, 3 (1976), 203–208.

[123] Joergensen, Rainer Georg. The fumigation-extraction method to estimate soil microbial biomass: calibration of the kec value. *Soil Biology and Biochemistry 28*, 1 (1996), 25–31.

[124] Jones, Ryan T, Robeson, Michael S, Lauber, Christian L, Hamady, Micah, Knight, Rob, and Fierer, Noah. A comprehensive survey of soil acidobacterial diversity using pyrosequencing and clone library analyses. *The ISME journal 3*, 4 (2009), 442–453.

[125] Kafri, Moshe, Metzl-Raz, Eyal, Jona, Ghil, and Barkai, Naama. The cost of protein production. *Cell reports 14*, 1 (2016), 22–31.

[126] Kaleta, Christoph, Schäuble, Sascha, Rinas, Ursula, and Schuster, Stefan. Metabolic costs of amino acid and protein production in escherichia coli. *Biotechnology journal 8*, 9 (2013), 1105–1114.

[127] Kallenbach, Cynthia M, Frey, Serita D, and Grandy, A Stuart. Direct evidence for microbial-derived soil organic matter formation and its ecophysiological controls. *Nature communications 7* (2016), 13630.

[128] Kassambara, Alboukadel. *ggpubr: 'ggplot2' Based Publication Ready Plots*, 2018. R package version 0.2.

[129] Keiblinger, Katharina M, Hall, Edward K, Wanek, Wolfgang, Szukics, Ute, Hämmerle, Ieda, Ellersdorfer, Günther, Böck, Sandra, Strauss, Joseph, Sterflinger, Katja, Richter, Andreas, et al. The effect of resource quantity and resource stoichiometry on microbial carbon-use-efficiency. *FEMS Microbiology Ecology 73*, 3 (2010), 430–440.

[130] Kembel, Steven W., Wu, Martin, Eisen, Jonathan A., and Green, Jessica L. Incorporating 16s Gene Copy Number Information Improves Estimates of Microbial Diversity and Abundance. *PLoS Computational Biology 8*, 10 (Oct. 2012), e1002743.

[131] Kembel, Steven W, Wu, Martin, Eisen, Jonathan A, and Green, Jessica L. Incorporating 16s gene copy number information improves estimates of microbial diversity and abundance. *PLoS Comput Biol 8*, 10 (2012), e1002743.

[132] Kembel, S.W., Cowan, P.D., Helmus, M.R., Cornwell, W.K., Morlon, H., Ackerly, D.D., Blomberg, S.P., and Webb, C.O. Picante: R tools for integrating phylogenies and ecology. *Bioinformatics 26* (2010), 1463–1464.

[133] Kempes, Christopher P, van Bodegom, Peter M, Wolpert, David, Libby, Eric, Amend, Jan, and Hoehler, Tori. Drivers of bacterial maintenance and minimal energy requirements. *Frontiers in microbiology 8* (2017), 31.

[134] Kielak, Anna M, Castellane, Tereza CL, Campanharo, Joao C, Colnago, Luiz A, Costa, Ohana YA, Da Silva, Maria L Corradi, Van Veen, Johannes A, Lemos, Eliana GM, and Kuramae, Eiko E. Characterization of novel acidobacteria exopolysaccharides with potential industrial and ecological applications. *Scientific reports 7* (2017), 41193.

[135] Kim, Dong-Myung, and Swartz, James R. Oxalate improves protein synthesis by enhancing atp supply in a cell-free system derived from escherichia coli. *Biotechnology Letters 22*, 19 (2000), 1537–1542.

[136] Klappenbach, J. A., Dunbar, J. M., and Schmidt, T. M. rRNA operon copy number reflects ecological strategies of bacteria. *Applied and Environmental Microbiology 66*, 4 (2000), 1328–1333.

[137] Kleber, M., Sollins, P., and Sutton, R. A conceptual model of organo-mineral interactions in soils: self-assembly of organic molecular fragments into zonal structures on mineral surfaces. *Biogeochemistry 85*, 1 (June 2007), 9–24.

[138] Koch, Arthur L. WHAT SIZE SHOULD A BACTERIUM BE? A Question of Scale. *Annual Review of Microbiology 50*, 1 (1996), 317–348.

[139] Koch, Arthur L. Oligotrophs versus copiotrophs. *BioEssays 23*, 7 (July 2001), 657–661.

[140] Koch, Benjamin J, McHugh, Theresa A, Hayer, Michaela, Schwartz, Egbert, Blazewicz, Steven J, Dijkstra, Paul, Gestel, Natasja, Marks, Jane C, Mau, Rebecca L, Morrissey, Ember M, et al. Estimating taxon-specific population dynamics in diverse microbial communities. *Ecosphere 9*, 1 (2018).

[141] Konstantinidis, Konstantinos T, Ramette, Alban, and Tiedje, James M. The bacterial species definition in the genomic era. *Philosophical Transactions of the Royal Society B: Biological Sciences 361*, 1475 (2006), 1929–1940.

[142] Koren, Sergey, Walenz, Brian P, Berlin, Konstantin, Miller, Jason R, Bergman, Nicholas H, and Phillippy, Adam M. Canu: scalable and accurate long-read assembly via adaptive k-mer weighting and repeat separation. *Genome research 27*, 5 (2017), 722–736.

[143] Kragh, Kasper Nørskov, Alhede, Maria, Rybtke, Morten, Stavnsberg, Camilla, Jensen, Peter Ø, Tolker-Nielsen, Tim, Whiteley, Marvin, and Bjarnsholt, Thomas. The inoculation method could impact the outcome of microbiological experiments. *Applied and environmental microbiology 84*, 5 (2018), e02264–17.

[144] Kreuzer-Martin, Helen W, Ehleringer, James R, and Hegg, Eric L. Oxygen isotopes indicate most intracellular water in log-phase escherichia coli is derived from metabolism. *Proceedings of the National Academy of Sciences 102*, 48 (2005), 17337–17341.

[145] Kreuzer-Martin, Helen W, Lott, Michael J, Ehleringer, James R, and Hegg, Eric L. Metabolic processes account for the majority of the intracellular water in log-phase escherichia coli cells as revealed by hydrogen isotopes. *Biochemistry 45*, 45 (2006), 13622–13630.

[146] Kristiansen, Anja, Saunders, Aaron M, Hansen, Aviaja A, Nielsen, Per H, and Nielsen, Jeppe L. Community structure of bacteria and fungi in aerosols of a pig confinement building. *FEMS microbiology ecology 80*, 2 (2012), 390–401.

[147] Kubitschek, HE. Constancy of the ratio of dna to cell volume in steady-state cultures of escherichia coli br. *Biophysical journal 14*, 2 (1974), 119.

[148] Kück, Patrick, and Longo, Gary C. Fasconcat-g: extensive functions for multiple sequence alignment preparations concerning phylogenetic studies. *Frontiers in zoology 11*, 1 (2014), 81.

[149] Kurland, CG. Translational accuracy and the fitness of bacteria. *Annual review of genetics 26*, 1 (1992), 29–50.

[150] Kuzyakov, Yakov, and Blagodatskaya, Evgenia. Microbial hotspots and hot moments in soil: concept & review. *Soil Biology and Biochemistry 83* (2015), 184–199.

[151] LaCroix, Ryan A, Sandberg, Troy E, O'Brien, Edward J, Utrilla, Jose, Ebrahim, Ali, Guzman, Gabriela I, Szubin, Richard, Palsson, Bernhard O, and Feist, Adam M. Use of adaptive laboratory evolution to discover key mutations enabling rapid growth of escherichia coli k-12 mg1655 on glucose minimal medium. *Appl. Environ. Microbiol. 81*, 1 (2015), 17–30.

[152] Lang, Jenna Morgan, Darling, Aaron E, and Eisen, Jonathan A. Phylogeny of bacterial and archaeal genomes using conserved genes: supertrees and supermatrices. *PloS one 8*, 4 (2013), e62510.

[153] Langille, Morgan GI, Zaneveld, Jesse, Caporaso, J Gregory, McDonald, Daniel, Knights, Dan, Reyes, Joshua A, Clemente, Jose C, Burkepile, Deron E, Thurber, Rebecca L Vega, Knight, Rob, et al. Predictive functional profiling of microbial communities using 16s rrna marker gene sequences. *Nature biotechnology 31*, 9 (2013), 814.

[154] Lauro, Federico M, McDougald, Diane, Thomas, Torsten, Williams, Timothy J, Egan, Suhelen, Rice, Scott, DeMaere, Matthew Z, Ting, Lily, Ertan, Haluk, Johnson, Justin, et al. The genomic basis of trophic strategy in marine bacteria. *Proceedings of the National Academy of Sciences 106*, 37 (2009), 15527–15533.

[155] Lavorel, Sandra, and Garnier, Éric. Predicting changes in community composition and ecosystem functioning from plant traits: revisiting the holy grail. *Functional ecology 16*, 5 (2002), 545–556.

[156] Le, Si Quang, and Gascuel, Olivier. An improved general amino acid replacement matrix. *Molecular biology and evolution 25*, 7 (2008), 1307–1320.

[157] Leckie, Sara E, Prescott, Cindy E, Grayston, Susan J, Neufeld, Josh D, and Mohn, William W. Comparison of chloroform fumigation-extraction, phospholipid fatty acid, and dna methods to determine microbial biomass in forest humus. *Soil Biology and Biochemistry 36*, 3 (2004), 529–532.

[158] Lee, Kuo-Chang, Webb, Richard I, Janssen, Peter H, Sangwan, Parveen, Romeo, Tony, Staley, James T, and Fuerst, John A. Phylum verrucomicrobia representatives share a compartmentalized cell plan with members of bacterial phylum planctomycetes. *BMC microbiology 9*, 1 (2009), 5.

[159] Lee, Zarraz M, and Schmidt, Thomas M. Bacterial growth efficiency varies in soils under different land management practices. *Soil Biology and Biochemistry 69* (2014), 282–290.

[160] Lehmeier, CA, Ballantyne IV, F, Min, K, and Billings, SA. Temperature-mediated changes in microbial carbon use efficiency and 13 c discrimination. *Biogeosciences Discussions 12*, 20 (2015).

[161] Lennon, Jay T, and Jones, Stuart E. Microbial seed banks: the ecological and evolutionary implications of dormancy. *Nature reviews microbiology 9*, 2 (2011), 119.

[162] Lennon, JT, Muscarella, ME, Placella, SA, and Lehmkuhl, BK. How, when, and where relic dna affects microbial diversity. *mBio 9*, 3 (2018), e00637–18.

[163] Lenth, Russell, Singmann, Henrik, Love, Jonathon, Buerkner, Paul, and Herve, Maxime. *emmeans*. Iowa State, 2019.

[164] Letunic, Ivica, and Bork, Peer. Interactive tree of life (itol) v3: an online tool for the display and annotation of phylogenetic and other trees. *Nucleic acids research 44*, W1 (2016), W242–W245.

[165] Lever, Mark A, Rogers, Karyn L, Lloyd, Karen G, Overmann, Jörg, Schink, Bernhard, Thauer, Rudolf K, Hoehler, Tori M, and Jørgensen, Bo Barker. Life under extreme energy limitation: a synthesis of laboratory-and field-based investigations. *FEMS microbiology reviews 39*, 5 (2015), 688–728.

[166] Li, Hui, Yu, Chan, Wang, Fei, Chang, Sae Jung, Yao, Jun, and Blake, Ruth E. Probing the metabolic water contribution to intracellular water using oxygen isotope ratios of po4. *Proceedings of the National Academy of Sciences 113*, 21 (2016), 5862–5867.

[167] Li, Jianwei, Wang, Gangsheng, Allison, Steven D, Mayes, Melanie A, and Luo, Yiqi. Soil carbon sensitivity to temperature and carbon use efficiency compared across microbial-ecosystem models of varying complexity. *Biogeochemistry 119*, 1-3 (2014), 67–84.

[168] Li, Jianwei, Wang, Gangsheng, Mayes, Melanie A, Allison, Steven D, Frey, Serita D, Shi, Zheng, Hu, Xiao-Ming, Luo, Yiqi, and Melillo, Jerry M. Reduced carbon use efficiency and increased microbial turnover with soil warming. *Global change biology* (2018).

[169] Linstrom, Peter J, and Mallard, William G. The nist chemistry webbook: A chemical data resource on the internet. *Journal of Chemical & Engineering Data 46*, 5 (2001), 1059–1063.

[170] Lipson, David A. The complex relationship between microbial growth rate and yield and its implications for ecosystem processes. *Frontiers in microbiology 6* (2015).

[171] Liu, J, Lee, F, Lin, C, Yao, X, Davenport, JW, and Wong, T. Alternative function of the electron transport system in azotobacter vinelandii: Removal of excess reductant by the cytochrome d pathway. *Applied and environmental microbiology 61*, 11 (1995), 3998–4003.

[172] Lofgren, Lotus A, Uehling, Jessie K, Branco, Sara, Bruns, Thomas D, Martin, Francis, and Kennedy, Peter G. Genome-based estimates of fungal rdna copy number variation across phylogenetic scales and ecological lifestyles. *Molecular ecology* (2018).

[173] Lorca, Graciela L, Barabote, Ravi D, Zlotopolski, Vladimir, Tran, Can, Winnen, Brit, Hvorup, Rikki N, Stonestrom, Aaron J, Nguyen, Elizabeth, Huang, Li-Wen, Kim, David S, et al. Transport capabilities of eleven gram-positive bacteria: comparative genomic analyses. *Biochimica et Biophysica Acta (BBA)-Biomembranes 1768*, 6 (2007), 1342–1366.

[174] Lu, Meng, Zhou, Xuhui, Yang, Qiang, Li, Hui, Luo, Yiqi, Fang, Changming, Chen, Jiakuan, Yang, Xin, and Li, Bo. Responses of ecosystem carbon cycle to experimental warming: a meta-analysis. *Ecology 94*, 3 (2013), 726–738.

[175] Lynch, William H, and Franklin, Mervyn. Effect of temperature on diauxic growth with glucose and organic acids in pseudomonas fluorescens. *Archives of microbiology 118*, 2 (1978), 133–140.

[176] Ma, Wenting, Peng, Donghai, Walker, Sharon L, Cao, Bin, Gao, Chun-Hui, Huang, Qiaoyun, and Cai, Peng. Bacillus subtilis biofilm development in the presence of soil clay minerals and iron oxides. *NPJ biofilms and microbiomes 3*, 1 (2017), 4.

[177] Maechler, Martin, and Ringach, D. Diptest: Hartigan's dip test statistic for unimodality—corrected. *R package version 0.75-7. See https://CRAN. R-project. org/package= diptest* (2015).

[178] Makino, W, Cotner, JB, Sterner, RW, and Elser, JJ. Are bacteria more like plants or animals? growth rate and resource dependence of bacterial c: N: P stoichiometry. *Functional Ecology 17*, 1 (2003), 121–130.

[179] Malik, Ashish A, Puissant, Jeremy, Buckeridge, Kate M, Goodall, Tim, Jehmlich, Nico, Chowdhury, Somak, Gweon, Hyun Soon, Peyton, Jodey M, Mason, Kelly E, van Agtmaal, Maaike, et al. Land use driven change in soil ph affects microbial carbon cycling processes. *Nature communications 9*, 1 (2018), 3591.

[180] Malik, Ashish A, Puissant, Jeremy, Goodall, Tim, Allison, Steven D, and Griffiths, Robert I. Soil microbial communities with greater investment in resource acquisition have lower growth yield. *Soil Biology and Biochemistry* (2019).

[181] Manzoni, Stefano, Taylor, Philip, Richter, Andreas, Porporato, Amilcare, and Ågren, Göran I. Environmental and stoichiometric controls on microbial carbon-use efficiency in soils. *New Phytologist 196*, 1 (2012), 79–91.

[182] Marchler-Bauer, Aron, Lu, Shennan, Anderson, John B, Chitsaz, Farideh, Derbyshire, Myra K, DeWeese-Scott, Carol, Fong, Jessica H, Geer, Lewis Y, Geer, Renata C, Gonzales, Noreen R, et al. Cdd: a conserved domain database for the functional annotation of proteins. *Nucleic acids research 39*, suppl_1 (2010), D225–D229.

[183] Martin, JP, Ervin, JO, and Shepherd, RA. Decomposition and aggregating effect of fungus cell material in soil 1. *Soil Science Society of America Journal 23*, 3 (1959), 217–220.

[184] Martiny, Adam C, Treseder, Kathleen, and Pusch, Gordon. Phylogenetic conservatism of functional traits in microorganisms. *The ISME journal 7*, 4 (2013), 830–838.

[185] Mayali, Xavier, Weber, Peter K, Mabery, Shalini, and Pett-Ridge, Jennifer. Phylogenetic patterns in the microbial response to resource availability: amino acid incorporation in san francisco bay. *PloS one 9*, 4 (2014), e95842.

[186] Maynard, Daniel S, Crowther, Thomas W, and Bradford, Mark A. Fungal interactions reduce carbon use efficiency. *Ecology letters 20*, 8 (2017), 1034–1042.

[187] Melillo, Jerry M, Butler, Sarah, Johnson, Jennifer, Mohan, Jacqueline, Steudler, Paul, Lux, Heidi, Burrows, Elizabeth, Bowles, Francis, Smith, Rose, Scott, Lindsay, Vario, Chelsea, Hill, Troy, Burton, Andrew, Zhou, Yu-Mei, and Tang, Jim. Soil warming, carbon–nitrogen interactions, and forest carbon budgets. *Proceedings of the National Academy of Sciences 108*, 23 (2011), 9508–9512.

[188] Melillo, Jerry M, Frey, Serita D, DeAngelis, Kristen M, Werner, William J, Bernard, Michael J, Bowles, Frank P, Pold, Grace, Knorr, Melanie A, and Grandy, A Stuart. Long-term pattern and magnitude of soil carbon feedback to the climate system in a warming world. *Science in review* (2017).

[189] Mendonça, André G, Alves, Renato J, and Pereira-Leal, José B. Loss of genetic redundancy in reductive genome evolution. *PLoS computational biology 7*, 2 (2011), e1001082.

[190] Merkl, Rainer. A survey of codon and amino acid frequency bias in microbial genomes focusing on translational efficiency. *Journal of molecular evolution 57*, 4 (2003), 453–466.

[191] Mishra, Nitish K, Chang, Junil, and Zhao, Patrick X. Prediction of membrane transport proteins and their substrate specificities using primary sequence information. *PLoS One 9*, 6 (2014), e100278.

[192] Molenaar, Douwe, Van Berlo, Rogier, De Ridder, Dick, and Teusink, Bas. Shifts in growth strategies reflect tradeoffs in cellular economics. *Molecular systems biology 5*, 1 (2009), 323.

[193] Mooshammer, Maria, Wanek, Wolfgang, Hämmerle, Ieda, Fuchslueger, Lucia, Hofhansl, Florian, Knoltsch, Anna, Schnecker, Jörg, Takriti, Mounir, Watzka, Margarete, Wild, Birgit, Keiblinger, Katharina M., Zechmeister-Boltenstern, Sophie, and Richter, Andreas. Adjustment of microbial nitrogen use efficiency to carbon:nitrogen imbalances regulates soil nitrogen cycling. *Nature Communications 5* (Apr. 2014).

[194] Morrison, Eric W, Sevigny, Joseph L., Thomas, W. Kelley, and DeAngelis, Kristen M. Life history traits and genomic markers predictive of microbial parameters relevant to terrestrial carbon cycle.

[195] Morrissey, Ember M, Mau, Rebecca L, Schwartz, Egbert, Caporaso, J Gregory, Dijkstra, Paul, van Gestel, Natasja, Koch, Benjamin J, Liu, Cindy M, Hayer, Michaela, McHugh, Theresa A, et al. Phylogenetic organization of bacterial activity. *The ISME journal* (2016).

[196] Mouginot, Céline, Kawamura, Rika, Matulich, Kristin L, Berlemont, Renaud, Allison, Steven D, Amend, Anthony S, and Martiny, Adam C. Elemental stoichiometry of fungi and bacteria strains from grassland leaf litter. *Soil Biology and Biochemistry 76* (2014), 278–285.

[197] Murali, Adithya, Bhargava, Aniruddha, and Wright, Erik S. Idtaxa: a novel approach for accurate taxonomic classification of microbiome sequences. *Microbiome 6*, 1 (2018), 140.

[198] Muscarella, Mario E, and Lennon, Jay T. Trait-based approach to bacterial growth efficiency. *bioRxiv* (2018), 427161.

[199] Muyzer, G. de Waal, E C. Uitterlinden A G. Profiling of complex microbial populations by denaturing gradient gel electrophoresis analysis of polymerase chain reaction-amplified genes coding for 16s rrna. *Applied and Environmental Microbiology 59*, 3 (1993), 695–700.

[200] Navarro Llorens, Juana María, Tormo, Antonio, and Martínez-García, Esteban. Stationary phase in gram-negative bacteria. *FEMS microbiology reviews 34*, 4 (2010), 476–495.

[201] Nedwell, David B. Effect of low temperature on microbial growth: lowered affinity for substrates limits growth at low temperature. *FEMS microbiology ecology 30*, 2 (1999), 101–111.

[202] Notredame, Cédric, Higgins, Desmond G, and Heringa, Jaap. T-coffee: a novel method for fast and accurate multiple sequence alignment1. *Journal of molecular biology 302*, 1 (2000), 205–217.

[203] Oksanen, Jari, Blanchet, F. Guillaume, Friendly, Michael, Kindt, Roeland, Legendre, Pierre, McGlinn, Dan, Minchin, Peter R., O'Hara, R. B., Simpson, Gavin L., Solymos, Peter, Stevens, M. Henry H., Szoecs, Eduard, and Wagner, Helene. *vegan: Community Ecology Package*, 2017. R package version 2.4-2.

[204] Oldfield, Emily E, Crowther, Thomas W, and Bradford, Mark A. Substrate identity and amount overwhelm temperature effects on soil carbon formation. *Soil Biology and Biochemistry 124* (2018), 218–226.

[205] Öquist, Mats G, Erhagen, Björn, Haei, Mahsa, Sparrman, Tobias, Ilstedt, Ulrik, Schleucher, Jürgen, and Nilsson, Mats B. The effect of temperature and substrate quality on the carbon use efficiency of saprotrophic decomposition. *Plant and Soil 414*, 1-2 (2017), 113–125.

[206] Orme, David, et al. The caper package: comparative analysis of phylogenetics and evolution in r. *R package version 5*, 2 (2013), 1–36.

[207] Padan, Etana, Bibi, Eitan, Ito, Masahiro, and Krulwich, Terry A. Alkaline ph homeostasis in bacteria: new insights. *Biochimica et biophysica acta (BBA)-biomembranes 1717*, 2 (2005), 67–88.

[208] Pagel, Mark. Inferring the historical patterns of biological evolution. *Nature 401*, 6756 (1999), 877–884.

[209] Pagès, H., Aboyoun, P., Gentleman, R., and DebRoy, S. *Biostrings: String objects representing biological sequences, and matching algorithms*, 2016. R package version 2.42.1.

[210] Papp, Katerina, Mau, Rebecca L, Hayer, Michaela, Koch, Benjamin J, Hungate, Bruce A, and Schwartz, Egbert. Quantitative stable isotope probing with h2 18 o reveals that most bacterial taxa in soil synthesize new ribosomal rna. *The ISME journal 12*, 12 (2018), 3043–3045.

[211] PARKINSON, D., and WILLIAMS, S. T. A method for isolateing fungi from soil microhabitats. *Plant and Soil 13*, 4 (1961), 347–355.

[212] Parks, Donovan H, Imelfort, Michael, Skennerton, Connor T, Hugenholtz, Philip, and Tyson, Gene W. Checkm: assessing the quality of microbial genomes recovered from isolates, single cells, and metagenomes. *Genome research 25*, 7 (2015), 1043–1055.

[213] Parton, Schimel, D. S., Cole, C. V., and Ojima, D. S. Analysis of factors controlling soil organic matter levels in Great Plains grasslands. *Soil Science Society of America Journal 51*, 5 (1987), 1173–1179.

[214] Petersen, Thomas Nordahl, Brunak, Søren, von Heijne, Gunnar, and Nielsen, Henrik. Signalp 4.0: discriminating signal peptides from transmembrane regions. *Nature methods 8*, 10 (2011), 785.

[215] Pfeiffer, Thomas, Schuster, Stefan, and Bonhoeffer, Sebastian. Cooperation and competition in the evolution of atp-producing pathways. *Science 292*, 5516 (2001), 504–507.

[216] Pietikäinen, Janna, Pettersson, Marie, and Bååth, Erland. Comparison of temperature effects on soil respiration and bacterial and fungal growth rates. *FEMS Microbiology Ecology 52*, 1 (2005), 49–58.

[217] Pietikäinen, Janna, Pettersson, Marie, and Bååth, Erland. Comparison of temperature effects on soil respiration and bacterial and fungal growth rates. *FEMS Microbiology Ecology 52*, 1 (Mar. 2005), 49–58.

[218] Pirt, S. J. The Maintenance Energy of Bacteria in Growing Cultures. *Proceedings of the Royal Society of London. Series B, Biological Sciences 163*, 991 (Oct. 1965), 224–231. ArticleType: research-article / Full publication date: Oct. 12, 1965 / Copyright © 1965 The Royal Society.

[219] Pirt, S John. Maintenance energy: a general model for energy-limited and energy-sufficient growth. *Archives of Microbiology 133*, 4 (1982), 300–302.

[220] Pisani, Oliva, Frey, Serita D, Simpson, André J, and Simpson, Myrna J. Soil warming and nitrogen deposition alter soil organic matter composition at the molecular-level. *Biogeochemistry 123*, 3 (2015), 391–409.

[221] Poeplau, Christopher, Helfrich, Mirjam, Dechow, Rene, Szoboszlay, Márton, Tebbe, Christoph C, Don, Axel, Greiner, Bärbel, Zopf, Dorit, Thumm, Ulrich, Korevaar, Hein, et al. Increased microbial anabolism contributes to soil carbon sequestration by mineral fertilization in temperate grasslands. *Soil Biology and Biochemistry 130* (2019), 167–176.

[222] Pold, Grace, Billings, Andrew F, Blanchard, Jeff L, Burkhardt, Daniel B, Frey, Serita D, Melillo, Jerry M, Schnabel, Julia, van Diepen, Linda TA, and DeAngelis, Kristen M. Long-term warming alters carbohydrate degradation potential in temperate forest soils. *Applied and environmental microbiology 82*, 22 (2016), 6518–6530.

[223] Pold, Grace, Conlon, Erin M, Huntemann, Marcel, Pillay, Manoj, Mikhailova, Natalia, Stamatis, Dimitrios, Reddy, TBK, Daum, Chris, Shapiro, Nicole, Kyrpides, Nikos, et al. Genome sequence of verrucomicrobium sp. strain gas474, a novel bacterium isolated from soil. *Genome announcements 6*, 4 (2018), e01451–17.

[224] Pold, Grace, and DeAngelis, Kristen M. Up against the wall: the effects of climate warming on soil microbial diversity and the potential for feedbacks to the carbon cycle. *Diversity 5*, 2 (2013), 409–425.

[225] Pold, Grace, Grandy, A Stuart, Melillo, Jerry M, and DeAngelis, Kristen M. Changes in substrate availability drive carbon cycle response to chronic warming. *Soil Biology and Biochemistry 110* (2017), 68–78.

[226] Pold, Grace, Huntemann, Marcel, Pillay, Manoj, Mikhailova, Natalia, Stamatis, Dimitrios, Reddy, TBK, Daum, Chris, Shapiro, Nicole, Kyrpides, Nikos, Woyke, Tanja, et al. Draft genome sequences of three strains of a novel rhizobiales species isolated from forest soil. *Genome announcements 6*, 5 (2018), e01452–17.

[227] Pold, Grace, Melillo, Jerry M, and DeAngelis, Kristen M. Two decades of warming increases diversity of a potentially lignolytic bacterial community. *Frontiers in microbiology 6* (2015), 480.

[228] Portillo, Maria C, Leff, Jonathan W, Lauber, Christian L, and Fierer, Noah. Cell size distributions of soil bacterial and archaeal taxa. *Appl. Environ. Microbiol. 79*, 24 (2013), 7610–7617.

[229] Qiao, Mingfeng, Xiao, Juan, Yin, Huajun, Pu, Xiaozhen, Yue, Bisong, and Liu, Qing. Analysis of the phenolic compounds in root exudates produced by a subalpine coniferous species as responses to experimental warming and nitrogen fertilisation. *Chemistry and Ecology 30*, 6 (2014), 555–565.

[230] Qiao, Yang, Wang, Jing, Liang, Guopeng, Du, Zhenggang, Zhou, Jian, Zhu, Chen, Huang, Kun, Zhou, Xuhui, Luo, Yiqi, Yan, Liming, et al. Global variation of soil microbial carbon-use efficiency in relation to growth temperature and substrate supply. *Scientific reports 9*, 1 (2019), 5621.

[231] R Core Team. *R: A Language and Environment for Statistical Computing*. R Foundation for Statistical Computing, Vienna, Austria, 2016.

[232] R Core Team. *R: A Language and Environment for Statistical Computing*. R Foundation for Statistical Computing, Vienna, Austria, 2016.

[233] Ratzke, Christoph, and Gore, Jeff. Self-organized patchiness facilitates survival in a cooperatively growing bacillus subtilis population. *Nature microbiology 1*, 5 (2016), 16022.

[234] Reddy, Vamsee S, and Saier, Milton H. Biov suite–a collection of programs for the study of transport protein evolution. *The FEBS journal 279*, 11 (2012), 2036–2046.

[235] Redmile-Gordon, M. A., Brookes, P. C., Evershed, R. P., Goulding, K. W. T., and Hirsch, P. R. Measuring the soil-microbial interface: Extraction of extracellular polymeric substances (EPS) from soil biofilms. *Soil Biology and Biochemistry 72* (May 2014), 163–171.

[236] Revell, Liam J. phytools: an r package for phylogenetic comparative biology (and other things). *Methods in Ecology and Evolution 3*, 2 (2012), 217–223.

[237] Roller, Benjamin RK, and Schmidt, Thomas M. The physiology and ecological implications of efficient growth. *The ISME Journal* (Jan. 2015).

[238] Roller, Benjamin RK, Stoddard, Steven F, and Schmidt, Thomas M. Exploiting rrna operon copy number to investigate bacterial reproductive strategies. *Nature microbiology 1*, 11 (2016), 16160.

[239] Rousk, Johannes, and Bååth, Erland. Growth of saprotrophic fungi and bacteria in soil. *FEMS Microbiology Ecology 78*, 1 (2011), 17–30.

[240] Sahin, Nurettin. Oxalotrophic bacteria. *Research in Microbiology 154*, 6 (2003), 399–407.

[241] Saier Jr, Milton H, Reddy, Vamsee S, Tsu, Brian V, Ahmed, Muhammad Saad, Li, Chun, and Moreno-Hagelsieb, Gabriel. The transporter classification database (tcdb): recent advances. *Nucleic acids research 44*, D1 (2015), D372–D379.

[242] Saifuddin, Mustafa, Bhatnagar, Jennifer M, Segrè, Daniel, and Finzi, Adrien C. Microbial carbon use efficiency predicted from genome-scale metabolic models. *Nature communications 10*, 1 (2019), 1–10.

[243] Santos, Valdinar B, Araújo, Ademir SF, Leite, Luiz FC, Nunes, Luís APL, and Melo, Wanderley J. Soil microbial biomass and organic matter fractions during transition from conventional to organic farming systems. *Geoderma 170* (2012), 227–231.

[244] Satinsky, Brandon M, Crump, Byron C, Smith, Christa B, Sharma, Shalabh, Zielinski, Brian L, Doherty, Mary, Meng, Jun, Sun, Shulei, Medeiros, Patricia M, Paul, John H, et al. Microspatial gene expression patterns in the amazon river plume. *Proceedings of the National Academy of Sciences 111*, 30 (2014), 11085–11090.

[245] Schaechter, Moselio, Maaløe, Ole, and Kjeldgaard, Niels O. Dependency on medium and temperature of cell size and chemical composition during balanced growth of salmonella typhimurium. *Microbiology 19*, 3 (1958), 592–606.

[246] Schimel, Joshua, and Schaeffer, Sean Michael. Microbial control over carbon cycling in soil. *Front Microbiol 3* (2012), 348.

[247] Schimel, Joshua P, and Schaeffer, Sean M. Microbial control over carbon cycling in soil. *The causes and consequences of microbial community structure* (2015), 155.

[248] Schmidt, Gavin A., Kelley, Max, Nazarenko, Larissa, Ruedy, Reto, Russell, Gary L., Aleinov, Igor, Bauer, Mike, Bauer, Susanne E., Bhat, Maharaj K., Bleck, Rainer, Canuto, Vittorio, Chen, Yong-Hua, Cheng, Ye, Clune, Thomas L., Del Genio, Anthony, de Fainchtein, Rosalinda, Faluvegi, Greg, Hansen, James E., Healy, Richard J., Kiang, Nancy Y., Koch, Dorothy, Lacis, Andy A., LeGrande, Allegra N., Lerner, Jean, Lo, Ken K., Matthews, Elaine E., Menon, Surabi, Miller, Ron L., Oinas, Valdar, Oloso, Amidu O., Perlwitz, Jan P., Puma, Michael J., Putman, William M., Rind, David, Romanou, Anastasia, Sato, Makiko, Shindell, Drew T., Sun, Shan, Syed, Rahman A., Tausnev, Nick, Tsigaridis, Kostas, Unger, Nadine, Voulgarakis, Apostolos, Yao, Mao-Sung, and Zhang, Jinlun. Configuration and assessment of the GISS ModelE2 contributions to the CMIP5 archive. *Journal of Advances in Modeling Earth Systems 6*, 1 (Mar. 2014), 141–184.

[249] Schmidt, Michael W. I., Torn, Margaret S., Abiven, Samuel, Dittmar, Thorsten, Guggenberger, Georg, Janssens, Ivan A., Kleber, Markus, Kögel-Knabner, Ingrid, Lehmann, Johannes, Manning, David A. C., Nannipieri, Paolo, Rasse, Daniel P., Weiner, Steve, and Trumbore, Susan E. Persistence of soil organic matter as an ecosystem property. *Nature 478*, 7367 (Oct. 2011), 49–56.

[250] Sengupta, Dipanjan, Datta, Sriparna, and Biswas, Dipa. Towards a better production of bacterial exopolysaccharides by controlling genetic as well as physico-chemical parameters. *Applied microbiology and biotechnology 102*, 4 (2018), 1587–1598.

[251] Setia, Raj, Verma, Suman Lata, and Marschner, Petra. Measuring microbial biomass carbon by direct extraction–comparison with chloroform fumigation-extraction. *European journal of soil biology 53* (2012), 103–106.

[252] Sihi, Debjani, Gerber, Stefan, Inglett, Patrick W, and Sharma Inglett, Kanika. Comparing models of microbial-substrate interactions and their response to warming. *Biogeosciences 13* (2016), 1733–1752.

[253] Silva-Sánchez, Alex, Soares, Margarida, and Rousk, Johannes. Testing the dependence of microbial growth and carbon use efficiency on nitrogen availability, ph, and organic matter quality. *Soil Biology and Biochemistry* (2019).

[254] Simpson, Rodney T, Frey, Serita D, Six, Johan, and Thiet, Rachel K. Preferential accumulation of microbial carbon in aggregate structures of no-tillage soils. *Soil Science Society of America Journal 68*, 4 (2004), 1249–1255.

[255] Sinsabaugh, Robert L., Manzoni, Stefano, Moorhead, Daryl L., and Richter, Andreas. Carbon use efficiency of microbial communities: stoichiometry, methodology and modelling. *Ecology Letters 16*, 7 (July 2013), 930–939.

[256] Sinsabaugh, Robert L, Moorhead, Daryl L, Xu, Xiaofeng, and Litvak, Marcy E. Plant, microbial and ecosystem carbon use efficiencies interact to stabilize microbial growth as a fraction of gross primary production. *New Phytologist 214*, 4 (2017), 1518–1526.

[257] Sinsabaugh, Robert L, Turner, Benjamin L, Talbot, Jennifer M, Waring, Bonnie G, Powers, Jennifer S, Kuske, Cheryl R, Moorhead, Daryl L, and Follstad Shah, Jennifer J. Stoichiometry of microbial carbon use efficiency in soils. *Ecological Monographs 86*, 2 (2016), 172–189.

[258] Sistla, Seeta A, Rastetter, Edward B, and Schimel, Joshua P. Responses of a tundra system to warming using scamps: a stoichiometrically coupled, acclimating microbe–plant–soil model. *Ecological Monographs 84*, 1 (2014), 151–170.

[259] Six, Johan, Frey, SD, Thiet, RK, and Batten, KM. Bacterial and fungal contributions to carbon sequestration in agroecosystems. *Soil Science Society of America Journal 70*, 2 (2006), 555–569.

[260] Smith, Daniel R, and Chapman, Matthew R. Economical evolution: microbes reduce the synthetic cost of extracellular proteins. *MBio 1*, 3 (2010), e00131–10.

[261] Soares, Margarida, and Rousk, Johannes. Microbial growth and carbon use efficiency in soil: Links to fungal-bacterial dominance, soc-quality and stoichiometry. *Soil Biology and Biochemistry* (2019).

[262] Spohn, Marie, Klaus, Karoline, Wanek, Wolfgang, and Richter, Andreas. Microbial carbon use efficiency and biomass turnover times depending on soil depth–implications for carbon cycling. *Soil Biology and Biochemistry 96* (2016), 74–81.

[263] Spohn, Marie, Pötsch, Erich M, Eichorst, Stephanie A, Woebken, Dagmar, Wanek, Wolfgang, and Richter, Andreas. Soil microbial carbon use efficiency and biomass turnover in a long-term fertilization experiment in a temperate grassland. *Soil Biology and Biochemistry 97* (2016), 168–175.

[264] Stamatakis, Alexandros. Raxml version 8: a tool for phylogenetic analysis and post-analysis of large phylogenies. *Bioinformatics 30*, 9 (2014), 1312–1313.

[265] Sterkenburg, Erica, Clemmensen, Karina E, Ekblad, Alf, Finlay, Roger D, and Lindahl, Björn D. Contrasting effects of ectomycorrhizal fungi on early and late stage decomposition in a boreal forest. *The ISME journal* (2018).

[266] Stevenson, Bradley S., Eichorst, Stephanie A., Wertz, John T., Schmidt, Thomas M., and Breznak, John A. New strategies for cultivation and detection of previously uncultured microbes. *Applied and Environmental Microbiology 70*, 8 (2004), 4748–4755.

[267] Stevenson, Bradley S, and Schmidt, Thomas M. Life history implications of rrna gene copy number in escherichia coli. *Applied and environmental microbiology 70*, 11 (2004), 6670–6677.

[268] Stoddard, Steven F, Smith, Byron J, Hein, Robert, Roller, Benjamin RK, and Schmidt, Thomas M. rrn db: improved tools for interpreting rrna gene abundance in bacteria and archaea and a new foundation for future development. *Nucleic acids research 43*, D1 (2014), D593–D598.

[269] Stouthamer, AH. A theoretical study on the amount of atp required for synthesis of microbial cell material. *Antonie van Leeuwenhoek 39*, 1 (1973), 545–565.

[270] Sugai, Susan F, and Schimel, Joshua P. Decomposition and biomass incorporation of 14 c-labeled glucose and phenolics in taiga forest floor: effect of substrate quality, successional state, and season. *Soil Biology and Biochemistry 25*, 10 (1993), 1379–1389.

[271] Suseela, Vidya, and Tharayil, Nishanth. Decoupling the direct and indirect effects of climate on plant litter decomposition: Accounting for stress-induced modifications in plant chemistry. *Global change biology 24*, 4 (2018), 1428–1451.

[272] Takriti, Mounir, Wild, Birgit, Schnecker, Jörg, Mooshammer, Maria, Knoltsch, Anna, Lashchinskiy, Nikolay, Alves, Ricardo J Eloy, Gentsch, Norman, Gittel, Antje, Mikutta, Robert, et al. Soil organic matter quality exerts a stronger control than stoichiometry on microbial substrate use efficiency along a latitudinal transect. *Soil Biology and Biochemistry 121* (2018), 212–220.

[273] Tang, Jinyun, and Riley, William J. Weaker soil carbon-climate feedbacks resulting from microbial and abiotic interactions. *Nature Climate Change 5*, 1 (2015), 56–60.

[274] Tate, KR, Ross, DJ, and Feltham, CW. A direct extraction method to estimate soil microbial c: effects of experimental variables and some different calibration procedures. *Soil Biology and Biochemistry 20*, 3 (1988), 329–335.

[275] Thiet, Rachel K, Frey, Serita D, and Six, Johan. Do growth yield efficiencies differ between soil microbial communities differing in fungal: bacterial ratios? reality check and methodological issues. *Soil Biology and Biochemistry 38*, 4 (2006), 837–844.

[276] Thompson, Luke R, Sanders, Jon G, McDonald, Daniel, Amir, Amnon, Ladau, Joshua, Locey, Kenneth J, Prill, Robert J, Tripathi, Anupriya, Gibbons, Sean M, Ackermann, Gail, et al. A communal catalogue reveals earth's multiscale microbial diversity. *Nature 551*, 7681 (2017), 457.

[277] Todd-Brown, K., Randerson, J., Post, W. M., Hoffman, F. M., Tarnocai, C., Schuur, E., and Allison, S. Causes of variation in soil carbon simulations from CMIP5 Earth system models and comparison with observations. *Biogeosciences 10*, 3 (2013), 1717–1736.

[278] Todd-Brown, KEO, Randerson, JT, Hopkins, F, Arora, V, Hajima, T, Jones, C, Shevliakova, E, Tjiputra, J, Volodin, E, Wu, T, et al. Changes in soil organic carbon storage predicted by earth system models during the 21st century. *Biogeosciences 11*, 8 (2014), 2341–2356.

[279] Treseder, Kathleen K, and Lennon, Jay T. Fungal traits that drive ecosystem dynamics on land. *Microbiology and Molecular Biology Reviews 79*, 2 (2015), 243–262.

[280] Valdivia-Anistro, Jorge A, Eguiarte-Fruns, Luis E, Delgado-Sapién, Gabriela, Márquez-Zacarías, Pedro, Gasca-Pineda, Jaime, Learned, Jennifer, Elser, James J, Olmedo-Alvarez, Gabriela, and Souza, Valeria. Variability of rrna operon copy number and growth rate dynamics of bacillus isolated from an extremely oligotrophic aquatic ecosystem. *Frontiers in microbiology 6* (2016), 1486.

[281] Van Bodegom, Peter. Microbial maintenance: a critical review on its quantification. *Microbial ecology 53*, 4 (2007), 513–523.

[282] van Hoek, Milan JA, and Merks, Roeland MH. Redox balance is key to explaining full vs. partial switching to low-yield metabolism. *BMC systems biology 6*, 1 (2012), 22.

[283] Vieira-Silva, Sara, and Rocha, Eduardo P. C. The Systemic Imprint of Growth and Its Uses in Ecological (Meta)Genomics. *PLoS Genet 6*, 1 (Jan. 2010), e1000808.

[284] Walker, Tom WN, Kaiser, Christina, Strasser, Florian, Herbold, Craig W, Leblans, Niki IW, Woebken, Dagmar, Janssens, Ivan A, Sigurdsson, Bjarni D, and Richter, Andreas. Microbial temperature sensitivity and biomass change explain soil carbon loss with warming. *Nature climate change 8*, 10 (2018), 885.

[285] Wallenstein, Matthew, Allison, Steven D, Ernakovich, Jessica, Steinweg, J Megan, and Sinsabaugh, Robert. Controls on the temperature sensitivity of soil enzymes: a key driver of in situ enzyme activity rates. In *Soil enzymology*. Springer, 2010, pp. 245–258.

[286] Wang, Gang, and Or, Dani. Hydration dynamics promote bacterial coexistence on rough surfaces. *The ISME journal 7*, 2 (2013), 395.

[287] Wang, Gangsheng, Mayes, Melanie A, Gu, Lianhong, and Schadt, Christopher W. Representation of dormant and active microbial dynamics for ecosystem modeling. *PloS one 9*, 2 (2014), e89252.

[288] Wang, Gangsheng, Post, Wilfred M, and Mayes, Melanie A. Development of microbial-enzyme-mediated decomposition model parameters through steady-state and dynamic analyses. *Ecological Applications 23*, 1 (2013), 255–272.

[289] Ward, Susan E, Orwin, Kate H, Ostle, Nicholas J, Briones, Maria JI, Thomson, Bruce C, Griffiths, Robert I, Oakley, Simon, Quirk, Helen, and Bardgett, Richard D. Vegetation exerts a greater control on litter decomposition than climate warming in peatlands. *Ecology 96*, 1 (2015), 113–123.

[290] Waschina, Silvio, D'Souza, Glen, Kost, Christian, and Kaleta, Christoph. Metabolic network architecture and carbon source determine metabolite production costs. *The FEBS journal 283*, 11 (2016), 2149–2163.

[291] Wickham, Hadley. *ggplot2: Elegant Graphics for Data Analysis*. Springer-Verlag New York, 2009.

[292] Wickham, Hadley. The split-apply-combine strategy for data analysis. *Journal of Statistical Software 40*, 1 (2011), 1–29.

[293] Wieder, William R, Allison, Steven D, Davidson, Eric A, Georgiou, Katerina, Hararuk, Oleksandra, He, Yujie, Hopkins, Francesca, Luo, Yiqi, Smith, Matthew J, Sulman, Benjamin, et al. Explicitly representing soil microbial processes in earth system models. *Global Biogeochemical Cycles 29*, 10 (2015), 1782–1800.

[294] Wieder, William R, Bonan, Gordon B, and Allison, Steven D. Global soil carbon projections are improved by modelling microbial processes. *Nature Climate Change 3*, 10 (2013), 909.

[295] Wieder, WR, Grandy, AS, Kallenbach, CM, and Bonan, GB. Integrating microbial physiology and physio-chemical principles in soils with the microbial-mineral carbon stabilization (mimics) model. *Biogeosciences 11*, 14 (2014), 3899–3917.

[296] Wieder, WR, Grandy, AS, Kallenbach, CM, Taylor, PG, and Bonan, GB. Representing life in the earth system with soil microbial functional traits in the mimics model. *Geoscientific Model Development 8*, 6 (2015), 1789–1808.

[297] Winogradsky, Sergei. Sur la microflora autochtone de la terre arable. *Comptes rendus hebdomadaires des seances de l'Acadamie des sceinces 178* (1924), 1236–1239.

[298] Wu, Hao, Fang, Yongjun, Yu, Jun, and Zhang, Zhang. The quest for a unified view of bacterial land colonization. *The ISME journal 8*, 7 (2014), 1358–1369.

[299] Xu, Xiaofeng, Thornton, Peter E, and Post, Wilfred M. A global analysis of soil microbial biomass carbon, nitrogen and phosphorus in terrestrial ecosystems. *Global Ecology and Biogeography 22*, 6 (2013), 737–749.

[300] Ye, Jian-Sheng, Bradford, Mark A., Dacal, Marina, Maestre, Fernando T., and García-Palacios, Pablo. Increasing microbial carbon use efficiency with warming predicts soil heterotrophic respiration globally. *Global Change Biology* (2019).

[301] Yin, Huajun, Li, Yufei, Xiao, Juan, Xu, Zhenfeng, Cheng, Xinyin, and Liu, Qing. Enhanced root exudation stimulates soil nitrogen transformations in a subalpine coniferous forest under experimental warming. *Global Change Biology 19*, 7 (2013), 2158–2167.

[302] Zak, Donald R, Ringelberg, David B, Pregitzer, Kurt S, Randlett, Diana L, White, David C, and Curtis, Peter S. Soil microbial communities beneath populus grandidentata grown under elevated atmospheric co2. *Ecological Applications 6*, 1 (1996), 257–262.

[303] Zhang, De-Chao, Schumann, Peter, Liu, Hong-Can, Xin, Yu-Hua, Zhou, Yu-Guang, Schinner, Franz, and Margesin, Rosa. Arthrobacter alpinus sp. nov., a psychrophilic bacterium isolated from alpine soil. *International journal of systematic and evolutionary microbiology 60*, 9 (2010), 2149–2153.

[304] Zheng, Qing, Hu, Yuntao, Zhang, Shasha, Noll, Lisa, Böckle, Theresa, Richter, Andreas, and Wanek, Wolfgang. Growth explains microbial carbon use efficiency across soils differing in land use and geology. *Soil Biology and Biochemistry 128* (2019), 45–55.

[305] Zhou, Yumei, Tang, Jianwu, Melillo, Jerry M, Butler, Sarah, and Mohan, Jacqueline E. Root standing crop and chemistry after six years of soil warming in a temperate forest. *Tree Physiology 31*, 7 (2011), 707–717.

[306] Zlatkin, IV, Nikitin, DI, and Sigalevich, PA. Investigation of unusual growth and phenotypic characteristics of plasmid-containing and plasmid-free strains of oligotrophic bacterium ancylobacter vacuolatus. *Microbiology 81*, 1 (2012), 35–43.